UNVEILING THE METABOLIC NETWORK UNDERLYING MITOCHONDRIAL AND NUCLEAR METABOLISM IN A MODEL DIFFERENTIATING STEM CELL

By
Sungwon Han

Thesis submitted in partial fulfillment
of the requirements for the degree of
Master of Science (MSc) in Chemical Sciences

School of Graduate Studies
Laurentian University
Sudbury, Ontario

THESIS DEFENCE COMMITTEE/COMITÉ DE SOUTENANCE DE THÈSE

Laurentian Université/Université Laurentienne
School of Graduate Studies/École des études supérieures

Title of Thesis Titre de la thèse	UNVEILING THE METABOLIC NETWORK UNDERLYING MITOCHONDRIAL AND NUCLEAR METABOLISM IN A MODEL DIFFERENTIATING STEM CELL
Name of Candidate Nom du candidat	Han, Sungwon
Degree Diplôme	Master of Science
Department/Program Département/Programme	Chemical Sciences
Date of Defence Date de la soutenance	July 30, 2013

APPROVED/APPROUVÉ

Thesis Examiners/Examinateurs de thèse:

Dr. Vasu Appanna
(Supervisor/Directeur de thèse)

Dr. Crestina Beites
(Committee member/Membre du comité)

Dr. Abdel Omri
(Committee member/Membre du comité)

Dr. William T. Self
(External Examiner/Examinateur externe)

Approved for the School of Graduate Studies
Approuvé pour l'École des études supérieures
Dr. David Lesbarrères
M. David Lesbarrères
Director, School of Graduate Studies
Directeur, École des études supérieures

ACCESSIBILITY CLAUSE AND PERMISSION TO USE

Abstract

Participation of metabolism in stem cell differentiation has been largely disregarded until recently. Here, functional proteomics and metabolomics were performed to unveil the mitochondrial and nuclear metabolism during dimethyl sulfoxide (DMSO)-induced differentiation of P19 cells. DMSO-treated cells were shown to exhibit increased glycolytic enzymes activities and fuel pyruvate into oxidative phosphorylation. Subsequently, enzymes of electron transport chain also had elevated activities upon differentiation. These changes in mitochondrial metabolism were concomitant with increased mitochondrial biogenesis as PGC-1α expression was higher in the differentiated cells. To study nuclear metabolism, particular focus was placed on delineating a potential role of nuclear lactate dehydrogenase (LDH). Nuclear LDH was found to exhibit higher expression in pluripotent cells. NAD^+ generated from LDH reaction was discovered to promote histone deacetylation via sirtuin-1 (SIRT1). Drastic alterations in mitochondrial and nuclear metabolism during differentiation point to a pivotal role of metabolism in deciding the final destination of stem cells.

Keywords: Stem cells, differentiation, mitochondrial metabolism, nuclear metabolism, mitochondrial biogenesis.

Acknowledgement

I would like to express my appreciation to Dr. Vasu Appanna and Dr. Crestina Beites for their guidance and support throughout the duration of my master's degree. I would like to extend a special thanks to Dr. V. Appanna for his continuous guidance and philosophy over the years I've worked in the lab. You are a true inspiration and your words will always motivate me to better myself.

I would also like to thank to the members of my committee Dr. Abdel Omri and my external examiner, Dr. William T. Self (University of Central Florida) for their assistance, and guidance with my thesis.

I would like to thank my lab mates past and present, Dr. Joseph Lemire, Christopher Auger, Sean HBP Thomas, Adam Bignucolo, Azhar Alhasawi, Varun Appanna and Jacob Costanzi for their friendship, mentorship, technical support and insights.

Finally, I would like to thank my friends and family for their continuous encouragements.

Table of Contents

List of Figures

List of Tables

List of Abbreviations

1,3 BPG	1,3-Bisphosphoglycerate
3PG	3-Phosphoglycerase
6PG	6-Phosphoglycoante
6PGDH	6-Phosphoglyconate dehydrogenase
6PGL	6-Phosphoglucolactone
6PGLase	6-Phosphoglycoolactonase
ACC	Acetyl-CoA carboxylase
ACL	ATP-citrate lyase
ACS	Acetyl-CoA synthase
ACT	Acylcarnitine carnitine translocase
AIF	Apoptosis-inducing factor
AKT	Protein kinase B
ATRA	*All-trans* retinoic acid
BMP-2	Bone morphogenic protein-2
BN-PAGE	Blue native polyacrylamide gel electrophoresis
CARD	Caspase-recruitment domain
CFE	Cell free extract
CPS-1	Carbamoyl phosphate synthase-1
CPT	Carnitine palmitoyl transferase
CRABP2	Cellular retinoic acid binding protein 2
CSF	Colony-stimulating factor
DHAP	Dihydroxyacetone phosphate
DMSO	Dimethyl sulfoxide
DNMT	DNA methyl transferase
dsRNA	Double-stranded RNA
E4P	Erythrose 4-phosphate
EB	Embryoid body
ECC	Embryonal carcinoma cell
ECM	Extracellular matrix
ER	Endoplasmic reticulum
ERK	Extracellular signal-regulated kinase
ESC	Embryonic stem cell
ETC	Electron transport chain
F16BP	Fructose-1,6-bisphosphatase
FAS	Fatty acid synthase
FBS	Fetal bovine serum
FGF2	Fibroblast growth factor 2
FGFR	Fibroblast growth factor receptor
G3P	Glyceraldehyde-3-phosphate
G6P	Glucose 6-phosphate
G6PDH	Glucose 6-phosphate dehydrogenase
GAPDH	Glyceraldehyde-3-phosphate dehydrogenase
GDH	Glutamate dehydrogenase
GPI	Glucose phosphate isomerase
HAT	Histone acetyltransferase

HDAC	Histone deacetylase
HIF-1α	Hypoxia inducible factor-1α
HK	Hexokinase
HSC	Hematopoietic stem cell
ICDH	Isocitrate dehydrogenase
ICM	Inner cell mass
IL	Interleukin
iPSC	Induced pluripotent stem cell
KGDH	α-ketoglutarate dehydrogenase
LDH	Lactate dehydrogenase
LIF	Leukemia inhibitory factor
LIFR	Leukemia inhibitory factor receptor
MAPK	Ras/mitogen-activated protein kinase
mCSB	Mammalian cell storage buffer
MDH	Malate dehydrogenase
MEL	Friend erythroleukimia
NF-κB	Nuclear factor-kappa B
OGlCNAc	O-linked N-acetylglucosamine
OGT	OGlcNAc transferase
PC	Pyruvate carboxylase
PDH	Pyruvate dehydrogenase
PEP	Phosphoenolpyruvate
PEPCK	PEP carboxykinase
PFK-1	Phosphofructookinase-1
PGC-1α	Peroxisome proliferator-activated receptor-γ coactiavtor-1α
PGK	Phosphoglycerate kinase
PGM	Phosphoglycerate mutase
PHD2	prolyl hydroxylase 2
PI3K	Phosphoinositide 3-kinase
PK	Pyruvate kinase
PTM	Post-translational modifications
Q	Ubiquinone
QH_2	Ubiquinol
R5P	Ribose 5-phosphate
RA	Retinoic acid
RAR	Retinoic acid receptor
RDH10	Retinol dehydrogenase 10
ROS	Reactive oxygen species
rRNA	Ribosomal RNA
RXR	Retinoid X receptor
SDH	Succinate dehydrogenase
siRNA	Small interfering RNA
SIRT1	Sirtuin 1
SRC-1	Steroid receptor coactivator 1
STAT3	Signal transducer and activator of transcription 3
TBS	Tris buffered saline
TCA	Tricarboxylic acid

TET1	Ten-eleven translocation 1
TGF-β	Transforming growth factor-beta
TIF-2	Transcriptional intermediary factor 2
TPI	Triose phosphate isomerase
TPO	Thrombopoietin
TTBS	Tween-20 tris buffered saline
VDAC	Voltage dependent anion channel
VEGF	Vascular endothelial growth factor
VLCFA	Very long chain fatty acyl-CoAs
α-MEM	α-minimum essential media
α-MHC	α-myosin heavy chain
β-MHC	β-myosin heavy chain

1. Introduction

1.1 Cellular metabolism

1.1.1 Metabolism

Metabolism involves the various essential biochemical reactions within the cells of viable organisms. It facilitates life by providing the necessary substituents required for growth, energy production, cellular communication and damage repair. These metabolic networks are mediated and interconnected by numerous enzymatic reactions making metabolism one of the most complex cellular processes [1]. The dynamics of metabolism is derived from these highly sophisticated connections among the biochemical reactions. Each reaction, however, plays a unique role in the system.

1.1.1.1Roles of metabolism

The role of metabolism can be divided into four categories. Anabolism constructs molecules from smaller units. Catabolism breaks down larger organic molecules into smaller units. Energy production generates the necessary energy currency required to facilitate cellular functions. Lastly, metabolism is also involved in signaling processes (Figure 1.1).

Carbohydrate, amino acid, nucleic acid and lipid anabolism are the major form of anabolism in cellular processes. Carbohydrate anabolism helps synthesize simple monosaccharides from organic acids, fatty acids from sugar and store energy reserves in form of glycogen and other molecules. Amino acid anabolism promotes production of 12 non-essential amino acids in humans, participates in the disposal of intercellular nitrogenous wastes and protein biosynthesis. Nucleotides are synthesized through purine/pyrimidine metabolism and become four nucleic acids. Lipid anabolism contributes in the formation of complex lipids such as steroids and sphingolipids.

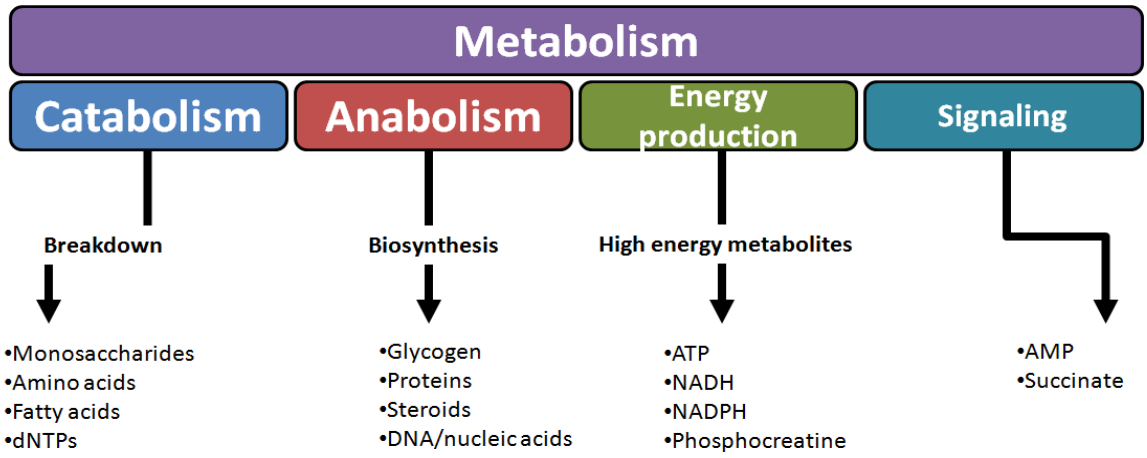

Figure 1. 1. Basic functions of metabolism

The function of metabolism is divided into catabolism, anabolism and energy production. Catabolism promotes breakdown of macromolecules. Anabolism synthesizes biomolecules such as glycogen, protein and nucleic acids. Energy metabolism provides the energy to operate cellular functions.

Catabolism promotes breakage of larger molecules into small molecules. These smaller molecules can be utilized in anabolic processes. For instance, fatty acids and glycerol can be broken down into acetyl-CoA, which can then be oxidized in the tricarboxylic acid (TCA) cycle and the electron transport chain (ETC) to generate ATP.

Energy is essential for any living organism to maintain proper function. The energy metabolic pathways, however, vary among the organisms as their source of energy differs. Chemoorganoheterotrophic organisms are often a focus in metabolic studies as it governs energy production in human. Once the complex carbohydrates are broken down into acetyl-CoA via processes such as glycolysis and β-oxidation of lipids (break down of complex lipid molecules), it can then enter the TCA cycle to undergo decarboxylation and produces NADH and $FADH_2$. The production of NADH and $FADH_2$ is facilitated by numerous dehydrogenases which assist in transferring high energy electrons to reduce

NAD^+ and FAD^{2+}. Subsequently, NADH and $FADH_2$ molecules transfer their electrons to Complex I and Complex II, respectively. ETC then relays the electrons to create ATP via ATP synthase [2].

More recently the role of metabolism in cellular signaling has begun to emerge. The plasticity of metabolic networks permit a cell to communicate information through appropriate metabolites generated or consumed. Mailloux et al (2007) have demonstrated that metabolism is used to pool specific metabolites in order to remove or remedy the effect caused by stressors [3]. AMP has also been found to be closely related to maintaining energy status of the cells via various mechanisms [4]. Metabolic feedback is another example where metabolism is used to coordinate the activities of a cell to sustain efficiency.

1.1.2 Metabolic regulation

Metabolic regulation helps control the direction of the metabolic reaction. Absence of regulation may promote production of undesired substrates. Thus, it is imperative that cells must strictly maintain metabolic regulations to ensure the synthesis of required products. Metabolic homeostasis is achieved via a series of mechanisms that control the direction of metabolites in response to the requirement of the organism. The metabolic network can be regulated by transcriptional regulations, posttranslational modifications and metabolic feedback mechanisms. These mechanisms can both act in an individual manner or operate in tandem (Figure 1.2).

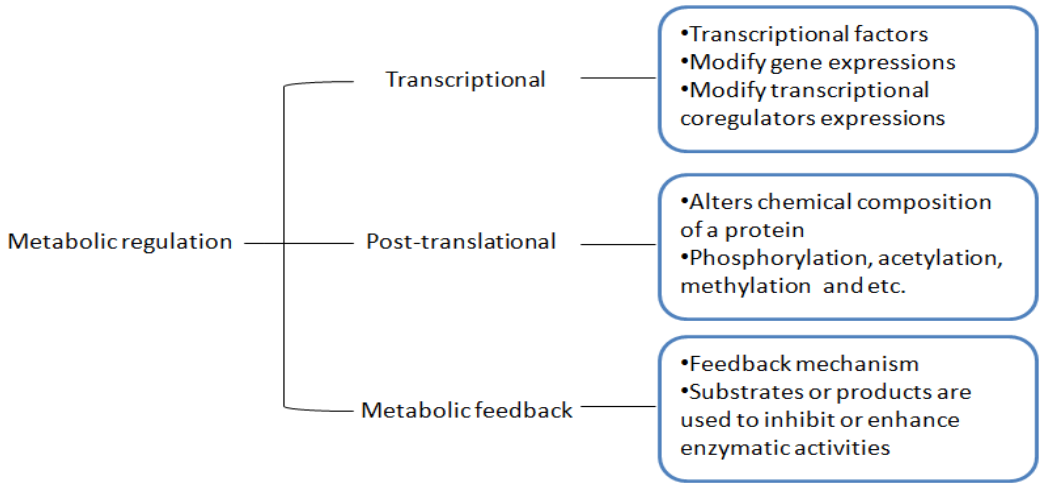

Figure 1. 2. Three major forms of metabolic regulation

The metabolism is regulated primarily by three forms: 1) transcriptional, 2) post-translational modification, and 3) metabolic feedback mechanisms. Transcriptional factors affect actual gene expression and modify transcription-linked gene expression. Post-translational modification is performed by changing the chemical composition of a protein via acetylation, phosphorylation, methylation, etc. Metabolic feedback mechanisms utilize substrates and products to either inhibit or enhance enzymatic activities.

1.1.2.1 Transcriptional regulation

Transcriptional regulations are crucial in maintaining the efficiency and organization of the metabolic network. These regulatory mechanisms involve transcription factors that directly interact with DNA to promote changes in gene expression and transcriptional coregulators or coactivators [5]. In recent years, there have been increased efforts in studying the cofactors of transcriptional regulation as they participate in fine-tuning of the transcriptional response. Cofactors such as PPAR gamma coactivator 1α (PGC-1α), steroid receptor coactivator 1 (SRC-1), and transcriptional intermediary factor 2 (TIF2) have provided clear evidence that genetic regulation maintains cellular metabolism [5].

PGC-1α is a master regulator of mitochondrial biogenesis and energy expenditure [6]. This particular coregulator has been related to various metabolic functions. In brown adipose tissue, PGC-1α acts as a protein that controls adaptive thermogenesis. Upon fasting, hepatic cells increase PGC-1α expression to promote gluconeogenesis. In skeletal and cardiac muscle, PGC-1α promotes mitochondrial biogenesis and respiration. Thus, it is evident that PGC-1α expression reflects the energy status and the energy needs of a cell. Transcription factors that are influenced by PGC-1α include PPARγ, PPARα, ERRα, FOXO1, HNF4α and NRF1 [7,8,9,10,11]. These pathways ultimately modulate the activity of metabolic pathways such as gluconeogenesis, fatty acid synthesis and oxidation and glycolysis.

1.1.2.2 Posttranslational modification

Post-translational modification (PTM) mechanisms involve altering the original chemical composition of a protein [12]. This process is commonly done by covalent addition of a small molecule to amino acid residues via specialized proteins [13]. Phosphorylation, acetylation, methylation, glycosylation, lipidation, flavinylation, ubiquitylation and proteolysis are common forms of PTM in eukaryotes [14]. Protein phosphorylation is, however, the most frequent and well studied. There are more than 2300 phosphoproteins in *Saccharomyces cerevisiae* and their production and activation are governed by a wide array of kinases and phosphatases [13]. The importance of phosphorylation is evident from many studies. In the yeast, 23 of 924 metabolic enzymes are known to be regulated by PTM via phosphorylation. However, an increasing number of studies indicate that there are even more enzymes in metabolic networks that are regulated by phosphorylation (Figure 1.3) [15,16,17,18]. More studies are required to

further understand the full extent of the influence of PTM on metabolic enzymes and the overall metabolic network.

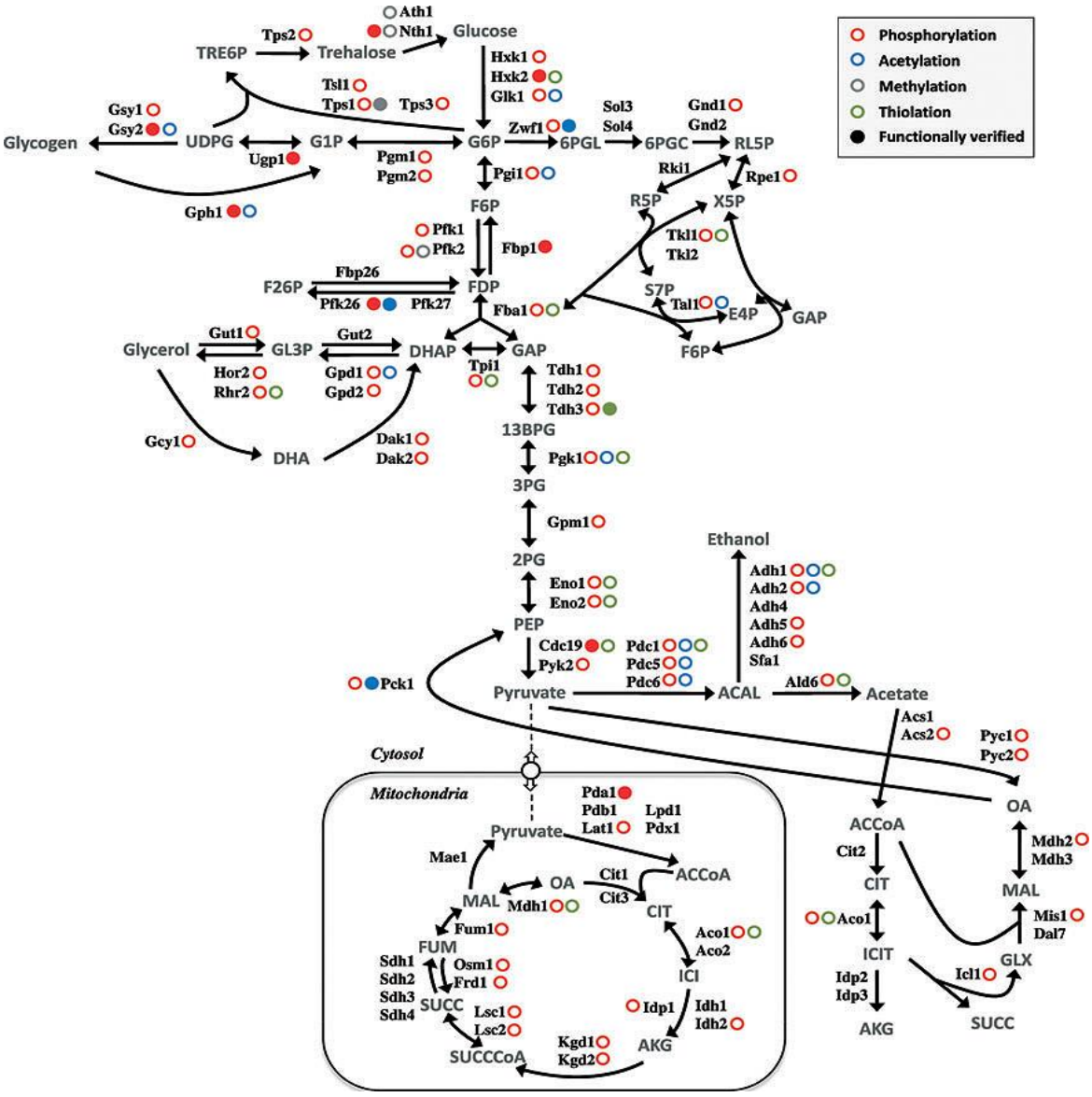

Figure 1. 3. Metabolic enzymes regulated by post-translational modification (PTM) in *Saccharomyces cerevisiae*.

The enzymes detected or verified to undergo phosphorylation (red), acetylation (blue), methylation (grey) and thiolation (green). Functionally verified PTMs are illustrated with solid circles. Open circles indicate detected but not yet functionally validated PTMs. Refer to [13].

1.1.2.3 Metabolic feedback

Metabolic feedback regulation is a well recognized route of enzyme inhibition, especially those in metabolic networks. Feedback mechanisms inhibit or activate enzymatic activities by utilizing the downstream product of the biochemical reactions. This process prevents overproduction of products. This means of modulating metabolic networks is similar to the regulation of cellular signaling, relaying on nodal enzymes or substrates to monitor the pathways [19].

Phosphofructokinase-1 (PFK-1) and pyruvate kinase (PK) are two well known examples of metabolic enzymes that are regulated through feedback mechanism. PFK-1 phosphorylates fructose-6-phosphate to generate fructose-1,6-bisphosphate. Phosphorylation of this enzyme is particularly important in regulating glycolysis as it is responsible for catalyzing the committed step of glycolysis. Metabolites such as AMP, ADP, ATP, fructose-2,6-bisphosphate and citrate are some of the recognized allosteric regulators of PFK-1 [20]. Glucose levels are also an important factor in regulating PFK-1. Under high glucose conditions, continuous production of fructose-6-phosphate is favoured. The fructose-6-phosphate is consumed by phosphofructosekinase-2 to produce fructose-2,6-bisphosphate. This metabolite is then used to positively reinforce the activity of PFK-1. If glucose levels are low, it leads to lower fructose-6-phosphate levels within the cell, subsequently causing the reduced level of fructose-2,6-bisphosphate production. Under decreased fructose-2,6-bisphosphate conditions, fructose-1,6-bisphophatase (F16BP) remains uninhibited and promotes the reaction in the opposite direction towards gluconeogenesis (Figure 1.4a). PK is another enzyme that modulates metabolism via allosteric inhibition. ATP is responsible for the inhibition of the enzyme, resulting in the accumulation of phosphoenolpyruvate (PEP). PEP causes inhibition of triosephosphate

isomerase, stimulating the pentose phosphate pathway and promoting production of NADPH, a crucial reducing agent. The production of NADPH makes the pentose phosphate pathway an important defense mechanism to counter the effects of reactive oxygen species (ROS) or other endogenous and exogenous oxidative stress causing agents [21] (Figure 1.4b).

a)

b)

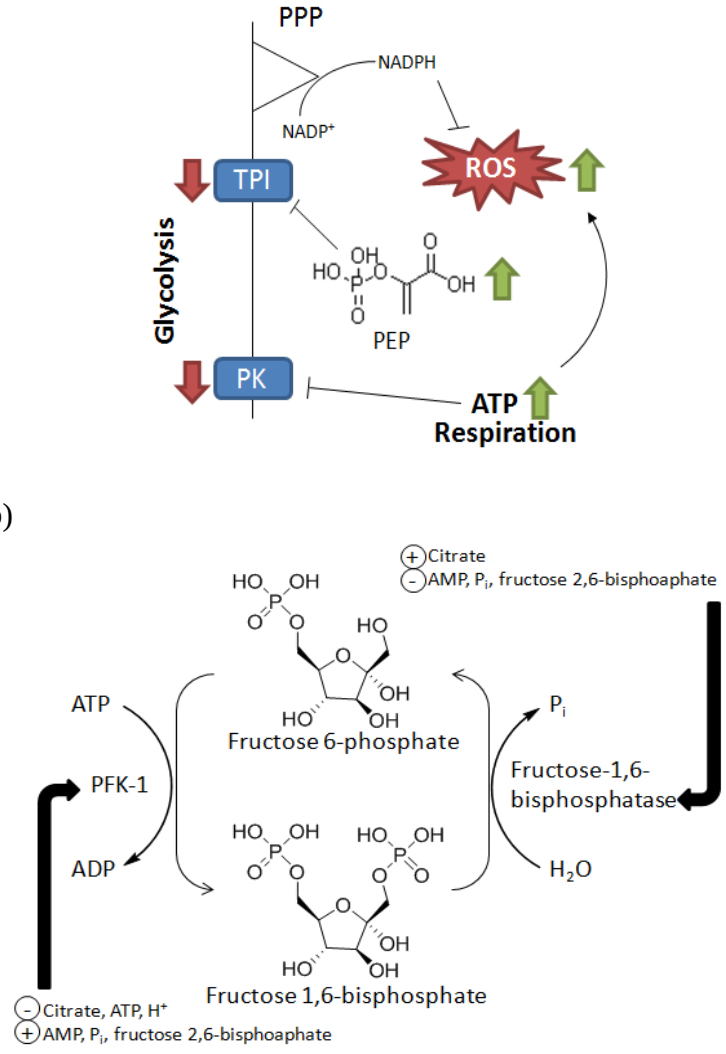

Figure 1. 4. Modulation of metabolism by feedback mechanism.

a) Increased cellular respiration promotes ATP and ROS generation. The ATP is used to inhibit pyruvate kinase and creates pools of PEP which can inhibit topoisomerase (TPI). Inhibition of glycolysis directs metabolites through the pentose phosphate pathway increasing production of NADPH, used to counteract the increased ROS. b) PFK-1 and

fructose-1,6-bisphosphatase are enzymes that regulate glycolysis and gluconeogenesis, respectively. Both enzymes are positively and negatively regulated by the metabolites illustrated in the figure.

1.1.3 Metabolic compartmentalization

Metabolic compartmentation refers to the non-homogenous allocation of metabolic pathways and enzymes within the cell. This differential localization of metabolism plays a key role in metabolic regulation as it concentrates and separates metabolites and enzymes within the organelles [22]. Present understanding of compartmentalization is based on the endosymbiotic origin of organelles [22]. Cellular compartments include most of the organelles found within the cell such as mitochondria, chloroplasts, peroxisomes, glycosome, lysosome, endoplasmic reticulum, nucleus and golgi apparatus. However, chloroplasts and mitochondria are the most studied examples of metabolic compartments. Chloroplasts were once free-living cyanobacteria that transformed into oxygen photosynthetic compartments of the eukaryotic cells [23,24]. Mitochondria are also believed to have evolved from proteobacteria to oxygen-dependent and oxygen independent pyruvate breakdown compartments of the organism [25,26]. Both organelles contain their own unique DNA, which further establishes the possibility that these organelles were once free-living organisms. Despite the reduced number of genomes in these organelles, chloroplasts and mitochondria can still contain several thousand proteins [27].

The origin of other organelles such as glycosomes and peroxisomes are not considered to be endosymbiotic. The unique metabolic pathways of these organelles must be transferred into their membrane enclosed compartments created by the endoplasmic reticulum. It would be highly burdensome to the cells to redirect individual enzymes one

at a time to the designated compartment. Thus, the whole metabolic pathway is suggested to be transferred. This transfer of entire metabolic pathways is theorized to originate during evolution and natural selection and may be derived from mistargeting of the proteins. It is clear that 100 percent protein targeting is not a realistic estimate. A small portion of enzymes will potentially end up in other organelles. Then, the mistargeting for all proteins of a pathway to incorrect organelles could also be possible. This would provide biochemically functional units and can potentially operate to increase or decrease natural selection of these particular changes [22].

The metabolic compartmentalization in eukaryotes plays a key role in metabolic homeostasis. Chemicals and enzymes in freely diffused form in cytoplasm would prove to be extremely inefficient as the right substrate-enzyme interaction would be left to chance. By providing a site and clustering of metabolites and enzymes, cells can maintain their metabolic efficiency [28].

1.1.3.1 Cytosolic metabolism

Cytoplasm, also called cytosol, is a viscous component residing within the cell membrane and surrounding the nucleus and the cytoplasmic organelles. Biochemical pathways such as glycolysis, pentose phosphate pathway, fatty acid synthesis, amino acid metabolism, steroid synthesis, glycogen synthesis and all other networks that are associated with these pathways can be found in the cytosolic portion of a eukaryotic cell.

Glycolysis is one of the key contributors in energy metabolism and it converts incoming glucose into pyruvate via a series of enzymatic reactions. Glucose is transported into the cell via glucose transport proteins (GLUT). The initial reaction of the glycolytic pathway is performed by hexokinase (HK), catalyzing the first committed step of glucose

metabolism by phosphorylating glucose and producing glucose 6-phosphate (G6P). By modifying the entering glucose, this crucial step maintains glucose concentration gradients and facilitates continuous glucose influx into the cell [29]. A subsequent reaction involves rearrangement of G6P into fructose 6-phosphate by glucose phosphate isomerase (GPI). The next step of the glycolysis involves an addition of another phosphate group, donated by ATP, to the F6P, producing fructose 1,6-bisphosphate. This rate limiting step of the glycolytic pathway is carried out by PFK-1 [20]. Then the fructose bisphosphate aldolase divides F16P into two triose sugars, dihydroxyacetone phosphate (DHAP) and glyceraldehydes-3-phosphate (G3P) [30]. Triose phosphate isomerase (TPI) is another enzyme that participates in both glycolysis and gluconeogenesis, as it provides rapid reaction changing DHAP into G3P. This provides additional G3P molecule that can be used in the second half of the glycolysis biochemical reactions [31]. A final reaction of glycolysis involves transfer of a phosphate group to ADP to generate one ATP and pyruvate. The net glycolysis reaction per one molecule of glucose yields 2 pyruvate, 2 ATP and 1 NADH. The NADH produced must be transported into mitochondria for subsequent biochemical reactions. This is done by the malate-aspartate and glycerol-3-phosphate shuttle (Figure 1.5).

Gluconeogenesis is considered the reverse of glycolysis. However, several enzymes involved in this metabolic pathway differ from that of glycolysis. Two key enzymes are pyruvate carboxylase (PC) and PEP carboxykinase (PEPCK). Pyruvate is carboxylated to form oxaloacetate by PC in the mitochondria. Next, oxaloacetate is transported out of the mitochondria into the cytosol and there PEPCK decarboxylates oxaloacetate to produce PEP, while hydrolyzing one GTP to GDP. The step converting PEP into fructose-1,6-bisphosphaste utilizes identical enzymes as the glycolysis, except in

the reverse reaction. F16BP and PFK-1 are two important rate determining steps of both glycolytic and gluconeogenesis pathways. This regulation helps to control the recycling process between fructose 6-phosphate and fructose 1,6-bisphosphate and maintains glycogenic/glyconeogenic flux in the cell [32]. Fructose-6-phosphate is then eventually converted into glucose (Figure 1.5).

The pentose phosphate pathway provides organisms with NADPH and pentose sugars. This pathway is considered a major source of NADPH for the cell. NADPH provides the reducing equivalent for various biosynthetic reactions and allows regeneration of glutathione, a protective mechanism against ROS toxicity. Two main pentoses produced from this pathway are ribose 5-phosphate (R5P) and erythrose 4-phosphate (E4P). R5P is a precursor in the synthesis of nucleotide and nucleic acid and E4P is used in aromatic amino acid biogenesis [33,34]. The pentose phosphate pathway is divided into two stages; an oxidative phase and a non-oxidative phase (Figure 1.5) [1].

Fatty acid synthesis involves the creation of fatty acids from acetyl-CoA and malonyl-CoA. This important lipogenesis is performed by acetyl-CoA carboxylase (ACC) and fatty acid synthases (FAS). ACC is responsible in converting acetyl-CoA into malonyl-CoA for the subsequent FAS reaction. Type I FAS is a multienzyme protein found in eukaryotes as the 10 enzymes in the system are covalently linked in multifunctional polypeptides. The overall reaction produces a 16-carbon palmitic acid from acetyl-CoA and malonyl-CoA.

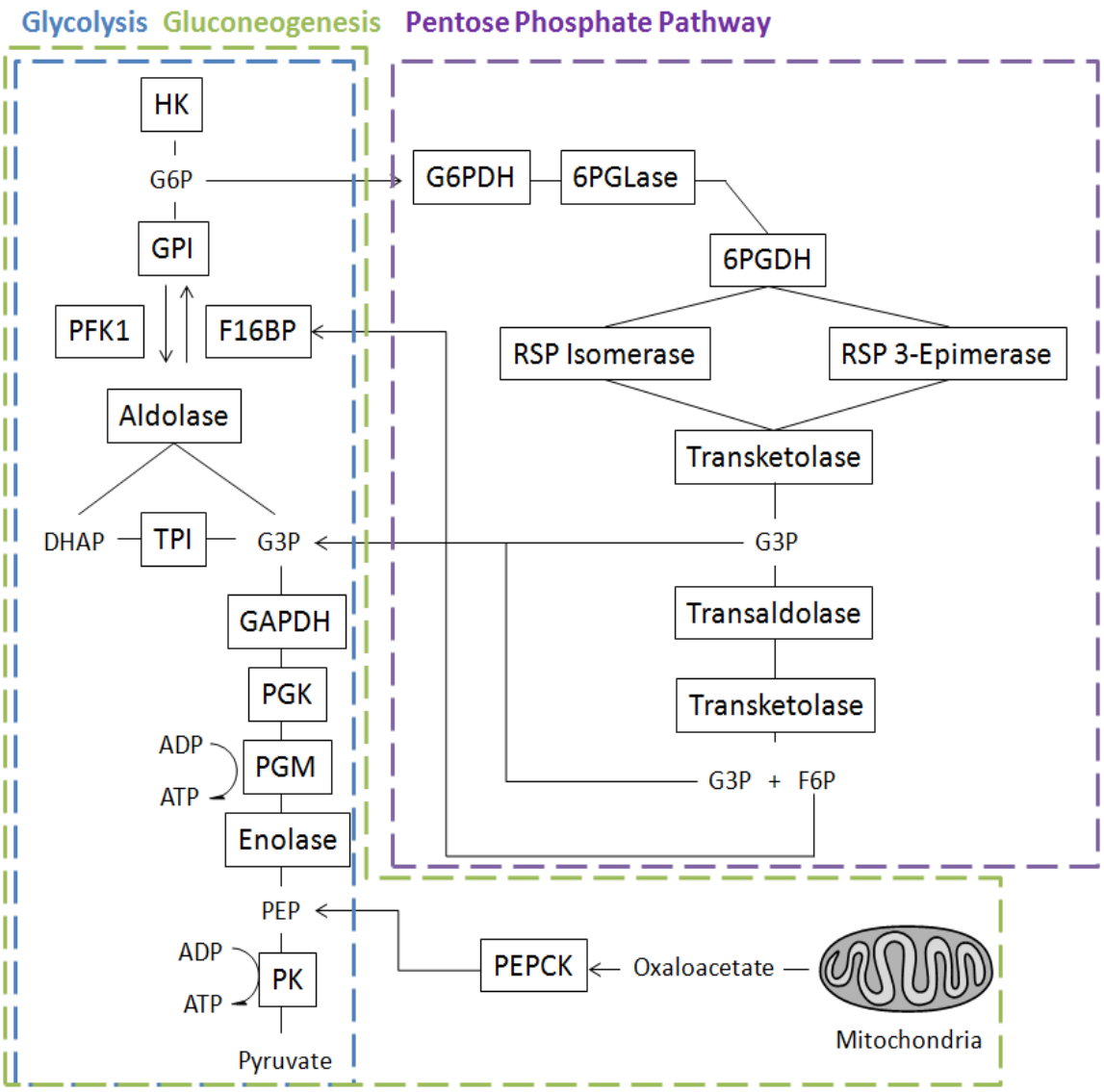

Figure 1. 5. Major cytosolic metabolic pathways.

Glycolysis is used to metabolize glucose into pyruvate for further energy production via oxidative phosphorylation. Glyconeogenesis, on the other hand, uses oxaloacetate derived from mitochondria to generate glucose. PFK-1 and F16BP are the only differences between the two opposite directed pathway. The pentose phosphate pathway is a pathway closely linked to glycolysis. This pathway is regulated by the amount of glucose 6-phosphate produced from HK. The later metabolite products of pentose phosphate pathway can be re-inserted into glycolysis. This illustrates a complex network of metabolism as the different pathways share metabolites for different purposes.

1.1.3.2 Mitochondrial metabolism

1.1.3.2.1 Energy metabolism

Mitochondria, the powerhouse of the cell, contribute in multiple ways in the energy status of the cell, mainly through the biochemical pathways such as TCA cycle, oxidative phosphorylation, β-oxidation, and initiation of gluconeogenesis. The one revolution of TCA cycle requires one acetyl-CoA. This reaction produces three NADH and one $FADH_2$, which produces ATP in the electron transport chain. The TCA cycle consists of a total of nine biochemical reactions driven by metabolic enzymes. The step involving the conversion of pyruvate into acetyl-CoA by pyruvate dehydrogenase (PDH) is often considered as the initiation process of the TCA cycle as the enzyme PDH is a key modulator of fluxes into the TCA cycle [2]. The second step involves citrate synthase, combining the incoming acetyl-CoA with recycled oxaloacetate from the previous TCA revolution to form citrate. Then the aconitase catalyzes the interconversion of citrate into isocitrate. Aconitase is an enzyme containing an iron-sulfur cluster [4Fe-4S] in its active site and because of this particular characteristic, this enzyme has been shown to be sensitive to ROS [35] (Figure 1.6).

Oxidative stress agents such as superoxide can rapidly remove an iron from the catalytic site to promote inactivation of the enzyme. Subsequently, this delays the electron transfer via the TCA cycle and ultimately ATP production is also affected. This mechanism, however, prevents further endogenous ROS production from oxidative phosphorylation, thus limiting the additional increase in ROS level. Next, isocitrate is oxidatively decarboxylated to produce NADH and α-ketoglutarate by isocitrate dehydrogenase (ICDH). There are two isoforms of ICDH in the TCA cycle, $NADP^+$-dependent ICDH and NAD^+-dependent ICDH. Under normal condition, the NAD^+-ICDH

is predominant in activity. However, in presence of oxidative stress the $NADP^+$-ICDH is upregulated to produce more NADPH in order to combat the ROS and reduce the level of endogenous ROS by limiting NADH production [3]. Figure 1.6 depicts the enzymes involved in the TCA cycle and oxidative phosphorylation.

The NADH and $FADH_2$ produced from the TCA cycle are then subjected to oxidative phosphorylation. The ETC couples the energy released in electron transfer to ATP production. The regulation of ETC depends on the amount of NADH, $FADH_2$ and the availability of ADP to phosphorylate. Complex I, NADH ubiquinone oxidoreductase, is responsible for the oxidation of NADH and Complex II, succinate ubiquinone reductase oxidizes $FADH_2$. These two initiators of the ETC transfer the electrons to the ubiquinone pool. During this process, Complex I also translocates a proton to the inner membrane space, while Complex II does not. The electrons in ubiquinol are then delivered to the cytochrome c via Complex III, cytochrome bc_1. Complex III also participates in generating a proton gradient by Q cycle mechanism. The ubiquinol (QH_2) binds to the Q_o site of complex III while ubiquinone (Q) binds to the Q_i site of complex III. Once bound, QH_2 transfers one electron to cytochrome c and the other to Q producing a semiquinone radical. This process releases hydrogen into the intermembrane space. The semiquinone radical is fully reduced in another cycle to produce QH_2. The complete Q cycle translocates 4 protons. The electrons transferred to the cytochrome c are delivered to the complex IV, cytochrome oxidase, which also pumps protons. Cytochrome c is a hemoprotein that can donate electrons on the cytoplasmic side of the mitochondrial inner membrane. Once the electrons are donated to the active site containing a heme iron and a copper, they are used to reduce molecular oxygen into two water molecules. The protein gradient established by the ETC can be used by Complex V, F_1F_0 ATPase to produce

ATP. The F0 domain is a membrane component of the complex V and the F_1 domain is a matrix component [36]. The F_0 region rotates counter-clockwise direction during the passage of a proton into the matrix of the mitochondria. The ADP-bound F_1 domain then uses the proton motive force to generate ATP with close to 100% efficiency [36] (Figure 1.6).

Another important metabolic role occurring in the mitochondria is β-oxidation. β-oxidation defines a process in which fatty acids are oxidized to produce energy. This phenomenon occurs mainly in heart and skeletal muscles. The fatty acids present in the cytosol are transported into the mitochodnria via carnitine palmitoyl transferase (CPT) and the acylcarnitine carnitine translocase (ACT). The CPT I is responsible for converting CoA into carnitine, then the carnitine acetyltransferase mediates transmembrane exchange of fatty acyl-carnitine for carnitine and the ACT catalyzes transfer of carnitine back to CoA form. Once in the mitochondria, β-oxidation is initiated by activating the fatty acid by forming CoA esters with ATP dependent acyl-CoA synthase. The short-chain and medium-chain acyl-CoA synthetases are both found in the matrix of the mitochondria. The long-chain acyl-CoA synthetases are found in the outer membrane, extending its CoA-binding domain into the cytosol. The activated fatty acids are metabolized first by acyl-CoA dehydrogenase, producing 2-enoyl-CoA and reducing FAD in the process. Then, the 2-enoyl-CoA hydratase catalyzes the hydration reaction to produce 3-hydroxyacyl-CoA. The next step involves dehydrogenation performed by 3-hydroxyacyl-CoA dehydrogenase yielding 3-oxalyl-CoA and NADH. Thiolytic cleavage serves as a last step to produce acetyl-CoA, which can be used by the TCA cycle, and shortened fatty acid intermediate, which can again undergo additional β-oxidation [37] (Figure 1.6).

Mitochondria are also an initial activation site of gluconeogenesis. Upon the activation signal caused by decreased glucose level, pyruvate is carboxylated by PC to produce oxaloacetate. Oxaloacetate is then transported out of the mitochondria by a malate-aspartate shuttle. Oxaloacetate is first converted into malate by MDH, and malate is converted back into oxaloacetate in the cytoplasm. Once the oxaloacetate arrives, gluconeogenesis can continue as PEPCK can convert oxaloacetate into PEP.

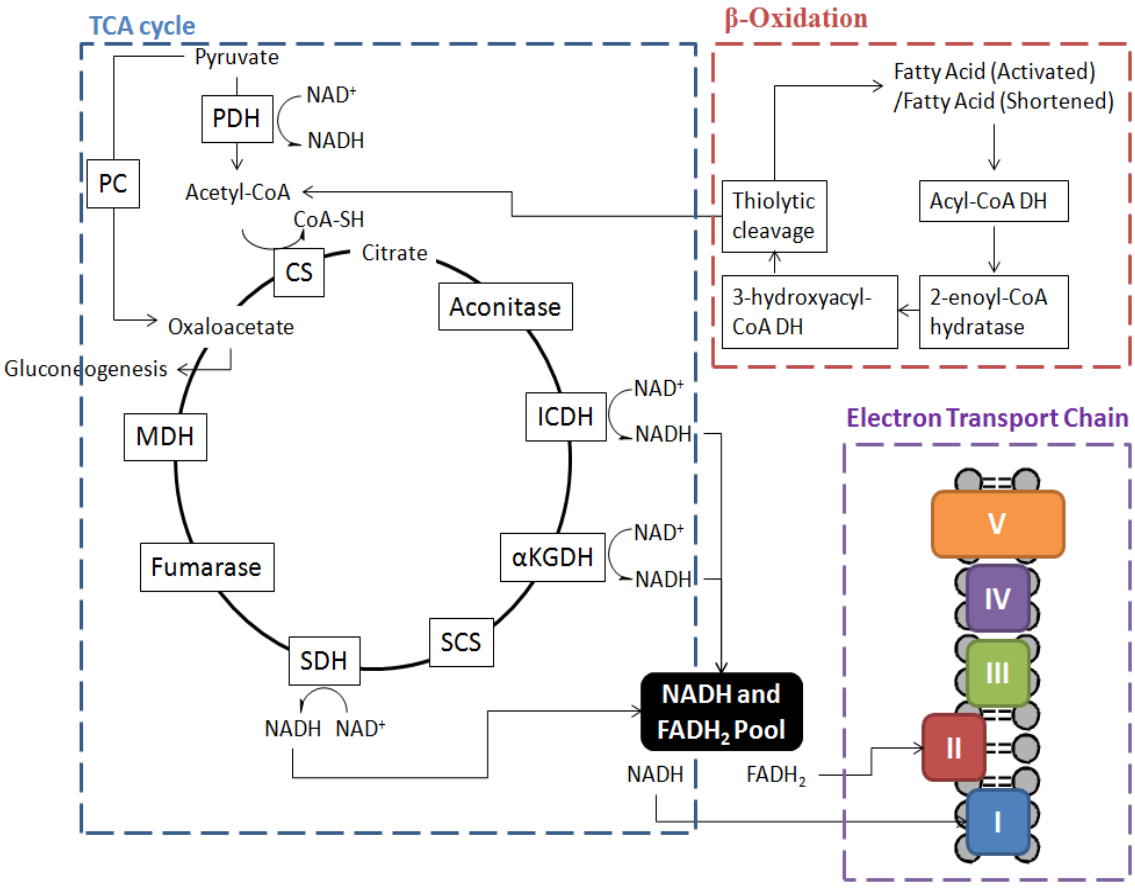

Figure 1. 6. Mitochondrial metabolic pathways.

Once pyruvate enters into mitochondria and is converted into acetyl-CoA, the TCA cycle is initiated for oxidative metabolism. The NADH generated from the TCA cycle can enter the electron transport chain to produce ATP. The β-oxidation is another major mitochondrial metabolism. The pathway is responsible for breaking down fatty acid into acetyl-CoA units, which can be funnelled into TCA cycle. The first step of

gluconeogenesis occurs in the mitochondria as malate dehydrogenase transports oxaloacetate out to the cytoplasm.

1.1.3.2.2 Other roles of mitochondria

Mitochondria have been considered to play a critical role in the life of a eukaryotic organism as it provides energy-yielding reactions to support all necessary cellular functions. The importance of mitochondrial metabolism is indeed evident from studies indicating the fatality resulting from interruption of this particular function of mitochondria. Recent studies, however, have begun to unravel various other roles of mitochondria. In particular, participation of mitochondria in signaling pathways gained substantial interests. Apoptosis, a programmed cell death, is one of the better understood models of mitochondria related signaling pathway. The effect of cytochrome c and apoptosis-inducing factor (AIF) release from mitochondria are prime examples demonstrating the participation of mitochondria during apoptosis. Release of cytochrome c is shown to initiate caspase activation. Once released to the cytosol, cytochrome c binds to Apaf-1, a cytosolic protein containing a caspase-recruitment domain (CARD). This causes a structural alteration that leads to oligomerization of the APAF-1 to form the apoptosome. The CARD domain of Apaf-1 is exposed to the cytosolic side and the multiple procaspase-9 are recruited and autoactivated. The AIF, a flavoprotein that resides in the mitochondrial intermembrane space, is released upon induction of apoptosis. The AIF is known to be translocated to the nucleus and causes chromatin condensation and large-scale DNA fragmentation [38] (Figure 1.7).

Calcium accumulation has long been established as a function of mitochondria. The functional significance, however, was unclear until recently. Mitochondrial calcium uptake serves several roles: it regulates membrane potential, acts as a spatial calcium ion

buffer by regulating the local calcium concentration and participates in apoptosis [39] (Figure 1.7).

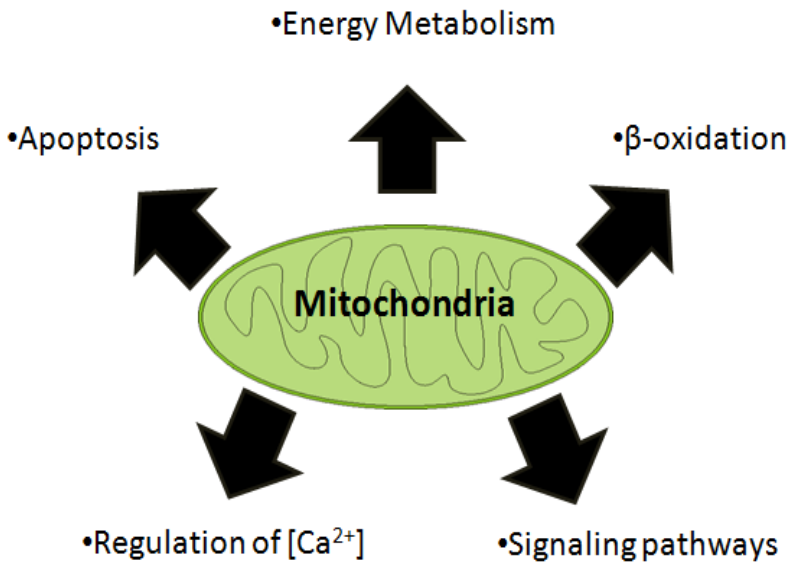

Figure 1. 7. Multiple cellular functions of mitochondria

Mitochondria serve multiple roles in the cell. Most well-known roles consist of energy metabolism and β-oxidation. However, studies reveal mitochondria also participate in apoptosis, signaling pathways and regulate intracellular calcium concentration.

1.1.3.3 Additional compartmentalized organelles

The peroxisome serves multiple roles in eukaryotic systems. As the name suggests, this organelle contains enzymes that use molecular oxygen to remove hydrogen from specific organic substrates in order to produce hydrogen peroxide [40]. Hydrogen peroxide produced from the reaction is used by an enzyme called catalase to oxidize other substrates. In liver and kidney cells, this type of oxidative reaction serves an important role as it provides a mechanism of detoxification of various toxic molecules entering the bloodstream. A major function of the oxidative reaction in peroxisomes involves the catabolism of fatty acid molecules, much like the mitochondrial β-oxidation process. The

peroxisome, however, is responsible for the breakdown of very long chain fatty acyl-CoAs (VLCFAs) and branched chain fatty acyl-CoAs as the mitochodnria lacks VLCFA synthases. The peroxisomal β-oxidation does not come to completion in the peroxisome, instead the shortened acyl-CoAs are exposed to the mitochondria for complete catabolism into acetyl-CoAs [41] (Figure 1.8).

The endoplasmic reticulum (ER) is another cellular compartment that contributes to the overall metabolism of the cell and helps to maintain cellular and organismic metabolic homeostasis. ER, particularly smooth ER, serves as an intermediary and complex lipid metabolic center. Among the lipids, ER plays a pivotal role in controlling the cholesterol levels. This organelle is also shown to participate in de novo synthesis of triglycerols, cholesterol and phospholipids [42] (Figure 1.8).

The compartmentalization of cellular metabolism is undoubtedly beneficial in terms of increasing and maintaining the efficiency of the system. However, this compartmentation does not strictly refer to complete isolation of each metabolic network within the organelle. It is evident that the enzymes that have specific roles in one pathway frequently have similar or varying roles in other pathways, and even in different compartments. Some of the metabolites also provide a connection between the compartments as enzymes often respond to each other via the availability of substrates or products and co-factors. Thus, the interplay between enzymes and metabolites play important roles in modulating cellular activities (Figure 1.8).

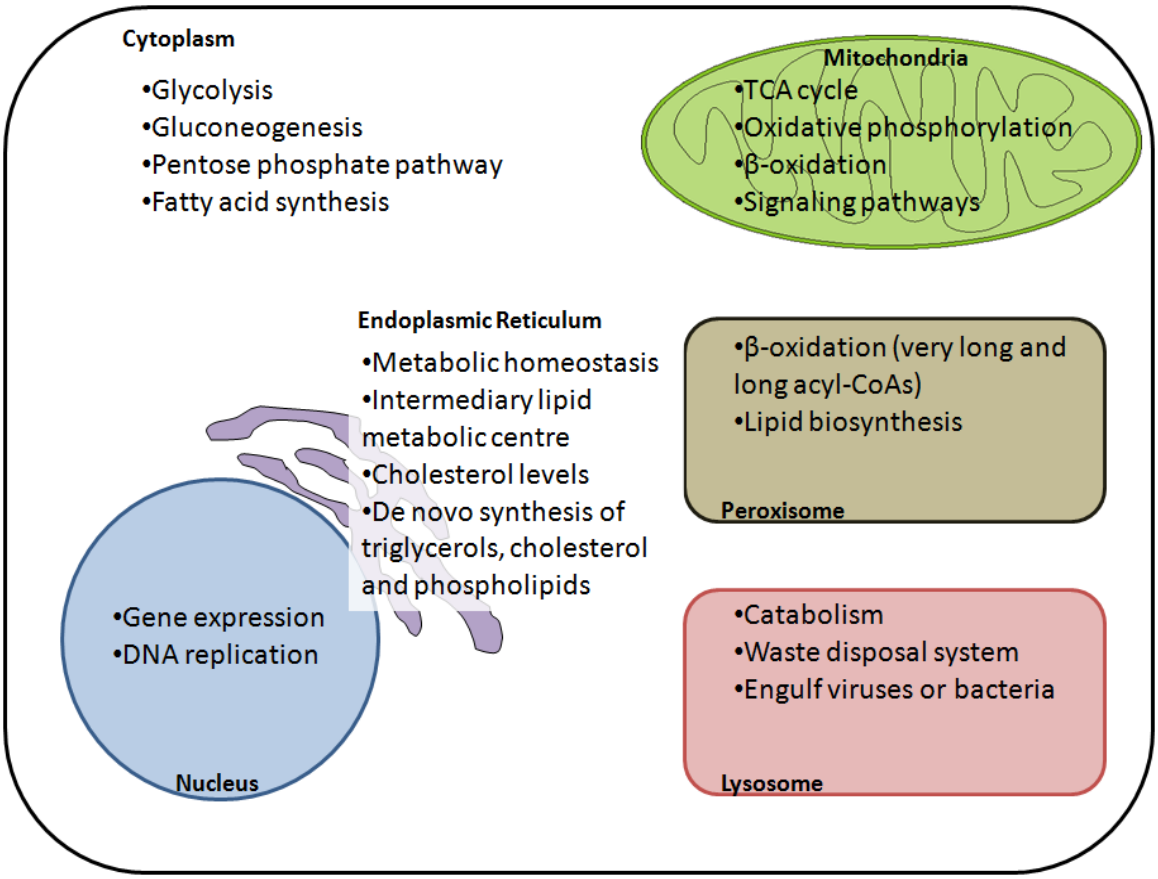

Figure 1. 8. Metabolic compartmentalization

Metabolism is compartmentalized into various sections. Nucleus, cytoplasm, mitochondria, peroxisome, lysosome and endoplasmic reticulum are some of the important metabolism regulating organelles of the cell.

1.1.4 Nuclear metabolism

Recent discoveries indicating the participation of metabolic enzymes and metabolic cofactors in transcriptional regulation demonstrate the presence of metabolic compartments within the nucleus itself. The role of metabolism or metabolic enzymes in the nucleus, however, still remains elusive to date. Several enzymes have already been identified to reside in the nucleus and partake in the process of transcriptional regulation. These enzymes include DNA methyl transferase (DNMTs), ATP-citrate lyase (ACL) and

acetyl-CoA synthase (ACS), phosphoglycerate kinase (PGK), glyceraldehydes-3-phosphate dehydrogenase (G3PDH) and lactate dehydrogenase (LDH).

1.1.4.1 Nuclear enzymes and epigenetics

Nuclear enzymes are commonly associated with DNA replication and transcription. Helicase, ligase, DNA and RNA polymerase are some of the nuclear enzymes that participate in this extremely crucial function of the cell. The metabolic enzymes, however, found in the nucleus are closely linked to epigenetic regulations. Epigenetics is a relatively new branch of genetics, related to changes in gene expression that are not dependent on a change in the nucleotide sequence [43]. The understanding of epigenetics requires an understanding of chromatin structure. Chromatins are organized in repeating structure of nucleosomes, which contain double stranded DNA wrapped around an octamer of histones. The histone octamers generally contain two copies of each core histones H2A, H2B, H3 and H4, structured in form of H3-H4 tetramer and two H2A-H2B dimers. Within the nucleosome, the negatively charged backbone of DNA and the hypoacetylated positively charged histones are tightly bound by electrostatic interactions (Figure 1.9).

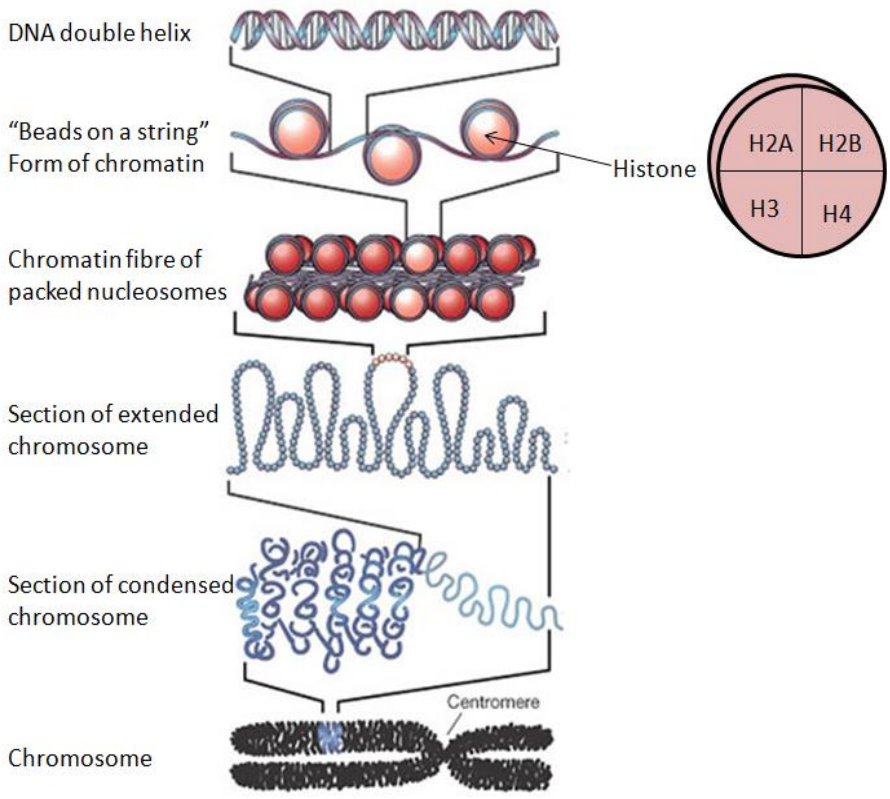

Figure 1. 9. Condensation of DNA and the overall structure of histone proteins.

The positive charge on the histone molecule is attracted to the negatively charged phosphate backbone of the DNA. This allows electrostatic interactions between DNA and histones. The DNA wraps around the histones forming "beads on a string" form of chromatin. DNA is further condensed and eventually becomes chromosomes. The histones are octameric proteins, consisting of two of each H2A, H2B, H3 and H4. Illustration is modified from [44].

Epigenetic modification involves alteration in the electrostatic nature of the chromatin or the affinity of chromatin-binding proteins. In particular, histones are subjected to several covalent modifications including methylation, acetylation, phosphorylation, ubiquitylation, sumoylation, succinylation and malonylation [45]. Among the list, histone acetylation and methylation are the most studied and best understood types of epigenetic modification. Histone methylation controls gene expression by covalently adding the methyl groups to the amino acids, most commonly to

the lysine resides. The binding of methyl groups can activate transcription by providing binding surface for the chromatin modifying enzymes such as histone acetyltransferases, histone deacetylases, methylases and ATP-chromatin remodeling enzymes. The silencing of gene expression via methylation occurs as lysine methylation blocks binding of proteins that interact with unmethylated histones or inhibiting modification of neighbouring residues.

Histone acetylation exerts its effect on the transcriptional regulation by altering the charges on the histone lysine residues. Acetylations on the proteins are executed by histone acetyltransferase (HATs). HATs are found in both the cytoplasm and nucleus of the cell. Cytoplasmic HATs acetylate histones prior to nuclear localization, while the nuclear HATs acetylate histones to activate or silence gene expression. The position of acetylation is located on the N-terminal lysine ε-amino groups and HATs utilize acetyl-CoA as a substrate to attach the acetyl group on these sites. All histones, H2A, H2B, H3 and H4, are shown to be capable of undergoing acetylation. However, modification of H3 and H4 are much more extensively characterized than H2A and H2B [46]. Some of the important sites of acetylation are located at H3 Lys 9 and 14 and H4 Lys 5, 8, 12 and 16 residues [47]. Once acetyl groups are attached to the lysine residues, the positive charges on the histones are removed. Elimination of positive charges decreases the interaction between histones and negatively charged phosphate groups of DNA. This process allows chromatin structures to adapt more relaxed structures, which is a requirement for greater gene transcription activity. Deacetylation of histones can be achieved by histone deacetylases (HDACs). HDACs restore the positive charges on histones by removing the acetyl group and ultimately allowing gene silencing by reinstating the interaction between histones and DNA (Figure 1.10). There are two protein families that can perform histone

deacetylation: SIRT2 family of NAD^+-dependent HDACs and the classical HDAC family [48]. Members of the classical HDAC family are divided further into class I and class II. Class I HDACs are found to be expressed in the majority of cell types, however, the class II HDACs involvements are suggested to be limited to differentiation and developmental processes [48]. As the roles of sirtuins are an important aspect of this study, it will be elaborated in detail.

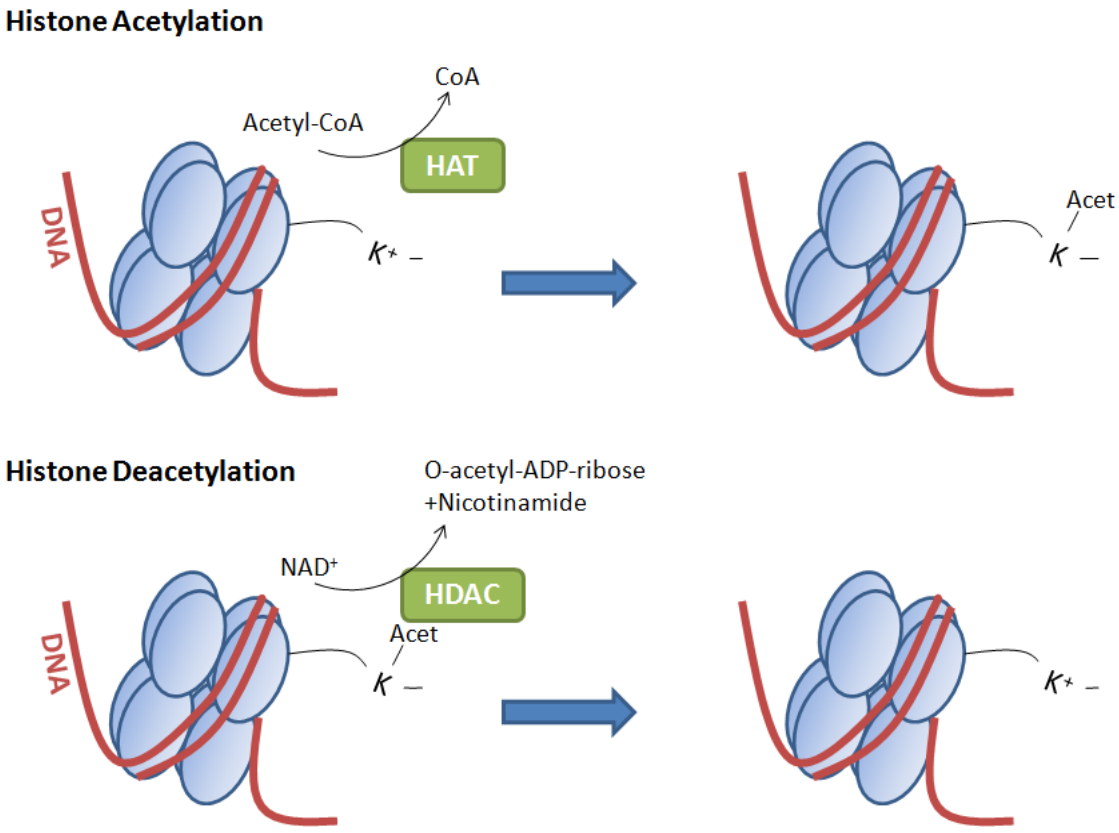

Figure 1. 10. Mechanism of histone acetylation.

Histone acetylation is one of the primary epigenetic modifications that modulate gene expression. Histone acetylation and deacetylation both occur on lysine residues of histones. HATs are known to be responsible for performing histone acetylation by using a acetyl-CoA. This causes the lysine residues to lose the positive charge, in turn neutralizing the electrostatic interaction between the DNA and the histone. This allows DNA to dissociate and permit transcriptional machinery to access the genes. Deacetylation of histone is executed by HDACs. Using NAD^+ as substrates, HDACs

allow the lysine residues regain the positive charge and reforming DNA-histone interactions. The acetylation typically promotes increase in gene expressions and the deacetylation causes the silencing of the genes.

1.1.4.2 Sirtuins

Sirtuins are NAD^+-dependent deacetylases, also called class III HDAC family. This recently discovered HDAC family is highly conserved from bacteria to human. In mammals, there are seven sirtuins, all containing a conserved NAD^+-binding and catalytic site, making them the only HDAC family that requires the presence of NAD^+ for their enzymatic activity [49] (Figure 1.11). The localization of sirtuins varies; SIRT1,2,6 and 7 in the nucleus, SIRT1 and 2 in the cytoplasm and SIRT3,4 and 5 in the mitochondria. The abundance of sirtuins speaks to its versatility. Sirtuins not only are able to acetylate histone but they can also acetylate non-histone protein substrates. The function of different Sirtuins also vary: SIRT1 and SIRT5 act as deacetylases, SIRT4 acts as a mono-ADP-ribosyl transferase, SIRT2, 3 and 6 can perform both deacetylase and mono-ADP-ribosyl transferase activity and the function of last sirtuin, SIRT7, has not been fully delineated to date [50]. Although the mechanism of action remains not fully understood, sirtuin-driven deacetylation generally consists of two steps. First, sirtuins cleave NAD^+ and produce nicotinamide (NAM) and in the second step the acetyl group is transferred from the lysine residue to the ADP-ribose moiety of NAD^+ to generate O-acetyl-ADP ribose.

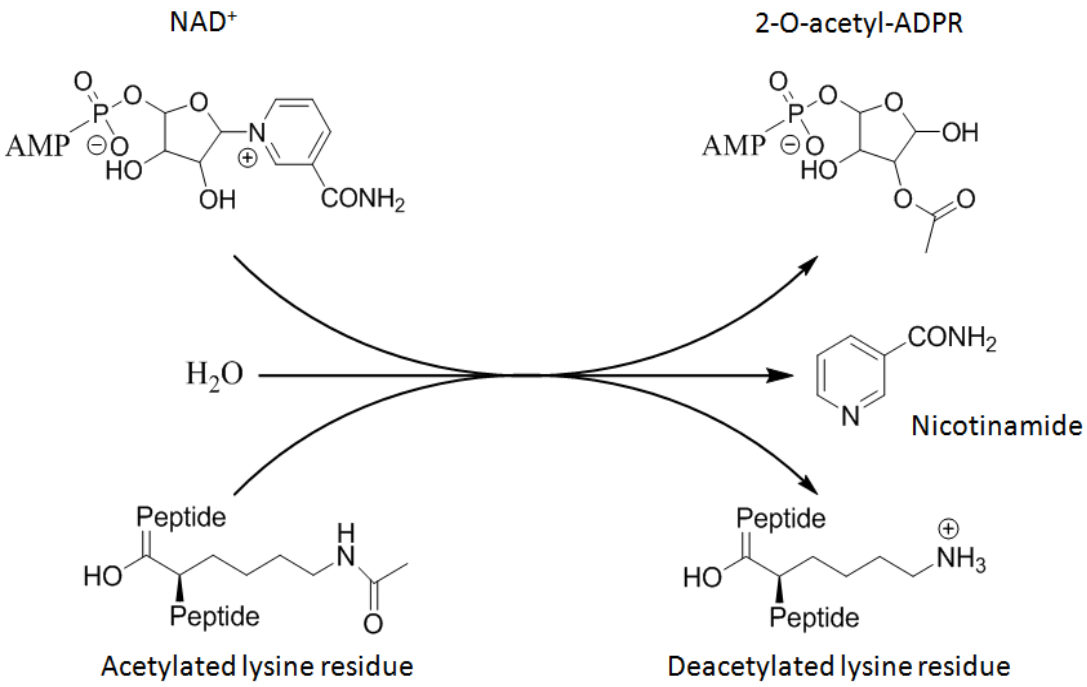

Figure 1. 11. Mechanism of sirtuin NAD^+-dependent histone deacetylation.

Sirtuin utilizes NAD^+ to perform deacetylation of lysine residues on proteins. The nicotinamide group from NAD^+ is replaced with acetyl group and the lysine residues deacetylated [49].

SIRT1 is the best characterized among the family member and although it resides in the nucleus it can be transported to the cytosol. SIRT1 activity is generally linked to the metabolic status of the cell. For instance, an increase in SIRT1 activity was displayed under energy and nutrient stress [50]. In the nucleus, SIRT1 deacetylation targets are key metabolic regulators, enhancing the suggestion that SIRT1 participates in metabolic transcriptional regulation. Some of the SIRT1 metabolic targets include p53 (mitochondrial activation), FOXOs (lipid metabolism and stress resistance), PGC-1α (mitochondrial biogenesis and lipid metabolism), PPARγ (adipocyte differentiation, lipid synthesis and lipid storage), LXRs (lipid anabolism and cholesterol regulation) and CREB

(gluconeogenesis) [50]. However, SIRT1 is also capable of exerting its effect on inflammatory response, cell proliferation, apoptosis and cancer [49].

SIRT2 is predominantly found in cytosol. It can, however, be transported into the nucleus in a cell cycle-dependent manner. SIRT2 migrates to the nuclei during the G2/M phase of the cell cycle, deacetylating histone H4 Lys16. This process modulates chromatin condensation during metaphase [51]. In addition, SIRT2 expression levels vary depending on the cell cycle phase and are commonly increased during mitosis. SIRT2 is also found to be responsible in deacetylation of α-tubulin, a major component of microtubules [52]. Thus, these observations implicate SIRT2 to be an important regulator of the cell cycle.

SIRT3 is preferentially localized in the mitochondria and accountable for targeting enzymes involved in energy metabolism process, including the ETC, TCA cycle, β-oxidation and ketogenesis [53]. Through modulating the metabolic enzymes in mitochondria, SIRT3 controls the flow of the oxidative pathways and regulates the rate of ROS production. Mitochondrial enzymes such as ACS, isocitrate dehydrogenase-2 and glutamate dehydrogenase has been identified to be a target of deacetylation by SIRT3 [54,55,56,57]. SIRT3 also plays a role in other metabolic processes such as acetate metabolism and brown adipose tissue thermogenesis [58]. In addition, genetic evidence and several mutation studies demonstrate the participation of SIRT3 in longevity [59].

SIRT4 is suggested to be a mitochondrial protein as SIRT4-GFP localized specifically to the mitochondria [60]. Although the SIRT4 consists of the NAD^+-binding sirtuin domain, it does not perform deacetylase activity [61].The mono-ADP-ribosytransferase activity is seldom found in all sirtuin family members and SIRT4 transfers ADP-ribosyl group from NAD^+ to histones. This PTM involves N- or S-

glycosidic linkage between an amino acid arginine or cysteine and ADP-ribose derived from NAD^+. The enzyme glutamate dehydrogenase (GDH) was the first mitochondrial protein to be discovered as being inactivated through SIRT4 mono-ADP-ribosylation [61]. SIRT4 has been linked to insulin secretion in pancreatic β cells. By inactivating GDH in the β cell mitochondria, SIRT4 limits the conversion of glutamine and glutamate into α-ketoglutarate [61]. Subsequently, this limits the production of ATP and hinders the amino acid-stimulated insulin secretion pathway.

SIRT5 is another mitochondrial residing protein. SIRT5, however, is localized in the matrix of the mitochondria. It was first discovered to deacetylate cytochrome c in the intermembrane space of mitochondria [56]. However, it is still unclear with regards to the mechanism of translocation of SIRT5 into the mitochondrial matrix. The confirmed substrate of SIRT5 thus far includes carbamoyl phosphate synthetase-1 (CPS1), the rate-limiting enzyme in the urea cycle [62]. The deacetylation activates CPS1 and it leads to overall up-regulation of ammonia detoxification. It has been shown experimentally that SIRT5 knock-out mice have elevated ammonia levels during starvation or on a high-protein diet [63].

SIRT6 is localized in the nucleus and is responsible in deacetylation of histone H3 Lys 9 and H3 Lys56. SIRT6 is specific in its substrate, as it displays low deacetylation for any other histones. In particular, H3 Lys56 deactylation has been associated with genomic stability and DNA damage sensitivity in eukaryotes [64]. The roles of SIRT6 have been suggested to be related to regulating telomeric chromatin, gene expression and the chromatin association of DNA repair factors. The deacetylation sites of SIRT6 are likely providing a change in chromatin structure at DNA double strand break locations for efficient association of repair proteins. The deacetylation at this site has also been linked

to transcriptional repression of nuclear factor-kappa B (NF-κB), a transcription factor in regulating aging, proliferation and inflammation gene expressions [65]. In addition, SIRT6 has been linked to metabolism by associating with HIF-1α.

SIRT7 is one of the least understood proteins of all other sirtuins. SIRT7 is proposed to be localized mainly in the nucleolus, where it participates in the regulation of ribosomal RNA (rRNA) transcription by controlling the activation of RNA polymerase I [65]. This activity of SIRT7 is particularly relevant in reactivation of rDNA transcription at the end of mitosis. The exact mechanism of how this protein operates, however, is still unknown. A recent study recognized a crucial role for SIRT7 in phenotype and transformation of cancer cells. It was found that SIRT7 specifically targets H3 Lys18 for deacetylation. This site is mainly found around the transcription start site of nuclear hormone receptors and hypoacetylation of H3 Lys18 site and it has been associated as a marker for malignancy in various human cancers [66].

The uniqueness of the sirtuin family arises from the fact that the activity of these proteins are directly related to the NAD^+:NADH ratio in the cell. The level of NAD^+ in the nucleus has been implicated to be the primary effector of the sirtuin-mediated silencing [67,68]. Thus, the biosynthetic and breakdown products of the NAD^+ in the cells play a crucial role regulating the activity of sirtuins. There are two main routes of NAD^+ biosynthesis in mammals: a *de novo* kynurenine pathway and a salvage pathway [69,70]. The kynurenine pathway involves degradation of tryptophan into NAD^+, while the salvage pathway utilizes nicotinic acid, nicotinamide and nicotinamide riboside. NAD^+:NADH ratio within the cells can also be modulated and influenced by the metabolic network itself. Thus, sirtuins are suggested to be directly linked to the cellular metabolic states and participate in orchestrating complex cellular processes such as

energy metabolism. Aforementioned, metabolic enzymes are often regulated by means of post-translational modification. Thus, many enzymatic activities in glycolysis, gluconeogenesis, TCA cycle, fatty acid metabolism and glycogen metabolism are modulated by acetylation. Sirtuin family members have been suggested to participate in an adjustment between storage and utilization of energy by direct deacetylation of metabolic enzymes. Deacetylation of the glycolytic, TCA cycle and fatty acid oxidation enzymes was linked to negative regulation. Gluconeogenesis enzymes, however, experienced positive regulation upon deacetylation (Figure 1.12).

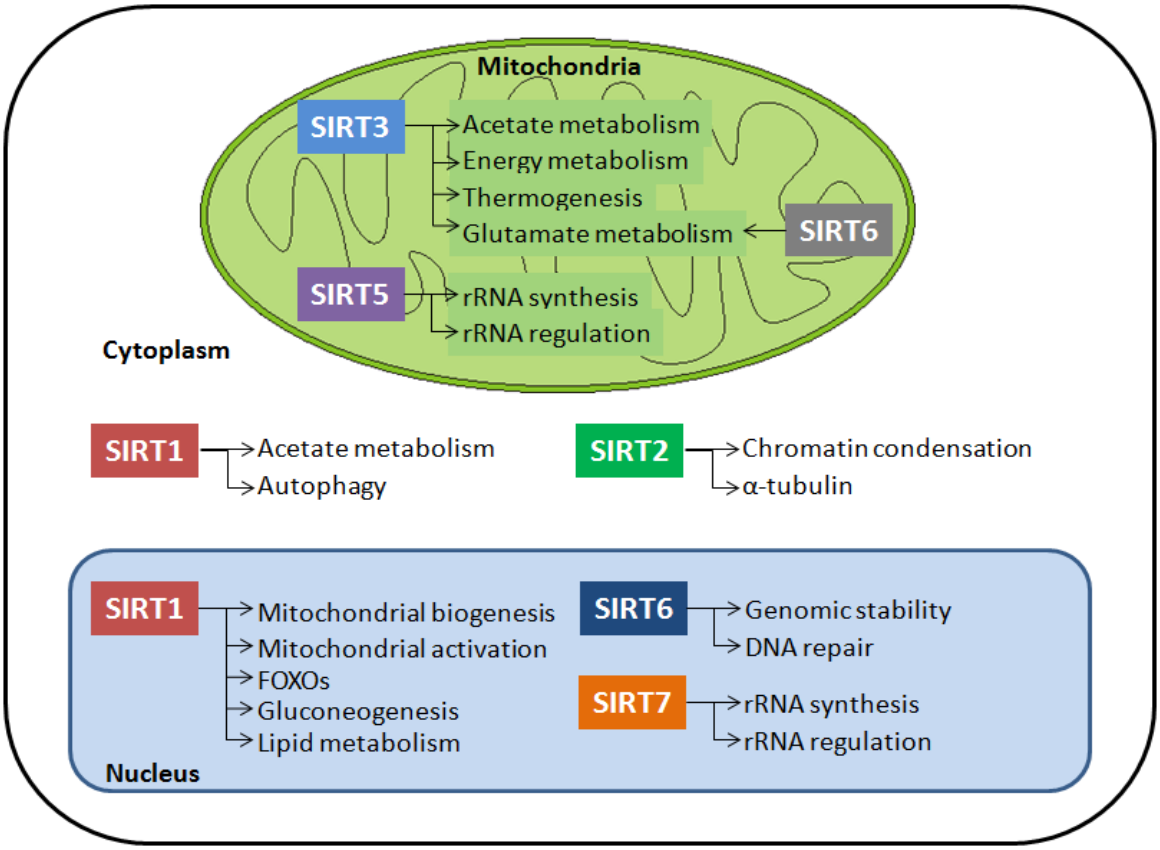

Figure 1. 12. Types and roles of Sirtuins.

Sirtuins are found throughout cellular compartments. There are a total of seven identified sirtuin family members that possess either deacetylase activity (SIRT 1, 2, 3, 5, 6) or mono ADP ribosyl transferase activity (SIRT 2, 3, 4,6). However, the activities of these

proteins are not limited to one or the other. The sirtuins are localized in the nucleus (SIRT 1,6,7), mitochondria (SIRT 3, 5, 6) and cytosol (SIRT 1, 2). As all the sirtuins use NAD^+ as a substrate, the level of NAD^+, which defines the cellular metabolic status, is responsible regulating sirtuin activity [71].

1.1.4.3 Metabolic cofactors

Any enzymes, especially metabolic enzymes, require the presence of necessary metabolites to execute biochemical reactions. This is no exception for enzymes found in the nucleus. These metabolites include NAD^+, AMP, acetyl-CoA, succinyl-CoA, malonyl-CoA, pyruvate and many more [72] (Figure 1.13). These metabolites help to regulate cellular events in the nucleus through epigenetics. Recent studies have begun to recognize the importance of the roles of nuclear enzymes in regulating the concentration of key epigenetic substrates. Enzymes such as sirtuin and HATs are some of the well-known proteins that require the common metabolites such as NAD^+ and acetyl-CoA, respectively. It is especially important to recognize that these enzymes are responsive to metabolic cues as they require metabolites generated or utilized by the metabolic enzymes. For histone acetylation, HATs have already been demonstrated to be associated with ACS, an enzyme which is responsible for generating acetyl-CoA from acetate. In mammals, however, acetate metabolism is not considered to be a major bioenergetic substrate. Thus, glucose metabolism related ACL has been suggested to be the regulator of acetyl-CoA concentration in the nucleus for the activity of HATs [73].

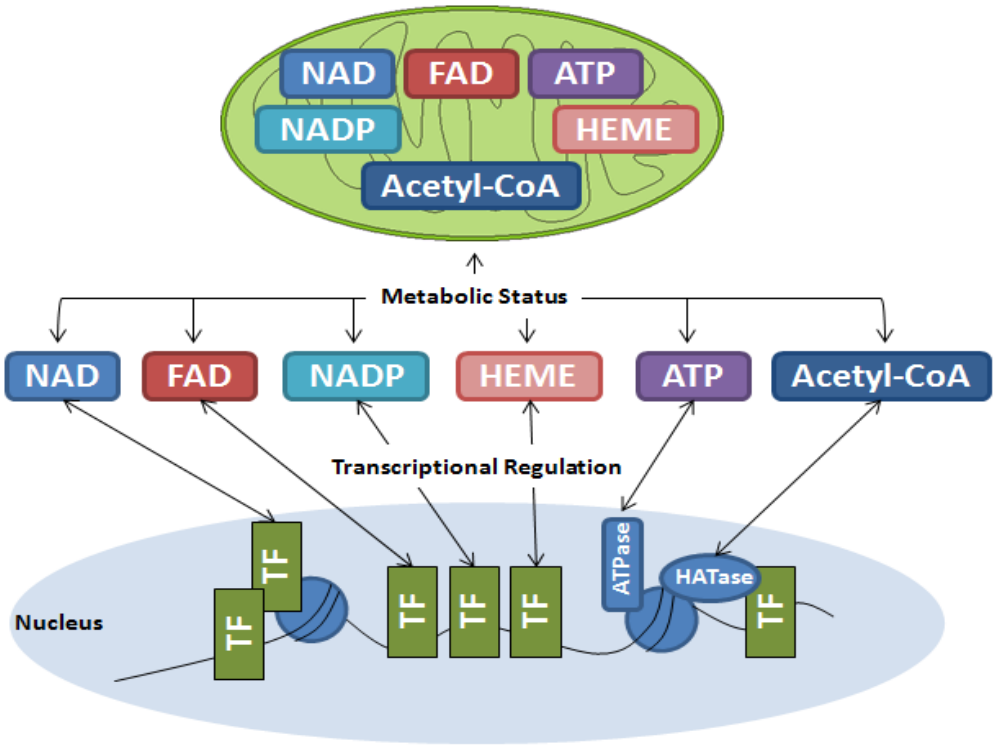

Figure 1. 13. Connection between cellular metabolism and gene transcription.

As the metabolic cofactors are common signatures of cellular metabolism, numerous metabolic cofactors are involved in modulating cellular metabolism via the regulation of transcription. The cofactors found in mitochondria and cytosol can enter the nucleus and induce changes in gene transcription level [72].

1.1.4.4 ATP-citrate lyase

The nuclear localization of an enzyme ACL has been illustrated recently [73]. This study bridged the gap between the epigenetic and metabolic enzymes by demonstrating that ACL is responsible for providing acetyl-CoA for HATs and affecting the expression of glycolytic enzymes through epigenetic modification. Silencing ACL expression in the cell significantly reduced the level of histone acetylation as HATs do not have acetyl-CoA, a substrate necessary to acetylate histones. Interestingly, Glut4 expression, an insulin-responsive glucose transporter and three key glycolytic enzymes hexokinase 2, PFK-1 and lactate dehydrogenase A (LDH-A) were all shown to be

suppressed under ACL silencing. Recovery by acetate was able to rescue these activities. Thus, this study demonstrated that ACL plays a crucial role in regulating the level of histone acetylation and contributes to the selective regulation of genes involves in glucose metabolism. In addition, the link between histone acetylation in adipocyte differentiation and ACL has been clarified. Adipocyte differentiation has been demonstrated to involve increased histone acetylation. Silencing ACL expression during the differentiation indeed caused the amount of histone acetylation to be significantly reduced, along with the inability of adipocytes to accumulate lipids (Figure 1.14). This research demonstrated how cellular metabolites can directly influence the metabolic compartments. The more citrate is available, ACL will up-regulate the glucose metabolizing enzymes via histone acetylation to generate more citrate. In turn, this produces a positive feedback loop to reinforce the expression of more glucose metabolizing enzymes via ACL-directed histone acetylation. Lower glucose conditions will produce opposite effects as citrate levels will also be diminished.

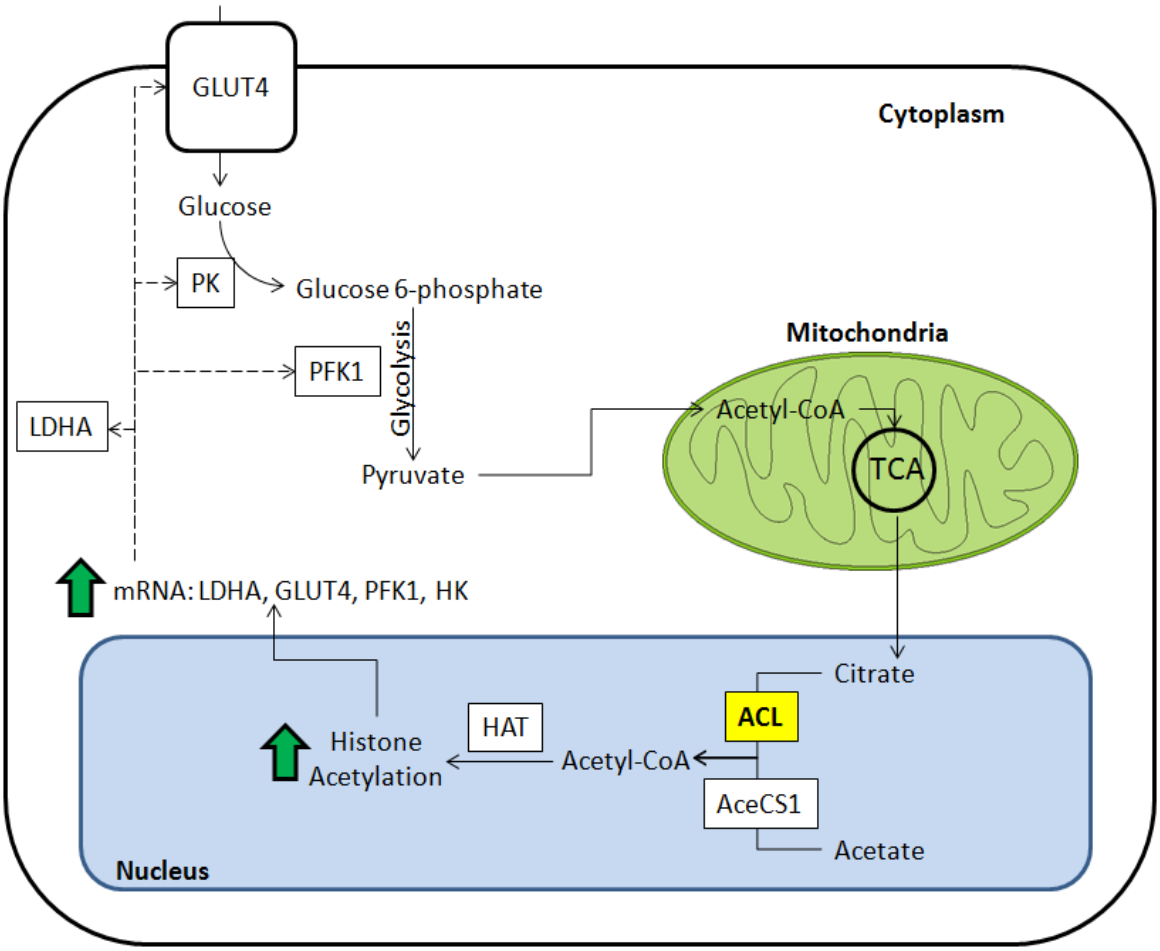

Figure 1. 14. ACL induced histone deacetylation modulates central metabolism.

Nuclear ATP-citrate lyase (nACL) was found to be responsible in creating acetate from citrate. The citrate level of the cell is shown to regulate the activity of nACL and directly influencing the activities of HATs, which regulate histone acetylation. The increase in histone acetylation caused by an increase in ACL activity induces increased expression of GLUT4, PK, PFK1 and LDHA, thus linking central metabolism to gene expression.

1.1.4.5 Lactate dehydrogenase

LDH is an enzyme that is responsible for the interconversion of pyruvate and lactate. There are five isoenzymes of LDH currently known: LDH-1, LDH-2, LDH-3, LDH-4 and LDH-5. Each isoenzyme is tetramer, constructed of four polypeptide chains. The subunits are made of two parent chains called LDH A (also called muscle (M) subunit) and LDH B (also called heart (H) subunit). The combination of the two subunits

form different isoenzymes of LDH. The combinations include BBBB (LDH-1), ABBB (LDH-2), AABB (LDH-3), AAAB (LDH-4) and AAAA (LDH-5) [74]. If more A subunits present, the enzyme will favour the formation of lactate from pyruvate, along with the oxidation of NADH. The A subunits are commonly found to complex with NADH, thus facilitating reaction that oxidizes NADH. On the contrary, if more B subunits arevpresent, the enzyme will favour the transformation of lactate into pyruvate, along with the reduction of NAD^+. The B subunit of LDH complexes with NAD^+, thus this complex further promotes the conversion of NAD^+ to NADH and lactate to pyruvate [75]. Interestingly, LDH-1 is maximally activated under low pyruvate concentration and inhibited by excessive presence of pyruvate but LDH-5 is resistant to the pyruvate inhibition. LDH-1 is comprised solely of heart or B subunit and found predominantly in heart, where the pyruvate levels do not or should not develop in high abundance as pyruvate would readily be oxidized by the mitochondria. Inhibition of LDH-1 by pyruvate is logical in attempt to favor oxidative metabolic pathway. Alternatively, LDH-5 is constructed with only A subunits and found primarily in skeletal muscle. Skeletal muscles rely on anaerobic glycolysis for the energy supply. Thus, it would be advantageous for skeletal muscle LDH to resist high pyruvate levels and be permitted to convert pyruvate into lactate.

All isoforms of LDH are found in the cell, but their concentration varies from tissue to tissue. In cytosol, LDH serves to complete the last step of lactic acid fermentation. The reaction involves reduction of pyruvate to lactic acid and providing NAD^+. The purpose of this reaction is to replenish the NAD^+ level for further glycolytic pathways to produce energy. LDH has also been shown in the mitochondria. Mitochondrial LDH has been suggested to participate in tissue lactate clearance and

oxidation. As glycolysis inevitably produces cytosolic lactate, mitochondrial LDH helps to balance the lactate produced from cytoplasm. LDH in mitochondria was also shown to generate ATP, maintain lactate homeostasis and modulate redox potential in human astrocytic cells [76]. LDH is also found in the nucleus. Phosphorylation at tyrosine 238 site has been linked to the restriction of LDH in the nucleus in PC12 cells [77]. In particular, LDH-5 has been exclusively found in the nucleus and has been previously suggested to complex with single-stranded DNA to stimulate DNA polymerase α-primase activation [78]. In addition, LDH has been hypothesized to modulate reparative and replicative DNA synthesis. Because LDH can enter the nucleus and potentially bind cofactors, substrates and inhibitors, this particular enzyme could establish a regulatory linkage between the energy states of a cell and the DNA replicative and reparative functions [78]. More recently, LDH has been shown to play a role in cancer progression by modulating HIF-1α and HIF-2α expression under low oxygen and energy conditions [79]. However, a clear role of nuclear LDH still remains elusive to date.

Recent work from our laboratory discovered that nuclear LDH in HepG2 cells are found to be linked to histone acetylation via sirtuin and the production of NAD^+. The sirtuin and nuclear LDH has been demonstrated to be physically linked, suggesting formation of multi-protein complexes during ROS stress [80].

1.2 Stem cells

1.2.1 Stem cells overview

Stem cells are undifferentiated cells that have the ability to self-replicate and transform into any cell type in an organism. Thus, two key prerequisites of stem cells are: 1) self-renewing ability and 2) plasticity to differentiate into an array of specialized cell

types. This process of conversion of stem cells into a committed and more mature specialized cell is called “differentiation”. Depending on the source of the stem cells, the potential for differentiation and the number of cell types they can transform into also varies. There are three categories of stem cells: totipotent stem cells, pluripotent stem cells and multipotent stem cells.

Totipotent stem cells are capable of giving rise to any and all human cells. After fertilization, the egg is divided several times to form morula. These cells are considered to be totipotent and any individual cell from the morula could in theory give rise to a complete human. After several cell divisions, the totipotent cells begin to specialize and form the inner cell mass of the blastocysts [81]. The inner cell mass is the source of embryonic stem cells, which are pluripotent. Pluripotent stem cells are defined by a stem cell that has the potential to differentiate into the three germ layers including endoderm, ectoderm and mesoderm, which adds up to 200 different cell types that makes up the human body. These pluripotent cells can differentiate into multipotent stem cells. The stemness of a multipotent stem cell is limited compared to a pluripotent stem cell, as they become more of a specialized progenitor cell. Multipotent cells give rise to cells that have a particular function and are commonly recognize to be destined to produce specific types of cells or tissues [82] (Figure 1.15). For example, hematopoietic stem cells are destined to differentiate into blood cell type cells such as lymphocytes, monocytes, neutrophiles and platelets [83], but cannot become non-blood cell types. Hematopoietic stem cells are found in the bone marrow of adults and are often used in clinical settings for transplantation to regenerate blood-forming components [84]. These progenitor cells are commonly characterized as adult or somatic stem cells and are found throughout the organism post-development.

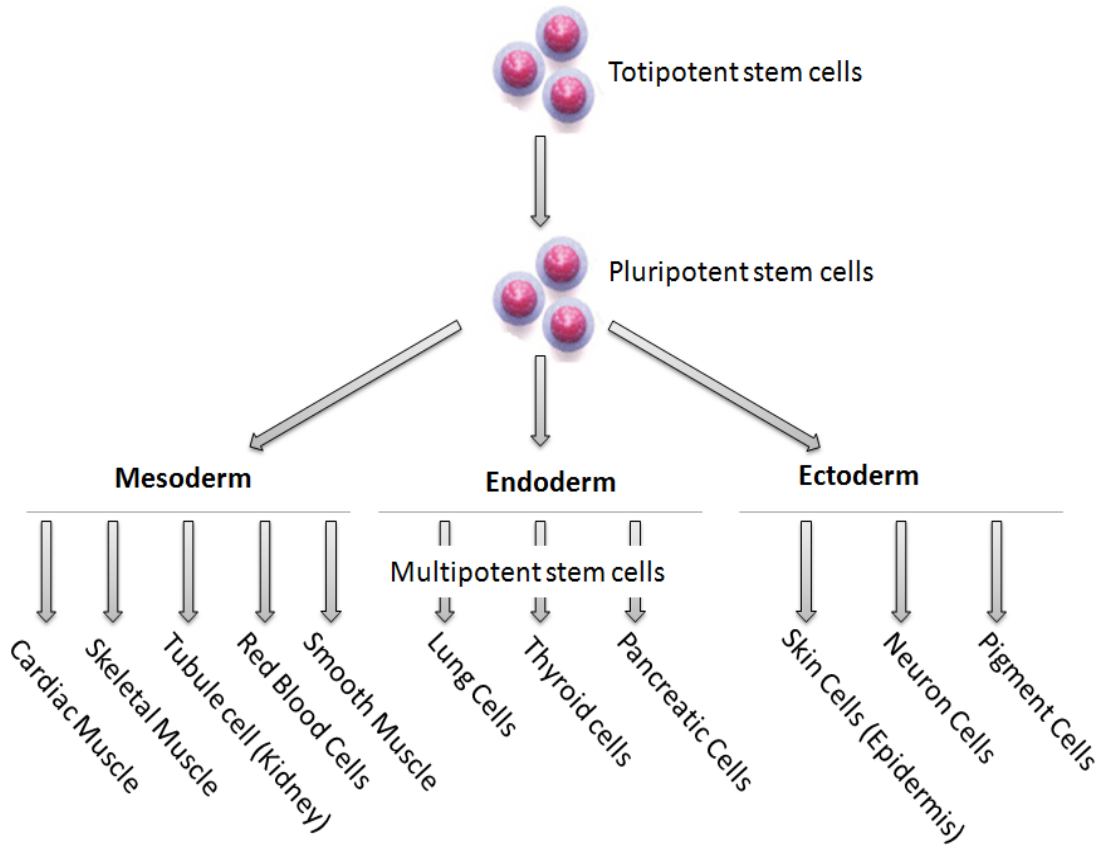

Figure 1. 15. Stem cell development and three germ layers.

There are three types of stem cells: totipotent, pluripotent and multipotent stem cells. Pluripotent stem cells have the potential to differentiate into three germ layers; mesoderm, endoderm and ectoderm. The three layers differentiate into multipotent progenitor cells and adult cells.

1.2.2 Development of the embryo and the three germ layer

To better understand the characteristics of stem cells and the process of differentiation, the development of the embryo should be discussed. Once fertilization occurs, the zygote starts to divide as it travels to the uterus . The duration of translocation is three to four days in mice and five to seven days in humans [81]. The zygote synchronously divides into 2 identical cells, 4, 8, 16 cells and so on. The 16-cell embryo

is defined as a morula. Compaction occurs and and the cells begin to divide into the trophectoderm, (outer rim of cells) and the inner cell mass. The inner cell mass continues to divide and differentiate and give rises to all embryonic tissues. By day 3 of embryonic development for mouse and day 5 to 6 for human, the embryo develops a cavity called the blastocoele. This cavitation allows a physical separation between the trophectoderm and the inner cell mass: the morula thusly becomes a blastocyst [85]. In day 4.5 in mice and day 8 to 9 in human, the blastocyst separates into the hypoblast and epiblast. The hypoblast give rise to the primitive endoderm and the epiblast, become the only pluripotent cells in the blastocyst (Figure 1.16). The epiblast further differentiates into the embryonic ectoderm and the primitive ectoderm.. The next major development occurs as the embryonic ectoderm becomes the three germ layers – endoderm, mesoderm and ectoderm. This phase of the embryonic development is termed gastrulation. The endoderm layer develops into the interior epithelial lining of the digestive and respiratory system. It also forms the lining of all glands which open into digestive tubes such as liver and pancreas. The mesoderm, or middle germ layer, gives rise to tissues and structures including bone, cartilage, muscle, connective tissue, blood, vascular, reproductive excretory and urinogenital systems. Lastly, the ectoderm differentiates into the nervous system, tooth enamel and the epidermis. It can also differentiate into the lining of the mouth, nostril, sweat glands, hair and nails.

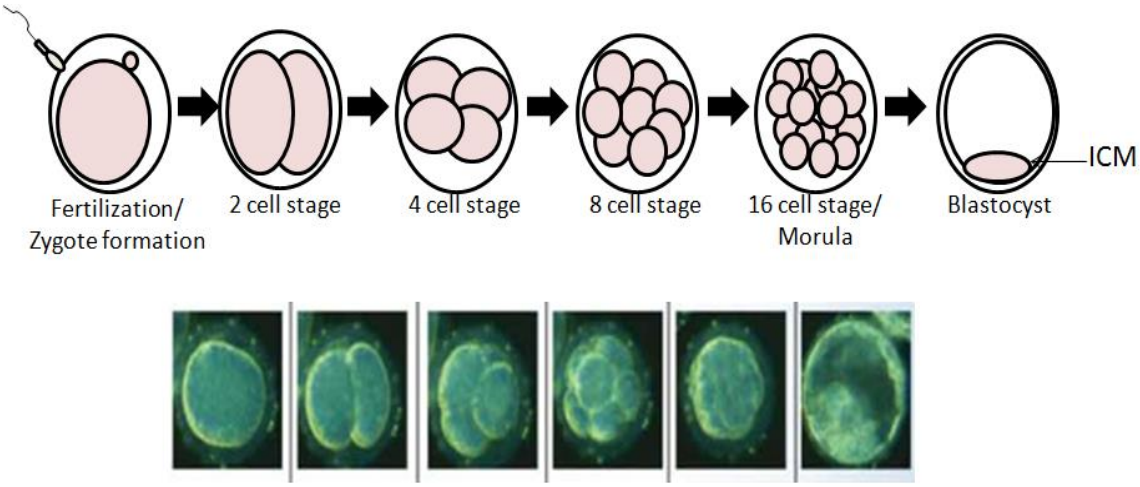

Figure 1. 16. Embryonic development

The zygote is formed when the sperm fertilizes the oocyote. The zygote then divides continuously through 2 cell, 4 cell, 8 cell and 16 cell stages (morula). Once past the morula stage, trophectoderm and inner cell mass (ICM) begin to develop. The embryonic stem cells are derived from the ICM [86].

1.2.3 Types of stem cells

There are many types of stem cells including early embryonic, blastocyst embryonic, fetal, adult, amniotic, cord blood and induced pluripotent stem cells. Adult, induced pluripotent and embryonic stem cells are, however, more commonly utilized in research. Adult or somatic stem cells are lineage-restricted cells and are found in tissues throughout the body. These types of stem cells are responsible for tissue homeostasis and regeneration [87]. Somatic stem cells are capable of an extended self-renewal period compared to other stem cells, as their continual self-replication is essential in maintaining tissue homeostasis. The microenvironment, or niche, which surround adult stem cells contain factors that are necessary for the long-term self-renewal of the cell [87]. The niche regulates cell to cell interaction between stem cells and neighbouring cells, controls oxygen availability, contains hormones, signaling molecules and metabolites to maintain the physiochemical status of the environment. Stem cells are localized in a small reservoir

and can replenish the tissues as needed when specific environmental cues occur. The hair follicle is one of the prime examples demonstrating the regulatory involvement of niches. During the degenerative phase of the hair cycle, receding follicles carry the dermal papilla, a specialized mesenchymal cell, from the base of the hair bulb up to the bulge. This alteration in the microenvironment stimulates progenitor cells to exit the niche and proliferate and differentiate [87] (Figure 1.17).

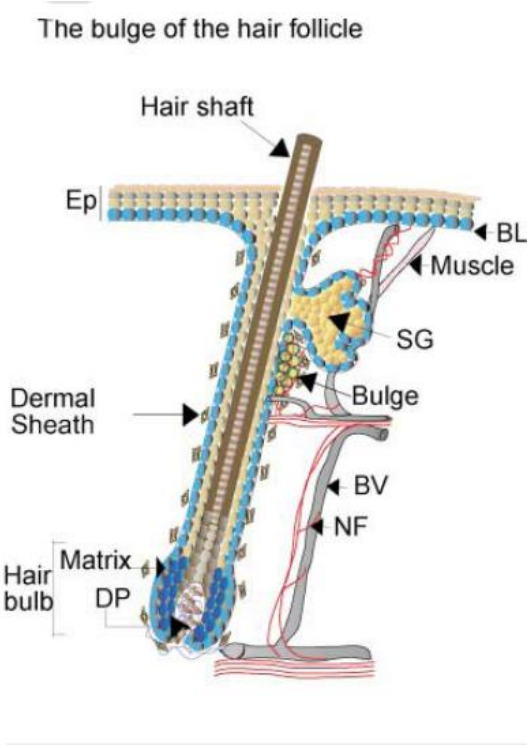

Figure 1. 17. Adult stem cells and their niche.

Hair follicles consist of multipotent stem cells found in the bulge. These adult stem cells give rise to transit-amplifying matrix cells, which differentiate into hair shaft and the channels that surrounds the shaft. The follicle is surrounded by a basement lamina which is surrounded in turn by a dermal sheath. The surrounding microenvironment of the follicle is shown to stimulate differentiation of these adult stem cells or allow the stem cells to maintain their stemness [87].

Induced pluripotent stem cells (iPSCs) are special stem cells that were first engineered by Takahashi and Yamanaka in 2006 [88]. This group was successful in reverting differentiated somatic cells back into the pluripotent state by transfecting the cells with four "stemness" transcription factors: SOX2, OCT4, KLF4 and c-MYC. Studies thus far suggest that iPSCs are similar to the natural embryonic stem cells in many aspects such as expression of stemness genes and proteins, embryoid body formation, teratoma formation and ability to differentiate, to name a few. However, the full extent of the relationship between iPSCs and natural pluripotent cells are still under investigation. The discovery of iPSCs is considered to be one of the major breakthroughs in stem cell research as these cells could potentially provide a mean of obtaining pluripotent cells without creating or destroying embryos [88]. In particular, iPSCs have been hypothesized to be a useful asset in clinical settings. As the undifferentiated stem cells are obtained from the host differentiated somatic cells, these stem cells are patient- and disease-specific [89]. This will allow exploration of *in vitro* disease modeling, high throughput drug discovery and screening and regenerative therapies, reducing possible immune-rejection in stem cell therapy [89]. It should, however, be recognized that iPSCs are still a recent discovery and further extensive investigation must be done to identify the true potential of these unique stem cells.

Embryonic stem cells (ESCs) are one of the most studied models in the field. ESCs are derived from the inner cell mass of the blastocyst or earlier morula stage embryos. These cells maintain their pluripotency and are considered immortal (self-renewal ability). However, these stem cells do require some extrinsic factors such as serum free media supplemented with a specific factor, inactivated embryonic fibroblast cells or other types of feeder layers to maintain their stemness [90]. For mouse ESCs,

leukemia inhibitory factor (LIF) and the LIF/signal transducer and activator of transcription 3 (STAT3) signaling pathway has been illustrated to play a crucial role in conserving pluripotent states. The pathway is initiated by binding of LIF to leukemia inhibitory factor receptor (LIFR) and acts via gp130 receptors to activate Jak kinases (JK) and STAT3 [91]. The STAT3 proteins are then transported into the nucleus to activate the transcription of key stemness maintenance genes, c-Myc and Klf4. The interaction between LIFR and gp130 also promotes activation of the phosphoinositide 3-kinase (PI3K)/ protein kinase B (AKT) signaling pathway and Ras/mitogen-activated protein kinase (MAPK)/extracellular signal-regulated kinase (ERK) pathway [92,93]. PI3K/AKT activates T-box3 and inhibits differentiation by preserving Nanog expression. Ras/MAPK/ERK activation leads to regulation of Myc and Elk transcription factors. The inhibition of ERK signaling has been shown to promote self-renewal in ESCs [94] (Figure 1.18).

The human ESCs require basic fibroblast growth factor 2 (FGF2) . Activin A\TGFβ signaling pathway is also an important in the self-renewal process of human ESCs [95]. Binding of FGF2 to the fibroblast growth factor receptor (FGFR) activates PI3K/AKT signaling to promote self-renewal of stem cells, similar to the effect of LIF on mouse ESCs. Consequently, this also inhibits BMP initiated signals which also promote self-renewal. Currently, there are many different types of ESCs available for research. Embryonal carcinoma cells (ECCs) are a variation of “normal” ESCs. ECCs are the malignant counterpart of ESCs and are derived from teratocarcinomas, a germ line tumour [96]. These teratocarnomas are isolated from malignant tumours in the testis of mice and human and contain a population of undifferentiated stem cells. These undifferentiated tumour cells are pluripotent and capable of self-renewing, an important

characteristic of all stem cells. F9 and P19 cell lines are two mouse ECCs commonly used in stem cell research. Although the clinical potential for these cells are limited due to their malignant characteristics, these cells are model systems: the cellular and molecular aspects of early differentiation are easily studied in these cells lines. The major advantages of ECCs are that they are easy to maintain, and to manipulate genetically [96]. Differentiation can also be controlled reproducibly with inducers such as *All-trans* retinoic acid (ATRA) and dimethyl sulfoxide (DMSO) [97].

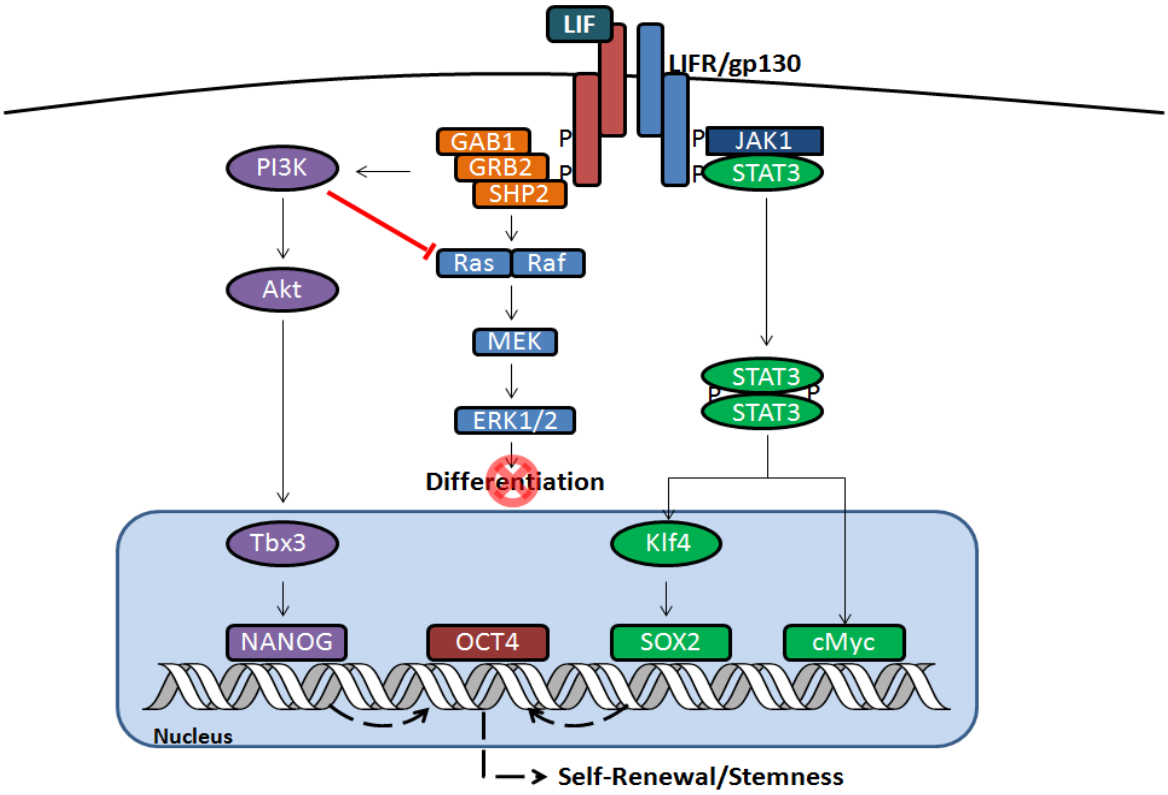

Figure 1. 18. Leukemia inducing factor helps to maintain pluripotency.

Binding of LIF to the LIF receptor (LIFR) promotes phosphorylation of the receptors. This recruits JAK1 and STAT3 proteins, activating STAT3 signaling pathway and promoting increased gene expression of SOX2 and cMyc. Phosphorylation of LIFR also induces PI3K/Akt pathway to initiate and promote enhanced expression of Nanog. Increased expression of both Nang and SOX2 promotes a feedback loop and subsequently maintains self-renewal and stemness of the stem cells.

1.2.4 Maintenance of pluripotency

The pluripotency of stem cells is shown to be governed by a unique set of transcription factors. Maintaining the expression of these factors allows cell to conserve their stemness. Many genes are crucial in maintain pluripotency such as Oct4, Sox2, Nanog, Tbx3, Essrb, Tcl1, Rif1, Nac1, Sall4, Dax1 and Zfp281[98]. Oct4, Sox2 and Nanog, however, are considered to be the core members among the stemness group [99,100]. Oct4 and Nanog share 345 genes in mouse ESCs. In human ESCs, Oct4, Sox2 and Nanog co-bind 353 target genes, demonstrating that a substantial fraction of target genes are shared among the three crucial factors [101]. The three factors are also in a feed-forward self-activating autoregulatory loop, while activating downstream self-renewal genes and repressing differentiation genes [58]. The autoregulatory loop is crucial in preserving the high levels of expression of the key stemness genes and preserving pluripotent states of the cell (Figure 1.19).

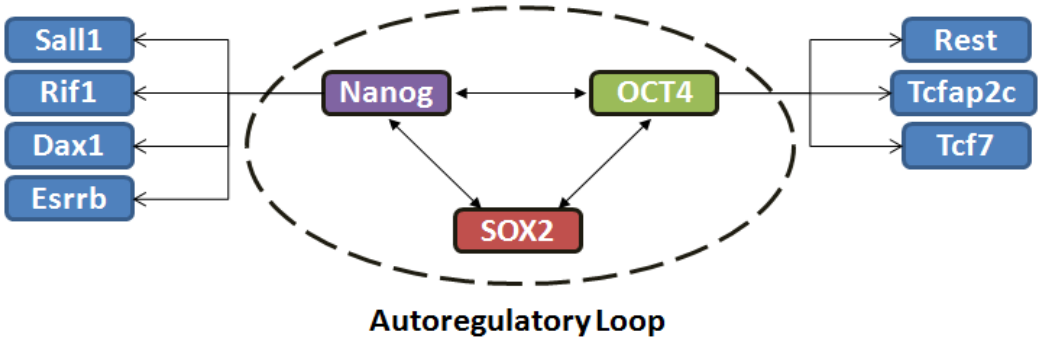

Figure 1. 19. Master regulators of self-renewal Oct4, Sox2 and Nanog.

The master regulators OCT4, SOX2 and NANOG are positioned inside the dashed circle. Presence of master regulators maintain the self-renewal characteristics of stem cells. Note that the initiation of pathways requires the expression of the master regulators. [102].

OCT4, also known as OCT3 or OCT3/4, is a Pou5f1 encoded transcription factor. OCT4 belongs to Pit-Oct-Unc (POU) transcription factor family. POU family members are known to target genes by binding an octameric sequence motif of an AGTCAAAT consensus sequence [103]. The POU domain of OCT4 binds DNA. N-terminal domain acts as transactivation domain and C-terminal domain acts as cell specific transactivation domain [104].This transcription factor is considered to be a master regulator for the initiation and maintenance of pluripotent cells during embryonic development. The expression of OCT4 remains high during pluripotent states and it rapidly disappears in differentiation. However, the level of Oct4 must also be maintained within a normal range to sustain pluripotency [105,106,107]. The expression level of OCT4 has been demonstrated to influence the fate of stem cells. For instance, reducing OCT4 expression by half promotes ESCs to differentiate into trophoblasts, while less than a twofold overexpression induces ESCs to become primitive endoderm and mesoderm [58].

SOX2 works concomitant with OCT4 to control pluripotency and it is also considered a master stemness gene [108]. SOX2 can heterodimerize with OCT4 to co-occupy HMG and POU motifs on regulatory DNA sequences [109]. Like OCT4, the expression of level of SOX2 is also tightly controlled in order to preserve pluripotency of stem cells. For instance, the loss of SOX2 is lethal to embryonic development, as the embryo fails to maintain an epiblast and cannot develop to a blastocyst stage [110].

NANOG is a homeobox-containing transcription factor and more recently described to play a crucial role in stem cell differentiation. NANOG regulates the cell fate of the pluripotent inner cell mass, maintains epiblast pluripotency and prevents differentiation to primitive endoderm [111,112]. Absence of NANOG leads to an embryo lacking proper epiblast [111]. For mouse ESCs, the overexpression of NANOG maintains

pluripotency without the need for the extrinsic factor LIF, (which has been shown to be crucial in maintaining stemness of mouse ESCs *in vitro* [113].)

1.2.5 Stem cell differentiation and *in vitro* protocols

When the factors that conserve pluripotency are removed, stem cells undergo differentiation. Under specific conditions, the differentiation can be directed to generate progeny consisting of derivatives of the three embryonic germ layers. In vitro, the formation of embryoid bodies (EBs) is one of the frequently used methods to induce differentiation. EB formation offers the advantage of providing three-dimensional structure that enhances multicelllular interactions. These are demonstrated to be a crucial element for differentiation process [114]. There are various ways to induce EB formation; however, only three commonly used techniques are discussed. These include suspension culture in a bacterial-grade dish, hanging drop culture and methylcellulose culture.

To induce EB formation in bacterial-grade dishes, the nontreated hydrophobic polystyrene dish is used [114]. This type of plate is necessary to ensure a liquid suspension culture and prevent cells from attaching to the surface, thus allowing cells to aggregate to one another. The bacteriological dish method for differentiation has been successfully demonstrated in both mouse and human ESCs, in which they form various types of specialized cells such as cardiomyocytes and insulin-producing cells [114]. Despite the level of successful differentiation and simplicity of the protocol, this method has drawbacks. In bacterial-grade dishes, the stem cells are allowed to spontaneously aggregate and form varying sizes of EBs each with different cell numbers.. This causes the size of EBs to be heterogenous in the culture and prevents synchrony in differentiation

[115]. Since uniformity and homogeneity in EB morphology is often an optimal condition for differentiation, other methods have been developed to resolve this issue.

The hanging drop culture overcomes the deficits of the bacterial-grade dish method. This method is now one of the most widely used technique to differentiate stem cells [116]. A specific number of cells can be seeded in the round shaped hanging droplets allowing a precise control of cell number in EB formation.. As the name suggests, the drop hangs on the petri dish lid and allows aggregation to take place. The disadvantage of this technique is often found in the size limit of the liquid volume and the complexity of the protocol. Because the droplets are hanging on the lid by surface tension, approximately 50 μL is the maximum volume that can be utilized. Subsequently, EBs from hanging drops are often transferred to suspension culture in bacteriological dishes to mature, thus being more laborious than the previous method [114].

Methylcellulose culture is another technique used to induce EB formation. This technique was originally employed to form cell aggregates of a clonal origin [117]. Unlike the other methods, stem cells in the methylcellulose matrix remain as a single cell and these single cells will proliferate and eventually develop into EBs. The semisolid characteristics of methylcellulose cultures are the disadvantage of this technique as the matrix of methylcellulose disturbs the mass transfer of factors added during an experiment and this causes difficulty in handling the semisolid solution. However, methylcellulose culture has been successfully utilized to differentiate ESCs into hematopoietic cells and endothelial cells [114] (Figure 1.20).

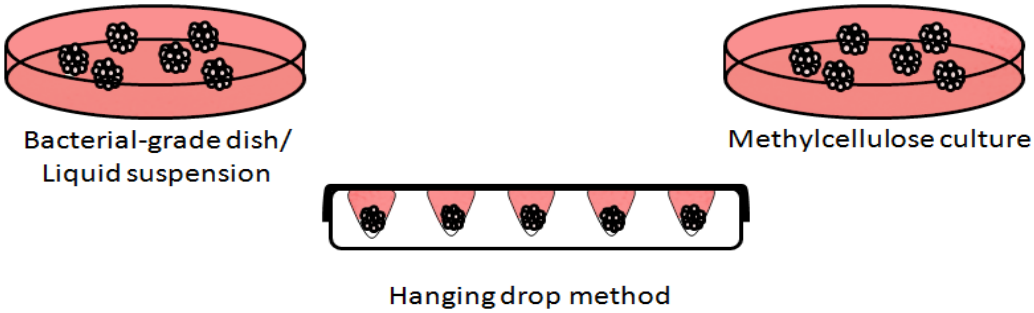

Figure 1. 20. Methods of embryoid body formation.

Embryoid body formation allows the stem cells to aggregate and enhances cell-to-cell interaction during the differentiation period. The three common methods include bacterial-grade dish, methylcellulose culture and hanging drop method. All three EB formation protocols permit liquid suspension of cells.

There are also differentiation techniques that do not involve the formation of EB. Stem cells can be cultured directly on stromal cells and differentiation can take place in contact with these supportive cells [118]. Stromal cells are connective tissue of organs and known to release growth factors that promote cell division. The most commonly used stromal cells in stem cells differentiation are OP9 cells. Co-culturing with stromal cells, however, consists of several shortcomings such as lack of knowledge with respect to the factors produced from the supportive cells, how these factors influence the differentiation process and the difficulty of isolating stem cells from stromal cells. The last protocol involves differentiating stem cells in a monolayer of extracellular matrix (ECM) protein. This type of approach is an attempt to mimic the niche microenvironment that houses stem cells. The ECM is a complex mixture of matrix molecules which are typically large glycoproteins such as fibronectins, collagens, laminins and proteoglycans that assemble into fibrils or other macromolecules [119]. The type of ECM could determine the fate of stem cell differentiation as it may influence the generation and survival of the developing cell types. The importance of the niche, however, is a relatively newer field in stem cell

research. This method therefore requires additional investigations in order to identify ECMs that contributes in differentiation and directing the fate of stem cells [119].

1.2.5.1 Mechanism of differentiation

Current stem cell research focuses on identifying factors and pathways that contribute to the fate of stem cells during differentiation. Studies exploring modifications in gene expression in undifferentiated and differentiated stem cells are one of the most utilized methods to discover specific factors that allow stem cells to transform into specific cell types. For the sake of relevancy only the mechanism of mesoderm differentiation will be discussed in detail.

1.2.5.1.1 Mesoderm differentiation

Mesoderm is one of the major germ layers that are being studied in stem cell differentiation. There are several factors already identified to be important in early mesoderm differentiation. These factors include bone morphogenic protein-2 (BMP-2), BMP-4, Brachyury, Homeobox protein MIXL-1, Nodal and Snail [120,121,122]. BMP-4 is a transforming growth factor-beta (TGF-β) superfamily member and it initiates complex formation of type I and type II receptors on the cell surface. This allows receptor II to phosphorylate the receptor I kinase domain. The phosphorylated type I receptor then phosphorylates Smad 1, 5, 8 (R-Smad). The two phosphorylated R-Smads and mediator Smad (Co-Smad) form a heterotrimeric complex, which then translocate into the nucleus. In the nucleus, this complex cooperates with transcription factors to modulate gene expressions [123] (Figure 1.21). Studies have demonstrated that this signaling cascade is a crucial requirement for mesoderm differentiation. Snail is another transcription factor

that is found to be involved in the development of mesoderm layers. Presence of this protein represses neuroectodermal differentiation by silencing genes such as rhomboid and single-minded in the mesodermal region [124]. Nodal factor has been demonstrated to play a role in mesodermal and endodermal differentiation. In mouse, high levels of nodal signaling has been suggested to be required to promote induction of posterior mesoderm [125].

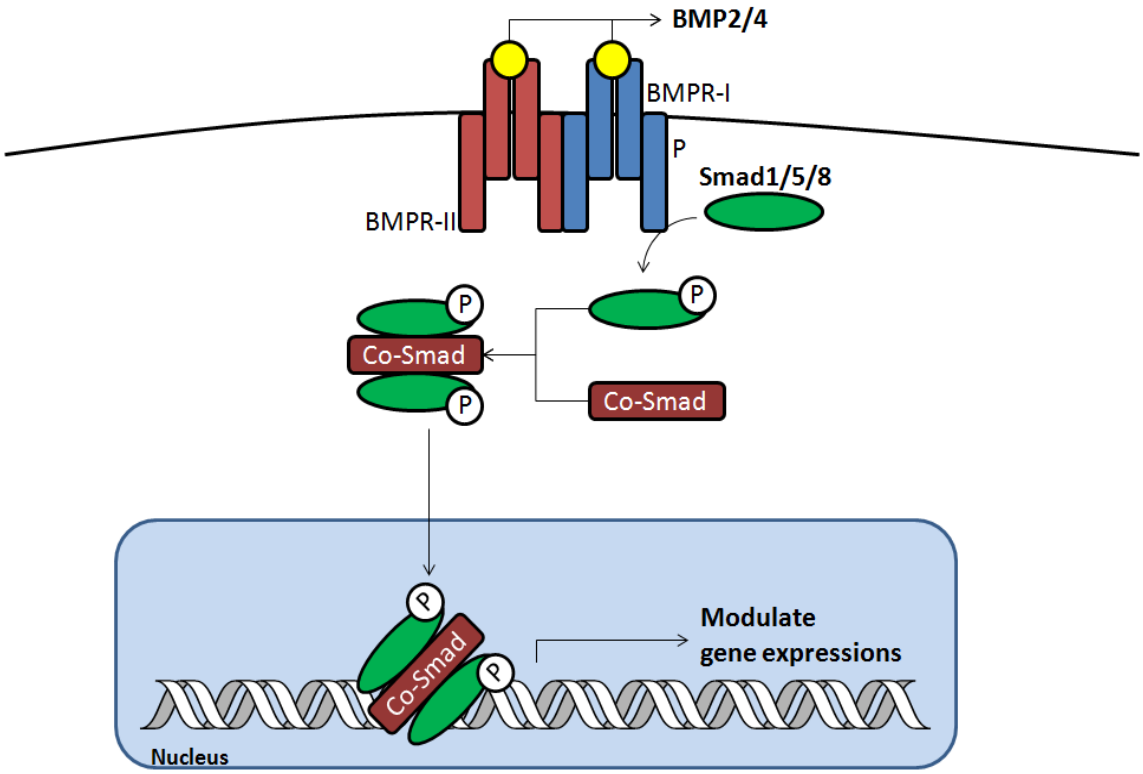

Figure 1. 21. BMP2/4 induce mesodermal differentiation.

Binding of BMP2/4 to the receptor promotes the formation of a BMPR-1 and BMPR-2 complex. Subsequently BMPR-2 phosphorylates BMPR-1 and allows BMPR-1 to recruit and phosphorylate Smad 1/5/8. Phosphorylated Smad protein can then complex with Co-Smad and be shuttled into nucleus to interact with other transcription factors thus modulating gene expression.

Once differentiated into mesoderm, this layer can further differentiate into mesenchymal, mesothelial, osteogenic, vascular, hematopoietic, cardiac cell and many other types. In particular, lineages such as hematopoietic and cardiac are among the easiest to differentiate from stem cells and have been studied in detail (Figure 1.22).

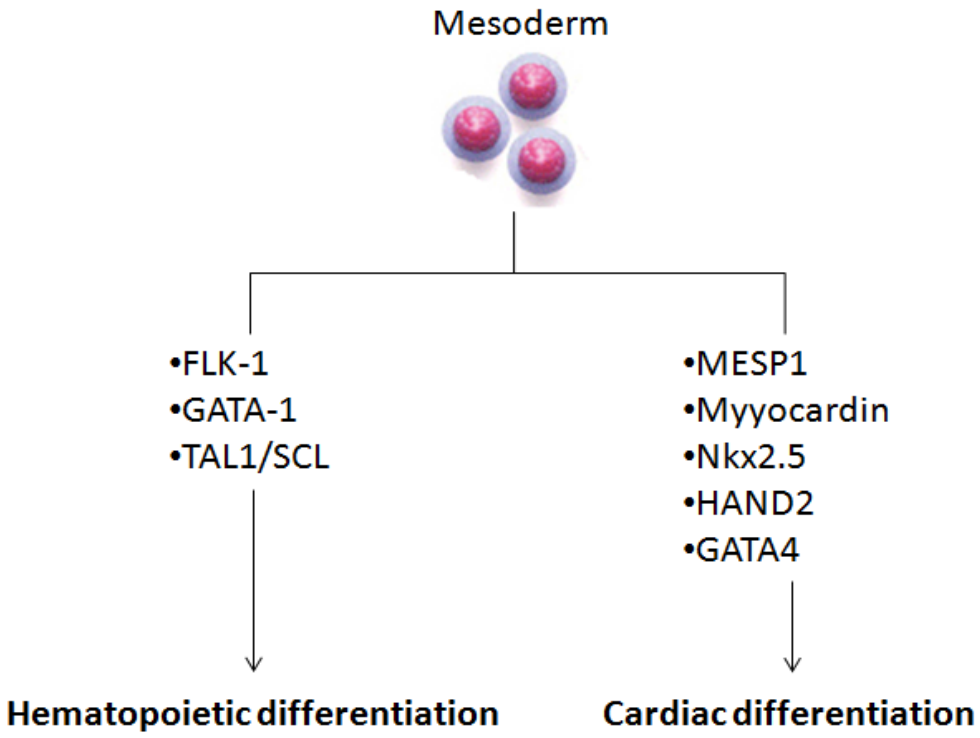

Figure 1. 22. Mechanism of hematopoietic and cardiac differentiation of mesoderm layer.

Mesoderm germ layer can differentiate into hematopoietic and cardiac cells. Transcription factors such as FLK-1, GATA-1 and TAL1/SCL promote hematopoietic differentiation. Mesp1, a master regulator of cardiac differentiation, promotes other cardiac related genes to promote cardiac differentiation.

The presence of hemoglobinized cells in EBs was first described in 1985 [126]. Since then, significant interest was placed in modeling the hematopoietic commitment of stem cells in order to allow readily accessible supply of transplantable stem cells in clinical settings. Studies identified important factors and markers in differentiation of ESCs into HSCs. FLK-1 is known to play a key role in hematopoietic and vascular

development [127]. In murine embryo, FLK-1 deficient mice do not develop blood vessels or yolk sac blood islands between 8 to 9 days [127]. FLK-1 positive cells express the GATA-1 transcription factors prior to endothelial or hematopoietic lineage markers [128,129], thus, indicating the importance of GATA-1 in hematopoietic differentiation of ESCs. The TAL1/SCL basic helix-loop-helix (bHLH) transcription factor, downstream of FLK-1 signaling pathway, is detected in the hematopoietic cells in later stages and in the yolk sac region in the mouse embryo [130]. Studies have indeed demonstrated that expression of TAL1 is essential for the development of all hematopoietic cells [131,132]. Human ESCs have also been successfully differentiated into hematopoietic cells under appropriate conditions. Hematopoietic development can be induced by addition of BMP4, Vascular endothelial growth factor (VEGF), and a mixture of hematopoietic cytokines such as interleukins (ILs), colony-stimulating factors (CSFs) and thrombopoietin (TPO) during either stromal cell-mediated differentiation or EB-mediated hematopoiesis [133].

Cardiomyocyte differentiation of ESCs is another mesodermal differentiation that is being studied extensively. In particular, investigations so far demonstrated that only pluripotent stem cells are capable of efficiently differentiating into spontaneously contracting cardiomyocyte-like cells *in vitro* [134]. Although the mechanism of cardiogenesis is still not fully understood, a number of key regulators of this process have been identified. Mesp1 is considered as the master regulator of cardiovascular development, initiating the cardiac transcription factor cascade to direct the formation of multipotent cardiac progenitor cells. Once Mesp1 is activated, it promotes increased expression of numerous other transcription factors such as Mef2c, Myocardin, Gata4, Nkx2.5 and Hand2 [135] (Figure 1.23). In particular, Nkx2.5 and Gata4 are crucial for specification of cardiac muscle phenotype differentiation. Nkx2.5 is shown to regulate the

transcription of several cardiac genes including α-sarcomeric actin and β-myosin heavy chain (β-MHC) [136]. Gata4 is a member of the cardiac GATA subfamily, consisting of Gata4, 5 and 6. These transcription factors bind to WGATAR motifs in promoter regions of cardiac- or gut-specific genes [137,138]. Once the differentiation is specified into cardiac lineage, the cardiomyocytes undergo a maturing phase. During this stage, several structural proteins are expressed such as α-actin, α-myosin heavy chain (α-MHC) and Troponin-T [134]. BMP-2/BMP-4 are also essential in mesodermal differentiation. These proteins have also been found to play a key role in recruiting mesoderm into cardiac lineage [139,140]. P19 clonal lines (P19C6noggin), consisting of noggin over-expression, exhibit hindered cardiac differentiation as noggin prevents activation of cardiac transcription factors and contractile proteins. It has been shown that addition of BMP proteins in the culture or overexpressing TAK1, a member of the mitogen-activated protein 3-kinase superfamily that transduces BMP signaling, can rescue P19C6noggin cells to differentiate into cardiomyocyte-like cells [141].

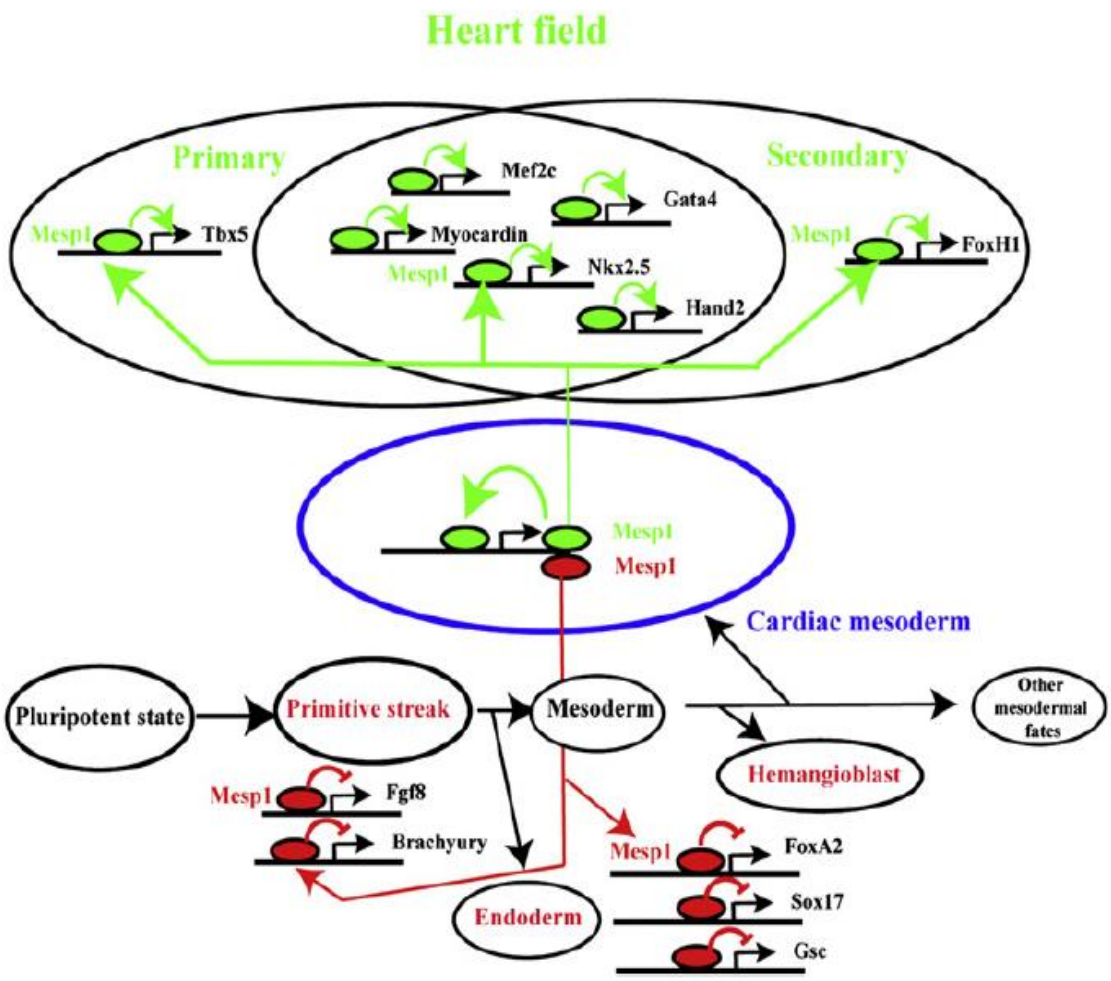

Figure 1. 23. Expression of Mesp1 acts as a master regulator for cardiac differentiation.

The green Mesp1 indicates increased expression and the red indicates decreased. Once the Mesp1 expression is enhanced, it induces a number of cardiac mesoderm linked gene expressions such as Nkx2.5, Tbx5, Mef2c, Gata4 and etc. On the other hand, Mesp1 downregulates several genes involved in primitive streak, endodermal and hemangloblast genes expressions [135].

1.2.5.2 Differentiation in P19 embryonal carcinoma cells

P19 cell lines are one of the most commonly used ECCs in stem cell research. The cells are derived from a teratocarcinoma formed following transplantation of 7.5 day embryos into the testis of C3H/He mice [142]. These isolated cells grow rapidly and are maintained as undifferentiated stem cells. Unlike other ECCs, P19 cells can undergo

efficient differentiation when the aggregates are exposed to non-toxic concentrations of a number of drugs . Retinoic acid (RA) and DMSO are two such drugs identified to be most effective in inducing differentiation of P19 cells. Both chemicals show no toxic effect to P19 cells at the doses used for differentiation, indicating that the drugs are not selecting the differentiated cells pre-existing in the cultures [142,143].

Retinoids are ubiquitous signaling molecules affecting nearly every cell types. In particular, these vitamin A (retinol) derived compounds are found to have profound effects on development, proliferation, differentiation and apoptosis [144]. Retinoids are synthesized from the diet as dietary vitamin A or generated enzymatically from the dietary precursor β-carotene [144]. Retinol dehydrogenase 10 (RDH10) is a primary enzyme that metabolizes vitamin A to retinaldehyde in a NAD^+ dependent manner. Retinaldehyde is then oxidized to RA via ALDH1a2 [145,146,147]. Once synthesized, RA is transported nucleus bound to cellular RA-binding protein 2 (CRABP2) and subsequently binds to the retinoic acid receptor (RAR) α, β or γ. Then the RARs can bind to one of the retinoid X receptors (RXRs) and promote formation of a heterodimer complex. This complex can bind to DNA and activates transcription of RA primary response genes. This step is considered to be the first step of the RA induced differentiation process and it occurs rapidly, within minutes to hours after the RA addition. The transcription factor Hoxa1 is identified as a primary response factor of this cascade. Primary response transcription factors are then used to promote synthesis of proteins that are involved in differentiation in the presence of RA [144] (Figure 1.24). In P19 ECC cultures, the concentrations of RA can be modified to produce all three primitive germ layers. Upon RA treatment of cell monolayers, P19 cells differentiate into endodermal and mesodermal pathways. Under suspension or aggregate conditions, however, RA

induces P19 cells to become neurons, glial and fibroblast-like cells. The dose of RA also dictates the process of differentiation. When aggregates are exposed to relatively higher doses (greater than 10^{-7}M), the P19 cells differentiate into neurons and astroglial cells. At lower doses (around 10^{-8}M), skeletal muscle is formed and fewer neurons are present. At even lower doses (around 10^{-9}M), cardiac muscle is formed while the number of skeletal muscles decrease in the culture [97].

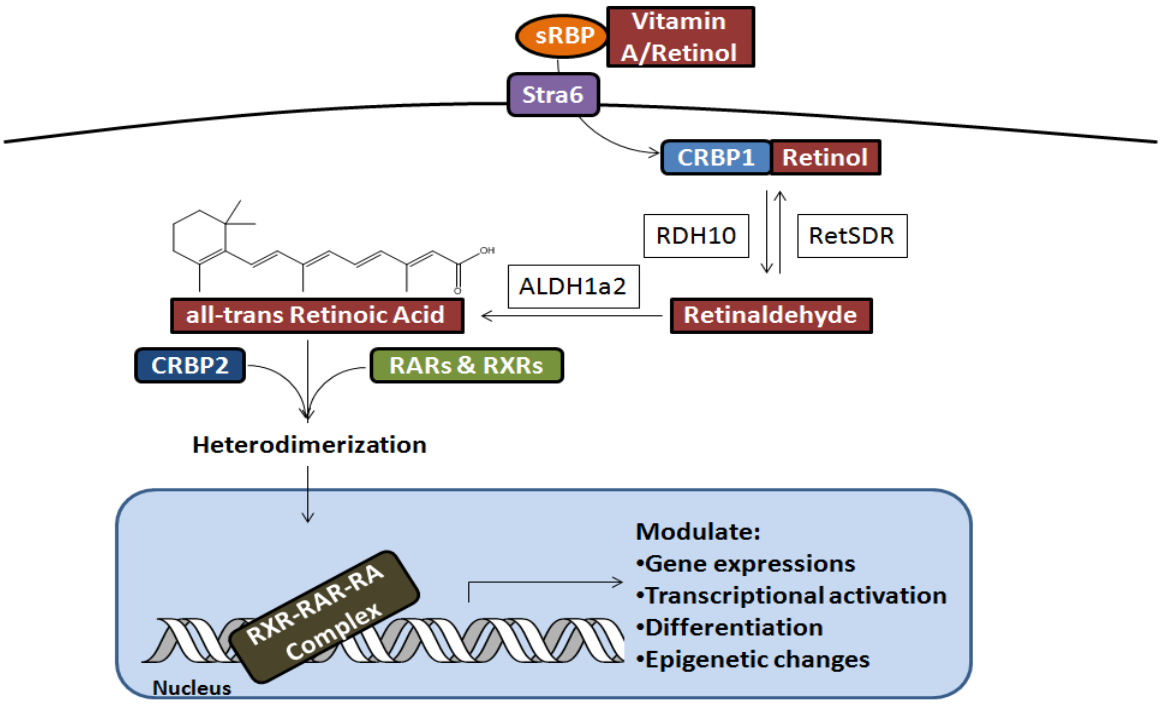

Figure 1. 24. Mechanism of retinoic acid-induced differentiation.

Vitamin A or retinol binds to serum retinol binding proteins (sRBPs). The Stra6 then transports the complex into the cell and the sRBP is replaced with cellular retinol binding protein (CRBP)-1. The enzyme RDH10 is responsible for converting retinol into retinaldehyde and ALDH1a2 subsequently uses retinaldehyde to produce all-trans retinoic acid (ATRA). ATRA is then complexed with CRBP2 first and binds to RARs and RXRs. This complex is then translocated into the nucleus to modulate gene expression, transcriptional activation, differentiation and epigenetic changes within the cell.

DMSO is an extensively studied chemical agent that is known to induce differentiation in ESCs and ECCs. It was demonstrated that P19 cells require 0.5-1% DMSO in order to differentiate into a variety of endodermal and mesodermal tissues. Although DMSO is identified to be a cell line specific inducer, its ability to initiate differentiation in other cells has been demonstrated previously. These cell lines include friend erythroleukemia (MEL) cells, neuroblastoma cells, lung cancer cells and mouse ESCs [148]. Although the DMSO-induced differentiation P19 cells produce numerous types of cells, cardiomyocytes-like cells are studied most frequently. The mechanism of DMSO-induced cardiac differentiation is still not fully understood, but studies revealed several signaling pathways involved in this process (Figure 1.25). DMSO is suggested to act via the oxytocin pathway as oxytocin antagonists have been shown to interfere with DMSO-induced cardiac myocyte differentiation [149]. Cardiac-like cells generated from P19 cells express similar transcriptional factors and signaling pathways observed in cardiac differentiation of ESCs. Gata4, Mef2c, Nkx2.5 and Tbx5 have been identified to be the crucial factors in DMSO-induced cardiomyocyte-like differentiation of P19 cells, which has also been found to play a key role in ESC-derived cardiac differentiation, [150]. The increased expression of BMP and TAK1 have also been identified during DMSO-induced differentiation, thus further indicating the similarity between the P19-derived and ESC-derived cardiomyocytes [148].

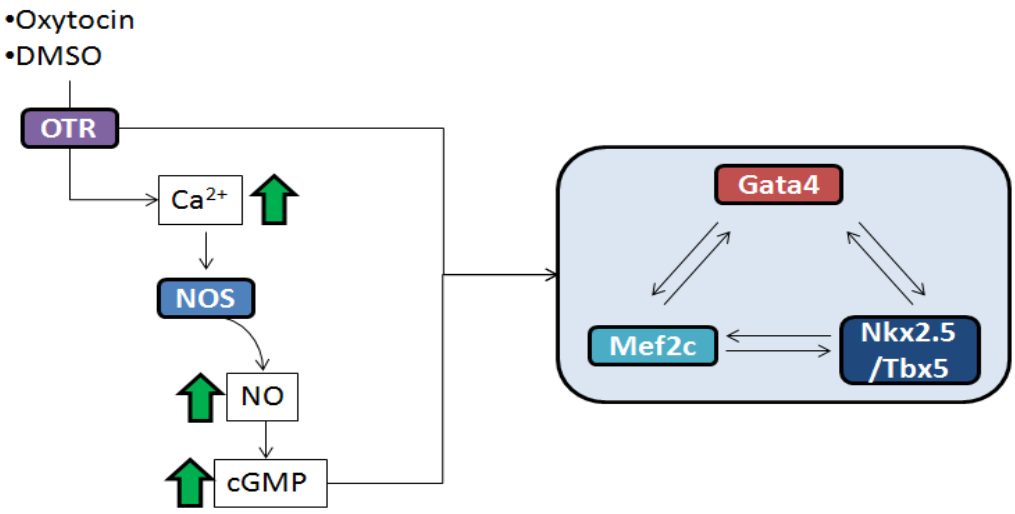

Figure 1. 25. Mechanism of DMSO-induced differentiation.

DMSO is demonstrated to act through the oxytocin/oxytocin receptor (OTR) pathway. Binding of DMSO to OTR causes intracellular calcium ion concentration to increase and causes increase in nitric oxide (NO) level via modulating the activity of nitric oxide synthase (NOS). This in turn increases the amount of cGMP. The pathway ultimately influences cardiac differentiation by inducing the expression of Gata4, Mef2c, Nkx2.5 and Tbx5 [151].

1.2.6 Metabolism and stem cell differentiation

Currently, the investigation to understand the molecular mechanisms of stem cell differentiation primarily relies on identifying the changes in gene expression, transcription factor expression and epigenetics. Evaluation of the global gene expression and identifying the key transcription factors in differentiation has provided important information about the process of differentiation. Although understanding the underlying genetic and epigenetic factors are crucial, other molecular aspects must be delineated in order to fully construct and identify the mechanisms governing cellular differentiation. Metabolomics is one of the emerging fields that show promising complementary to the other techniques in the exploration of the stem cell characteristics [152]. Among the

metabolic compartments, mitochondrial metabolism is studied most extensively in an attempt to link metabolism to stem cell differentiation.

1.2.6.1 Mitochondrial metabolism and differentiation

Although there are studies indicating the participation of the mitochondrion during differentiation, its precise role has yet to be fully uncovered. There is mounting evidence demonstrating the significance of mitochondrial morphology, biogenesis and activity during this process. In both human and mouse ESCs, undifferentiated stem cells consist of few and poorly developed cristae containing mitochondria [153]. These mitochondria were found to be localized perinuclearly [154]. Once differentiated and matured, however, these cells contain higher mitochondrial DNA content and mass [155,156]. The up-regulation of energy production via oxidative metabolism has been demonstrated in differentiated cells. For instance, oxidative phosphorylation was suggested to be crucial for the functional excitation-contraction in cardiac cells [157]. Neural and cardiac differentiation of ESCs was substantially increased when the differentiating cells were exposed to the natural metabolites associated with oxidative metabolism [152,158,159]. These findings suggest that mitochondria experience drastic changes in morphology and activity during the differentiation process. Despite these findings, the studies often fail to delineate the possible role of mitochondrial modification and oxidative metabolism in regulating differentiation.

1.2.6.2 Nuclear metabolism and differentiation

In contrast to well understood metabolic networks in the mitochondria, nuclear metabolism remains relatively elusive to date. There are several nuclear residing

metabolic enzymes and cofactors that have been recently identified. As these enzymes are metabolism-linked, the roles of these proteins are often suggested to be related to modulating metabolic status of the cells by regulating specific gene expression. There are, however, limited studies dedicated to understanding the nuclear metabolism in stem cell differentiation. Recently, ACL has been shown to play a role in histone acetylation during differentiation of murine 3T3-L1 preadipocyte into adipocyte [73]. O-linked N-acetylglucosamine (OGlcNAc) transferase (OGT) activity is found to be essential in ESC viability and development. Nuclear OGT of ESCs forms a stable partner with ten-eleven translocation-1 (TET1) and regulates CpG island methylation. This in turn modifies several important transcriptional regulators such as SP1, HCFC1, MYC and OCT4 [160].

2. Thesis objectives

The objective of this study is to investigate the role of metabolism in the differentiation of stem cells. Although genomic and transcriptional studies have been explored, there is limited information on the functional proteomics and metabolomics of differentiating stem cells. Using P19 embryonal carcinoma cells as a model, cytoplasmic, mitochondrial and nuclear metabolism were analysed. The alterations in glycolytic and mitochondrial enzymes and the fluctuation in metabolite levels involved in the central energy metabolism were studied. The variations in the nature and concentrations of metabolites coupled with activities of key enzymes involved in ATP synthesis provide a holistic illustration of all the participants in the DMSO-induced differentiation process. The significance of nuclear metabolism in pluripotency and the final fate of stem cells in response to nuclear metabolism are only beginning to emerge. The modulation of NAD^+, a key contributor to epigenetic changes was probed. Particular attention was given to the role of lactate dehydrogenase (LDH) and NAD^+ in epigenetic changes. Sirtuins are known to modify histone by removing acetyl groups, thus controlling the flow of genetic information. Such a role of LDH will help establish the intimate connection between cellular metabolism and epigenetic modulation. This investigation will assist in generating a global perspective on how metabolism, the end-product of any genetic cue, is indeed an important communicator and regulators of stem cells. This information will be pivotal in designing technologies that allow guiding pluripotent cells to any desired destination.

3. Materials and Methods

3.1 Cell culturing

3.1.1 P19 embryonal carcinoma cells

P19 embryonal carcinoma cells CRL-1825 were acquired from the American Type Culture Collection (ATCC). The cells were maintained in α-minimum essential media (α-MEM) supplemented with 5% fetal bovine serum (FBS) and 1% antibiotics (streptomycin and penicillin) in an incubator kept at 37˚C with a 5% CO_2 humidified atmosphere [161].

3.1.2 Culture initiation and passaging

P19 cells were cryogenically frozen in 5% DMSO. Prior to use, the frozen cells were thawed in a 37˚C water bath. Once thawed, the cells were pelleted at 2000 RPM for 5 minutes (Sorvall Legend RT Centrifuge). The media was removed and the pellet was resuspended in 1 mL of α-MEM + 5% FBS + 1% antibiotics (Growth media). The cells were seeded into a 75 cm^2 tissue culture flask in a final volume of 10 mL growth medium. The cells were allowed to grow for 2 days, until confluent. Cultures were then passaged by removing the adherent cells via trypsinization (1X trypsin in phosphate buffer saline (PBS, [136 mM sodium chloride, 2.5 mM potassium chloride, 1.83 mM dibasic sodium phosphate and 0.43 mM monobasic potassium phosphate, pH 74.]). The cells were then diluted to $1.0x10^6$ cells/mL and seeded into a new 75 cm^2 culture flask containing 10 mL total volume of growth medium. Each culture was maintained until the passage number was 30 (Figure 3.1)

3.1.3 Cell storage

The cells from first, second and third passages were isolated for cryogenic storage. The cells were detached from the flask by trypsinization and centrifuged at 2000 RPM for 10 minutes at 4˚C (Sorvall Legend RT Centrifuge). Low speed centrifugation prevents plasma membrane damage. The supernatant was removed and the pellets were rinsed with PBS. The pellets were then resuspended in 2 mL of DMSO containing cell storage media (Gibco) and aliquoted into 2 mL cryovials. The cells were frozen first at -20˚C for 2 hours followed by 1 day at -80˚C prior to cryogenic storage to avoid rapid freeze fracturing of the cells.

3.1.4 Differentiation

The protocol for DMSO-induced differentiation of P19 ECCs was performed as described in [149,162]. To induce differentiation, $1x10^6$ undifferentiated cells were seeded in a 10 cm bacteriological petri dish with a total volume of 10 mL growth medium under standard conditions of 5% CO_2 at 37˚C. The petri dishes were covered with a thin layer of 1% agar to prevent adhesion of the cells. DMSO was added to a final concentration of 1% and cells were allowed to form EBs (day 0). After 2 days, the medium was removed carefully and replaced with 10 mL of fresh medium with DMSO. Cells were then incubated for an additional 2 days (day 4). At day 4, the cells were either isolated or plated for further analysis (Figure 3.1) [149,162]. OCT4 expression was monitored via western blot to assess the differentiation.

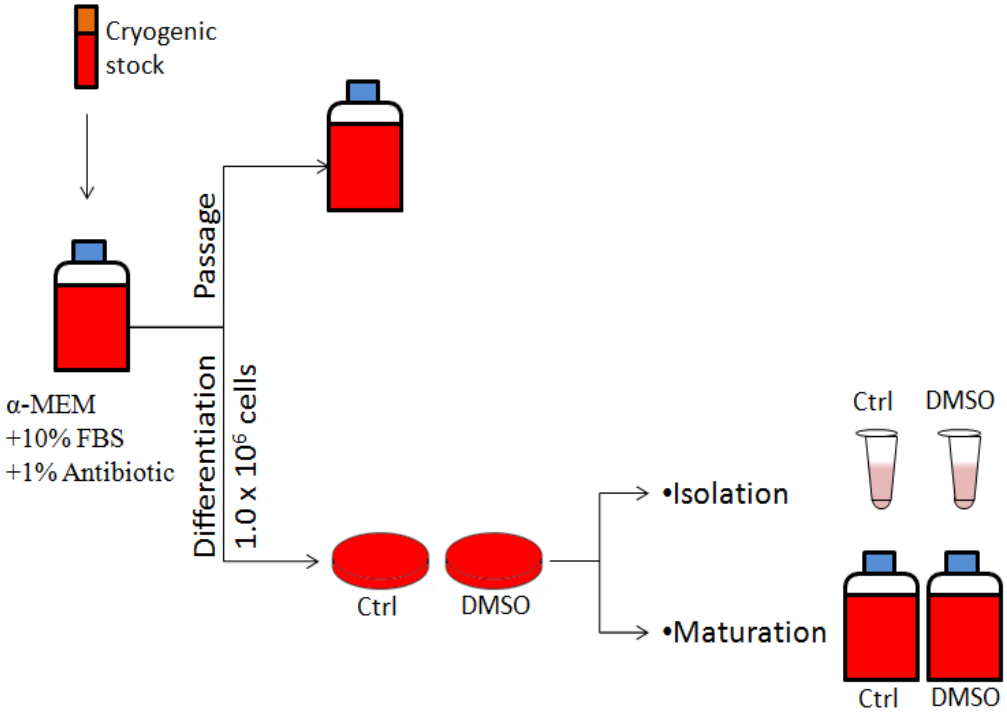

Figure 3. 1. Cell growth and differentiation.

P19 cells were thawed from a cryogenic stock and grown until confluent (approximately 2 days). Cells are either propagated or subjected to differentiation. To differentiate, P19 cells were trypsinized and the cell number was counted. 1 x 10^6 cells were seeded per agar-coated petri dish to allow aggregation (day 0). By day 4, the embryoid bodies were disaggregated and either isolated or seeded in new flasks for maturation.

To plate EBs, the day 4 aggregates of P19 cells were transferred to a 50 mL tube and centrifuged at 2000 RPM for 5 minutes. Subsequently, the media was removed and the cells were washed with PBS. The pellets were then subjected to 25% trypsin in PBS and incubated at 37˚C for 5 minutes. The pellets were gently resuspended, promoting disaggregation. Afterwards, 5 mL of fresh growth medium was added to deactivate the trypsin. The cells were centrifuged at 2000 RPM for 10 minutes and the supernatant was discarded (Sorvall Legend RT centrifuge). The cell pellets were resuspended in fresh media and counted. For plating, cells were seeded at 2x10^6 cells in a 75 cm^2 tissue culture

grade flask. The media was replenished every 2 days in order to provide fresh nutrients and remove waste products.

3.1.5 Cell isolation and subcellular fractionation

Cells were isolated at day 3, day 4 and day7 throughout the differentiation process. The aggregates (day 3 and day 4) were transferred to the centrifuge tubes immediately. Plated cells (day 7), however, were isolated by trypsinization and gentle tapping of the flask. The cells were removed from the medium by centrifugation at 2000 RPM for 10 minutes (Sorvall Legend RT Centrifuge). The pellets were washed twice in ice-cold PBS then resuspended in 1 mL of ice-cold mammalian cell storage buffer (mCSB) [50 mM Tris-HCl, 1 mM phenylmethylsulfonylfluoride, 1 mM dithiothreitol, 250 mM sucrose, 1 mg/mL pepstatin, 0.1 mg/mL leupeptin, and 2 mM citrate, pH 7.4] and stored at -80˚C.

When the cells were needed, they were thawed and centrifuged at 400 x g for 10 min at 4C. The cells were then resuspended in 30μL of mCSB and homogenized on ice with a sonic dismembrator operating at 36% amplitude. The sonication was performed 4 times for 10 seconds in 1 second bursts to disrupt the cell membrane. The suspension was kept on ice for 5 minutes between each round of sonication to prevent damage to intracellular organelles and proteins. The subcellular fractions were obtained by using differential centrifugation [163].

Whole cells were first removed by centrifugation at 150 x g for 10 min at 4˚C. The supernatant containing cell free extract (CFE) was centrifuged at 800 x g for 20 minutes at 4˚C to produce a nucleus pellet. The pellet was resuspended in 50 μL of mCSB before being processed for further experimentation. The supernatant was further centrifuged at 12,000 x g for 45 minutes at 4˚C to isolate mitochondria from the

remaining CFE. The mitochondrial fraction was resuspended in 50 µL of mCSB (Figure 3.2). Purity of these fractions was ascertained by anti-actin (for nucleus, anti-voltage dependent anion channel (VDAC) (for mitochondria) and Lamin B1 (for nucleus).

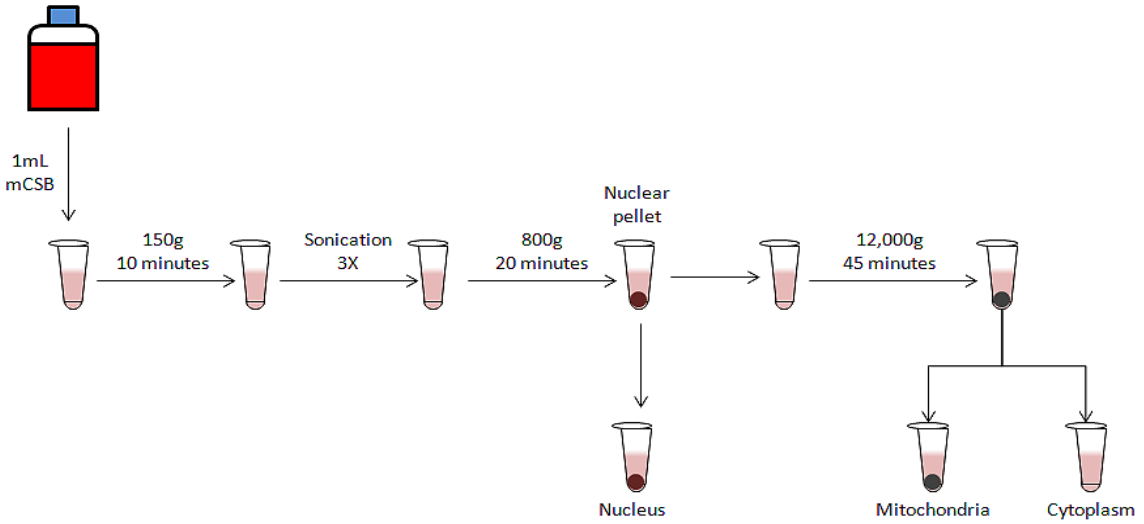

Figure 3. 2. Subcellular fractionation

Cells are isolated and resuspended in 1 mL of mammalian cell storage buffer (mCSB) and stored at -80˚C until needed. When the cells were needed, they were thawed and the pellet was isolated by centrifugation at 400 x g. The pellet was resuspended in 50µL of mCSB then sonicated 3 times. Whole cells were removed and supernatants were centrifugated at 800 x g for 20 minutes to yield a nuclear pellet. Supernatant was again spun down at 12,000 x g for 45 minutes to obtain a mitochondrial pellet and cytoplasmic fraction.

3.2 Blue native polyacrylamide gel electrophoresis

BN-PAGE was used to perform functional proteomics on metabolic enzymes. This technique provides a unique tool to monitor enzymatic activities in their native state (Figure 3.3) [164]. Subcellular protein fractions were quantified and normalized by the Bradford assay [165]. Protein was diluted to its desired concentration in blue native buffer (1.5 M €-aminocaproic acid, 150 mM BisTris (pH 7 at 4^{o}C)]. To the mitochondrial fraction, 10% maltoside, a mild detergent, was added to release membrane-bound proteins while maintaining their activity. Samples were kept on ice for 30 minutes in order to keep

proteins native during maltoside treatment. Prepared proteins were stored at -20˚C for up to one week before usage.

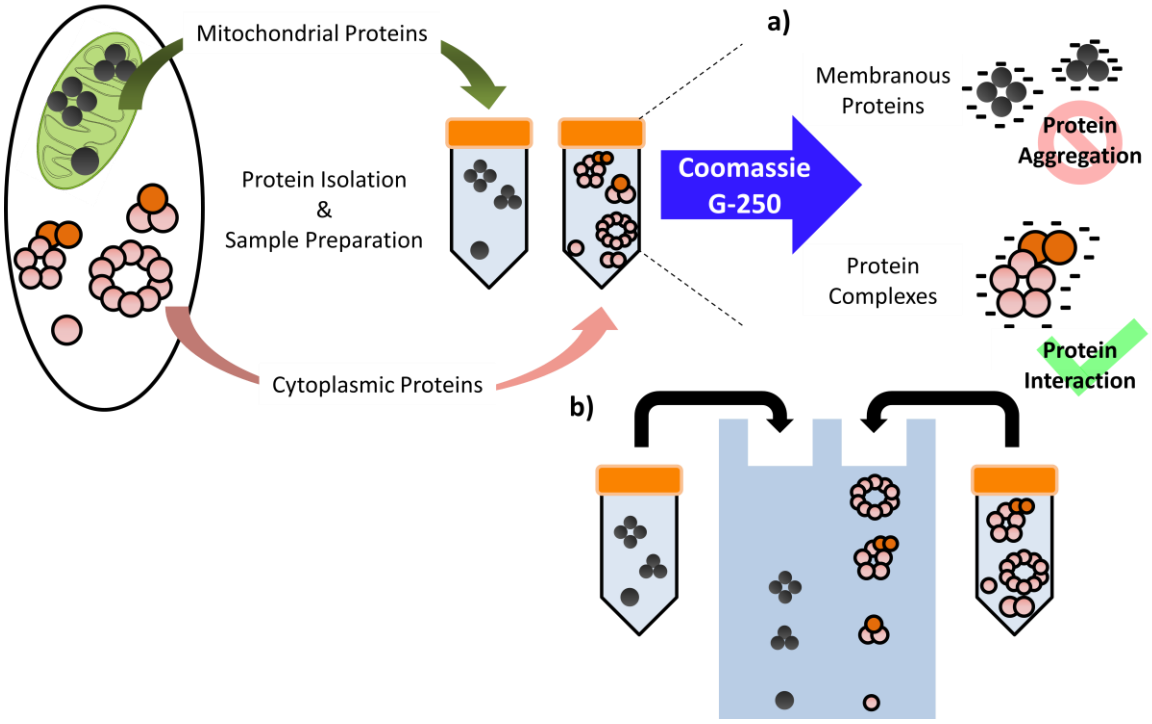

Figure 3. 3. Blue native polyacrylamide gel electrophoresis.

Subcellular fractions can be isolated and prepared for BN-PAGE analysis. a) Coomassie G-250 dye prevents protein aggregation in membranous proteins, while maintaining their protein-protein interactions. b) BN-PAGE separates proteins based on their size and maintain their native conformation during electrophoresis [164].

3.2.1 Gel formation

Native polyacrylamide gel electrophoresis gels were formed by a modified method described in [166]. Gels (dimension 8x7cm^2) were cased using 1 mm spacers in the Bio-Rad MiniProtean^{TM}2 system. A 4-16% gradient gel was used in all blue native polyacrylamide gel electrophoresis (BN-PAGE) experiments. The 4% acrylamide gel solution was made separately from 16% acrylamide gel solution and mixed using a

gradient former and a peristaltic pump to create a 4-16% resolving gel. A stacking gel was poured over the resolving gel after the gel was solidified (Table 3.1).

Table 3. 1. Reagents for gradient BN-PAGE gel

Volume of reagents required to compose resolving and stacking gels.

Reagent	**16%**	**4%**	**Stacking Gel**
48% Acrylamide +1.5% Bisacrylamide	1879 µL	234 µL	273 µL
3X BN Buffer	967 µL	967 µL	1136 µL
ddH2O	654 µL	1699 µL	2000 µL
75% (v/v) Glycerol	773 µL	-	-
10% (w/v) APS	7.4 µL	9.4 µL	50 µL
TEMED	3 µL	3 µL	10 µL

3.2.2 Electrophoresis

The prepared BN-PAGE protein samples were introduced into the wells along with molecular mass standards (Apo-ferritin = 480kDa, BSA = 120kDa and 66 kDa). The molecular weight standards are used to ensure that gels resolve appropriately. The gel cassettes were then assembled in the Bio-Rad MiniProtean^{TM}2 system. Once the proteins were loaded, the gel was overlaid with blue cathode buffer. The inner chamber of the electrophoresis system was then filled with the coloured cathode buffer and the outer chamber was filled with clear anode buffer (Table 3.2). Coomassie staining was used to ensure the equal loading of proteins.

Table 3. 2. Reagents for BN-PAGE

Composition of solutions required for BN-PAGE electrophoresis. Note: pH correction of blue cathode, clear cathode and anode buffers must be performed at 4˚C

Reagent	Blue Cathode Buffer	Colourless Cathode Buffer	Anode Buffer	3X Blue Native Buffer
Tricine (mM)	50	50	-	-
Bis-Tris (mM)	15	15	50	150
Coomassie Blue G-250 (%)	0.002	-/0.002	-	-
pH	7.0	7.0	7.0	7.0

The electrophoresis was performed at 4˚C to prevent denaturation of proteins. Electrophoresis was performed at 80 V to allow proteins to properly stack prior to resolving gel. Upon reaching the resolving gel, the voltage was increased to 150 V and no higher than 25 milliamps. When the proteins had run halfway through the gel, the blue cathode was replaced with a colourless cathode. The removal of coloured cathode allows visualization of the gel and partially removes the stain, so the activity band could be visualized more readily.

3.2.3 In-gel activity assays

Upon completion of electrophoresis, the gel slab was removed carefully from the unit and placed in reaction buffer [25 mM Tris, 5 mM $MgCl_2$, pH7.0] for 15 minutes in order to remove remaining buffer salts. Subsequently, the gels were placed in reaction mixture and kept at 37˚C in the dark. Each reaction container contained a reaction mixture containing substrates, cofactors and linking enzymes specific to the enzymes under investigation. The reaction was stopped with destaining solution [50% methanol,

10% glacial acetic acid, 40% ddH_2O] which helped remove the coomassie staining on the gel. The reaction mixtures for each enzyme are elaborated in table 3.3.

Table 3. 3. Enzymatic activity reaction mixtures

Enzyme	Reaction Mixture	Reaction Type
Glucose 6-phosphate dehydrogenase [EC 1.1.1.49]	5 mM glucose 6-phosphate 0.5 mM $NADP^+$ 0.3 mg/mL PMS 0.5 mg/mL INT	NAD(P)H producing reaction
Isocitrate dehydrogenase-$NAD(P)^+$ [EC 1.1.1.41] [EC 1.1.1.42]	5 mM isocitrate 0.5 mM $NAD(P)^+$ 0.3 mg/mL PMS 0.5 mg/mL INT	NAD(P)H producing reaction
Malate dehydrogenase [EC 1.1.1.37]	5 mM malate 0.5 mM NAD^+ 0.3 mg/mL PMS 0.5 mg/mL INT	NAD(P)H producing reaction
Malic enzyme [EC 1.1.1.82]	5 mM malate 0.5 mM $NADP^+$ 0.3 mg/mL PMS 0.5 mg/mL INT	NAD(P)H producing reaction
Lactate dehydrogenase [EC 1.1.1.27]	5 mM lactate 0.5 mM NAD^+ 0.3 mg/mL PMS 0.5 mg/mL INT	NAD(P)H producing reaction
Pyruvate kinase [EC 2.7.1.40]	5 mM phosphoenolpyruvate 0.5 mM ADP 0.5 mM NADH 2.8 μg/mL DCIP 0.5 mg/mL INT 3.3 units/mL lactate dehydrogenase	Enzyme linked reaction (LDH linked)
ATP-citrate lyase [EC 2.3.3.8]	20 mM citrate 0.75 mM CoA 0.37 mM ATP 1.5 mM NADH 2.8 μg/mL DCIP 0.5 mg/mL INT 13 units/mL malate dehydrogenase	Enzyme linked reaction (MDH linked)
Complex I	5 mM NADH	NADH oxidation reaction

[EC 1.6.5.3]	0.5 mg/mL INT	
Complex IV [EC 1.9.3.1]	10 mg/mL diaminobenzidene 10 mg/mL cytochrome C 562 mg/mL sucrose	Diaminobenzidene reduction

Four types of reaction are studied, including NAD(P)H producing, LDH linked, MDH linked, NADH oxidation and diaminobenzidene reduction reactions. NAD(P)H generating enzymes are visualized when NAD(P)H transfers electrons to INT using PMS as a electron mediator. The reduced INT forms an insoluble red formazan precipitate at the region where the enzyme is active (Figure 3.4) [167].

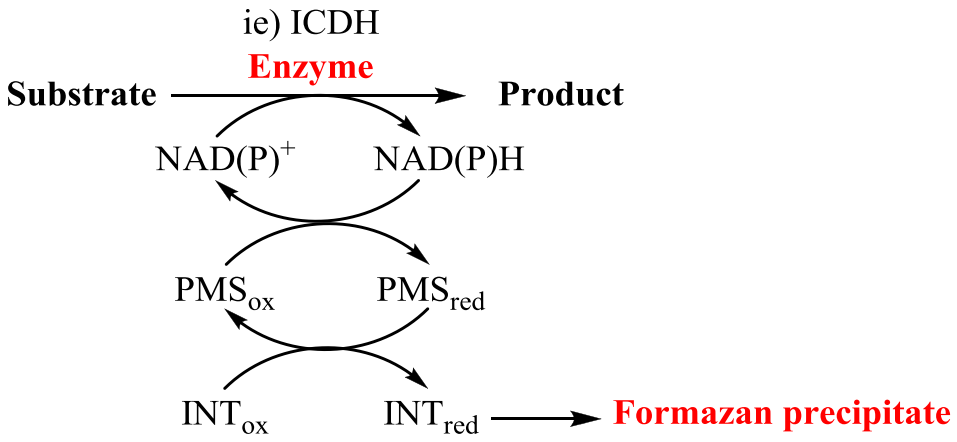

Figure 3. 4. NAD(P)H producing enzyme activity assay.

Reduction of $NAD(P)^+$ to NAD(P)H via an enzymatic reaction. NAD(P)H then transfers electrons to reduce PMS which reduces INT. Reduced INT forms a red-formazan precipitate.

LDH and MDH-linked enzymatic activity assays uses exogenous MDH and LDH to detect the enzyme of interest. MDH and LDH will then reduce NAD^+ to form NADH or oxidize NADH to NAD^+. The former reaction leads to the reduction in PMS and the latter uses DCIP as an electron mediator to reduce INT (Figure 3.4) [76,167].

a)

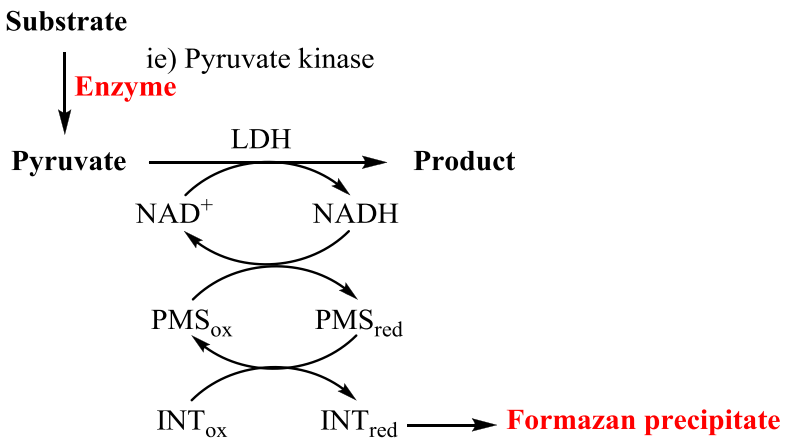

b)

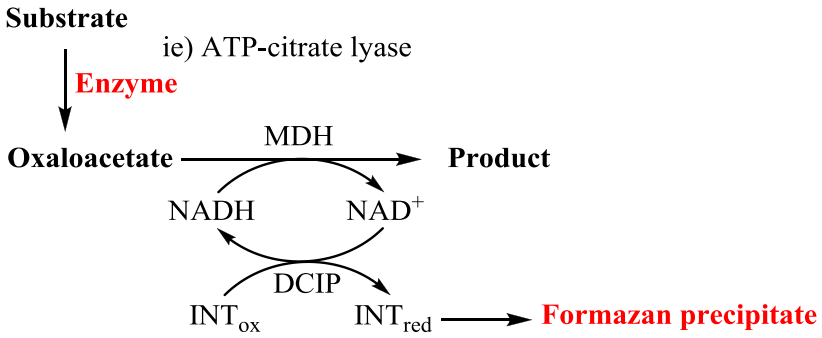

Figure 3. 5. Malate dehydrogenase and lactate dehydrogenase-linked enzyme activity assays.

a) Pyruvate formed by an enzyme of interest is used by exogenous LDH. Electrons are transferred from NADH to INT to produce a formazan precipitate. b) An enzyme of interest produced oxaloacetate which can then be metabolized by exogenous MDH. DCIP serves as an intermediate to reduce INT from the MDH reaction and create the formazan precipitate.

The activity of Complex I and Complex IV of the electron transport chain was monitored. Although Complex I oxidizes NADH, it does not require an electron mediator such as PMS or DCIP as the reaction itself has sufficient electropotential to reduce INT. The in-gel activity of cytochrome C oxidase (Complex IV) was examined via the reduction of diaminobenzidene [76]. The latter accepts the electrons from cytochrome C

and undergoes oxidative polymerization at the site of enzyme activity. This polymer of diaminobenzidene is insoluble and precipitate out of the solution with a brown colour. Enzymes probed in this study are illustrated in figure 3.5.

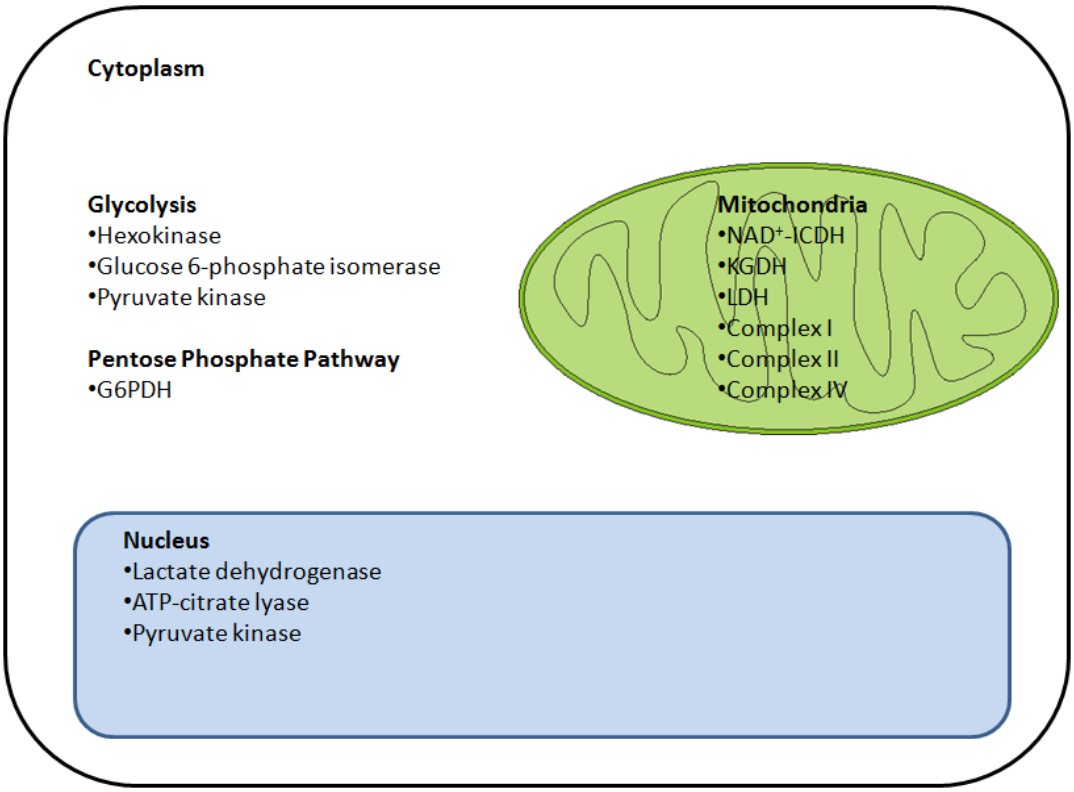

Figure 3. 6. Enzymatic activities probed in various cellular compartments.

Enzymes of central metabolism and nuclear metabolic enzymes were probed via BN-PAGE. Glycolysis and the pentose phosphate pathway were studied in the cytoplasm. TCA cycle and electron transport chain enzymes were analyzed in the mitochondria. Nuclear lactate dehydrogenase, ATP-citrate lyase and pyruvate kinase was examined in the nucleus.

The enzyme activity was confirmed by HPLC analysis. The activity band was excised from the gel and placed in a reaction mixture containing the appropriate substrates for 30 min (refer to activity assay recipe in Table 3.3). The consumption of substrates and formation of products was monitored by HPLC.

3.3 HPLC analysis

Samples were filtered and diluted ten-fold with Milli-Q water prior to HPLC analysis. These were then placed in the automated sampler of the Waters 2695 Aliance HPLC. The EMPOWER software allowed programming of the protocol and automatic injection of the samples. Prior to the 30 min sample injections, the column was equilibrated for 10 min. The volume of sample injected was between 50 to 100 μL depending on the desired resolution of the peaks. The HPLC was standardized using a five-point calibration protocol prior to each injection. A Phenomenex C-18 column with a polar cap was used in conjunction with HPLC grade mobile phase (20 mM KH_2PO_4, pH of 2.9) to retain organic acids. A Waters 2487 dual λ absorbance detector operating at 210 nm for carbonyl functions, and 254 nm, for C to N conjugation, was used to detect the organic acids. The flow rate was kept at 0.7 mL/min for all experiments. The identities of the peaks were determined by comparing to know standards and by spiking the samples with specific standards to confirm their identity.

3.3.1 CFE, cytoplasmic and mitochondrial fractions

Both control and DMSO-differentiated subcellular fractions were collected and analyzed. Samples were equalized by the cell counts performed prior to isolation (e.g., subcellular fractions were obtained from same amount of control and DMSO cells). All subcellular fractions were subjected to two analyses: 1) metabolic profile and 2) the monitoring of specific substrate consumption. The CFE was treated with 2 mM acetoacetate and 2 mM succinate in order to assess the substrate consumption. To examine the ATP producing ability of the mitochondria, the mitochondrial fractions were subjected to 2 mM succinate or 2 mM malate with 0.5 mM ADP for 1 hour.

3.3.2 Nuclear fraction

To analyse nuclear fraction form the control and differentiated cells, nuclear proteins were isolated from an equal cell number of both control and DMSO-treated cells. A metabolic profile of the nucleus was first obtained to assess the level of metabolites present. The nuclear NAD^+ consumption was monitored by incubating nuclear fractions with 0.5 mM NAD^+ for varying period of time at 37˚C in reaction buffer. Subsequently, the nuclear proteins were boiled for 10 minutes to lyse the nuclei. Solid materials were then removed by centrifugation and filtered prior to sample injection in the HPLC.

3.4 Histone acetylation

Histone extraction and purification was performed as outlined in [168]. Cells were grown and were pelleted at 300 x g for 10 minutes. The pellets were washed with PBS and again subjected to centrifugation at 300 x g for 10 minutes. Cells were then resuspended in 1 mL of hypotonic lysis buffer [10 mM Tris-HCl, 1 mM KCl, 1.5 mM MgCl2, 1 mM DTT, 1 mg leupeptin and 0.5 μL pepstatin, pH 8.0] and incubated on a rotator for 30 minutes at 4˚C to promote swelling and lysis by mechanical sheering. Next, a nuclear pellet was obtained by centrifugation at 10, 000 x g for 10 minutes at 4˚C. The supernatant was discarded and nuclei were resuspended in 400 μL of 0.4 H_2SO_4 and incubated on a rotator at 4˚C overnight. Histones were precipitated from the supernatant (400 μL) by adding 132 μL of ice cold trichloroacetic acid drop-wise at a final concentration of 33%. The samples were left on ice overnight and centrifuged the next day at 16, 000 x g for 10 minutes at 4˚C. The histone pellets were washed twice with ice cold acetone and centrifuged at 16, 000 x g for 5 minutes at 4˚C in order to completely

remove the acid. The remaining acetone was dried at room temperature for 20 minutes and the pellets were resuspended in 50 µL of ddH_2O.

To determine the level of acetylation on histones, the acetyl groups were removed by hydrolysing the histones. The hydrolysis step includes incubating histones in 6 N H_2SO_4 at 100˚C for 5 hours [169]. Following hydrolysis samples were prepared for HPLC analysis (Figure 3.6).

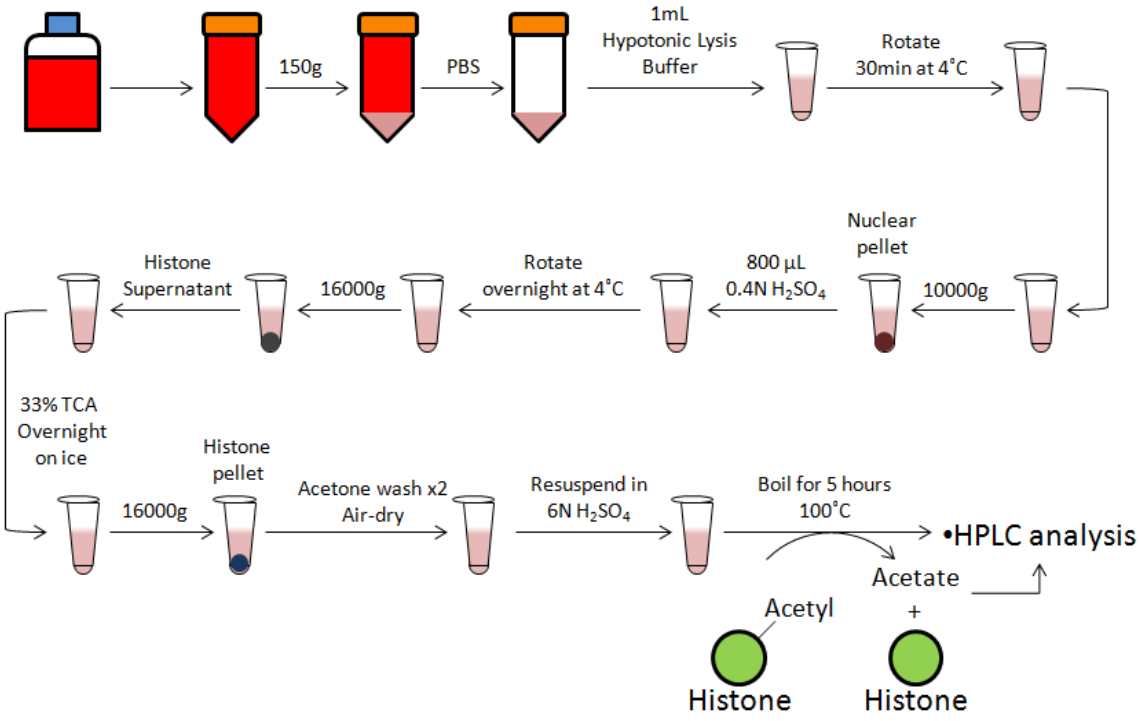

Figure 3. 7. Histone extraction and hydrolysis protocol.

Cells were collected and lysed using hypotonic lysis buffer and nuclei were isolated by centrifugation at 10, 000 x g for 10 minutes. Nuclei were resuspended in 0.4N H_2SO_4 and allowed to rotate overnight at 4˚C. Cellular debris was removed from the soluble histones by centrifugation at 16, 000 x g for 10 minutes. Histones were precipitated by TCA precipitation and centrifuged at 16, 000 x g for 10 minutes at 4˚C. The pellet was washed with acetone and allowed to dry. Histones were resuspended in a solution of 6N H_2SO_4 at 100˚C for 5 hours. Histone acetylation levels were measured by analyzing acetate by HPLC [168].

3.5 Fluorescence microscopy

After day 4 of differentiation, embryoid bodies were disaggregated and transferred to glass coverslips in a 35 mm X 10 mm petri plate or in 96 well plates. Cells were seeded at a density of 4.0 x 10^5 cells/mL in 2 mL of growth media. It was essential to seed the proper cell number as high cell density causes cell clumping prior to the attachment. The analysis of fluorescence microscopy was performed on a Zeiss deconvolution microscope at 60X ocular magnifications and in the dark to prevent photobleaching. An OdysseyTM infrared imager from LiCor was used to visualize 96-well plates during in-cell western blots.

3.5.1 Rhodamine dye

Rhodamine dye was used to visualize membrane potential generated in mitochondria. Rhodamine B fluoresces when it is protonated by the acidic gradient created by active mitochondria, thus making this dye ideal to observe the mitochondrial activity level in the cell. The cells grown on the coverslips were incubated with rhodamine B (15μg/mL in 2 mL of growth media) for 30 minutes at 37˚C, followed by PBS/EDTA wash [76].

3.5.2 Immunofluorescence microscopy

At a predetermined time, the growth media was removed and the cells were washed twice with PBS. Cells were then fixed with a 3:1 methanol:acetic acid solution for 10 minutes and air-dried for 1 minute. The cells were washed with PBS twice prior to Hoescht 33528 (2.5 μg/mL in PBS) treatment for 10 minutes. Hoescht is used to visualize the nucleus. Cells were washed twice with tris buffered saline (TBS) [2.42g Tris, 8g NaCl

in 1 L ddH_2O, pH 7.6] before the blocking step [TBS + 1% tween-20 + 5% FBS]. Tween serves to permeabilize the membrane for antibody binding and FBS is responsible for blocking non-specific binding sites. Blocking was done for an hour on a gentle agitator. The coverslips were washed 3 times for 5 minutes after removing the blocking solution. The cells were then exposed to the primary antibody (anti-OCT4 1:800, anti-VDAC 1:1000) at an appropriate dilution in 1% tween-20 TBS (TTBS) for 2 hours on gentle agitation at room temperature. After three washings with TBS for 5 minutes, the cells were incubated with secondary antibody (dilution 1:10000 in TTBS) for1 hour (table 3.4). Next, the secondary antibodies were washed away with TBS three times for 5 minutes and the coverslips were mounted on slides. Hoescht was measured at $\lambda_{excitation}$ = 355 nm and $\lambda_{emission}$ = 495 nm and FITC was detected at $\lambda_{excitation}$ = 495 nm and $\lambda_{emission}$ = 520 nm [76].

3.5.3 Ninety six-well plate in-cell western blot

In-cell western assays were performed as described in the Odyssey Infrared Imaging System protocol document (LiCor doc# 988-08332). Embryoid bodies were first disaggregated and seeded in 96-well plates at $1.0x10^6$ cells/mL. After 24 hours, the cells were washed three times with PBS and fixed with 37% formaldehyde for 20 minutes at room temperature. Then, the cells were rinsed with 0.1% tween-20 in PBS and blocked using Odyssey blocking buffer for 2 hours. Following the blocking step, the cells were exposed to primary antibody overnight at 4˚C. Primary antibodies were diluted to 1:200 in blocking buffer (anti-LDH, anti-acetylated lysine, anti-SIRT1). Secondary antibody (1:500 dilution in blocking buffer) incubation was performed for 2 hours with gentle shaking in the dark. The infrared signals were detected with an Odyssey Infrared Imager.

3.6 SDS-PAGE

All protein samples were prepared in 6X sample buffer [62.5 mM Tris-HCl, 2% (w/v) SDS and 2% (v/v) β-mercaptoethanol, pH 6.8] at a final protein concentration of 1 mg/mL in a 30 μL volume. Samples were boiled for 10 minutes and subjected to electrophoresis. A 10% isocratic SDS gel was used for protein separation [9.2% (w/v) acrylamide, 0.8% (w/v) bis-acrylamide, 0.15M Tris-HCl, 0.1% (w/v) SDS, 0.17% (v/v) TEMED, 0.86% APS, pH 8.8]. Stacking gel [9.2% (w/v) acrylamide, 0.8% (w/v) bis-acrylamide, 0.15M Tris-HCl, 0.1% (w/v) SDS, 0.17% (v/v) TEMED, 0.86% APS, pH 6.8] overlayed the resolving gel. The pH difference between the stacking and resolving gel allows proper stacking of the proteins. Electrophoresis was done in an electrophoresis buffer [0.025 mM Tris, 0.192 mM glycine, 0.1% (w/v) SDS, pH 8.3] and electrophoresed at 80V until the protein reached into the resolving gel. Once the protein entered the resolving gel, the voltage was increased to 150 V until completion. The gels were subjected to either Coomassie staining or immunoblot assays.

3.6.1 Coomassie staining

The gels were subjected to fixing solution containing 50% methanol, 10% acetic acid and 40% ddH_2O. After 45 minutes, fixing solution was removed and 0.2% Coomassie Brilliant Blue R-250 solution was added and the gels were incubated for 45 minutes at room temperature. Destaining was performed until the desired resolution of the bands was achieved [170].

3.6.2 Immunoblotting

Protein expression levels were determined using SDS-PAGE followed by Western blotting. After SDS-PAGE electrophoresis, the resolving gel was incubated in protein transfer buffer (PTB) [3.03g Tris-base, 14.4 glucine in 1 L ddH_2O] for 15 minutes. Two sponges, 2 Whatman^{TM} papers and a nitrocellulose membrane were submerged in PTB prior to assembling the protein transfer apparatus. Nitrocellulose membrane was placed between two pieces of Whatman paper^{TM} with sponges on either side. A Biorad Mini-Trans Blot^{TM} transfer unit was used to perform protein transfer from the gel to the nitrocellulose membrane. The unit was subjected to a constant voltage of 25 V for 16 hours at 4˚C. Subsequently, the membrane was removed and washed three times with TTBS then placed in 5% non-fat skim milk in TTBS for 1 hour in order to block non-specific binding sites. Following the blocking, the membrane was washed twice for 10 minutes in TBS then probed with the primary antibody at an appropriate concentration for 2 hours (table 3.4). Following this step, the membrane was washed three times with TTBS for 10 minutes and subjected to secondary antibodies at an appropriate concentration for 1 hour (table 3.4). The membrane was washed three times with TTBS for 10 minutes prior to analysis on Odyssey^{TM} infrared imager. The gel was scanned with the Odyssey^{TM} software which detected an infrared signal from the infrared conjugated antibody at $\lambda_{excitation}$=778nm, $\lambda_{emission}$=795nm (IR 800) or $\lambda_{excitation}$=676nm, $\lambda_{emission}$=693nm (IR 680) [171].

Table 3. 4. Antibodies

List of primary and secondary antibodies and their dilutions.

1˚ Antibody	Dilution	2˚ Antibody	Dilution
anti-VDAC/Porin	1/200	Anti-mouse FITC	1/500
Goat anti-LDH	1/700	Anti-goat FITC	1/500
Rabbit anti-acetylated lysine	1/200	Anti-rabbit FITC	1/500
Rabbit anti-SIRT1	1/200	Anti-rabbit FITC	1/500

3.7 LDH siRNA

To decrease the expression of nuclear LDH in P19 cells, these were plated in 75 cm^2 culture grade flask and grown to 80-90% confluency in α-MEM with 5% FBS in the absence of antibiotics at standard culture conditions. Antibiotics are known to cause cell death during transfection. The siRNA solution was prepared as described in the manufacturer's protocol with adjusted volumes. Solution A included 25 μL of siRNA duplex or negative control siRNA (ctrlRNA) diluted in 475 μL of transfection medium. Solution B was comprised of 25 μL of transfection reagent in 475 μL of transfection medium. Solution A and B was combined and incubated for 30 minutes at room temperature. The cells were rinsed with 3 mL of transfection medium and the mixture of Solution A and B was added to the culture flask. The cells were overlaid for 6 hours at 37˚C in 5% CO_2. After, 2X FBS and 2X antibiotics-containing α-MEM was added without removing the transfection mixture. The cells were incubated for an additional 24 hours. The cells were either isolated at this stage or subjected to differentiation as described previously. Histones were extracted and purified from all samples and the level of histone acetylation was determined by HPLC analysis as described previously (Figure 3.7).

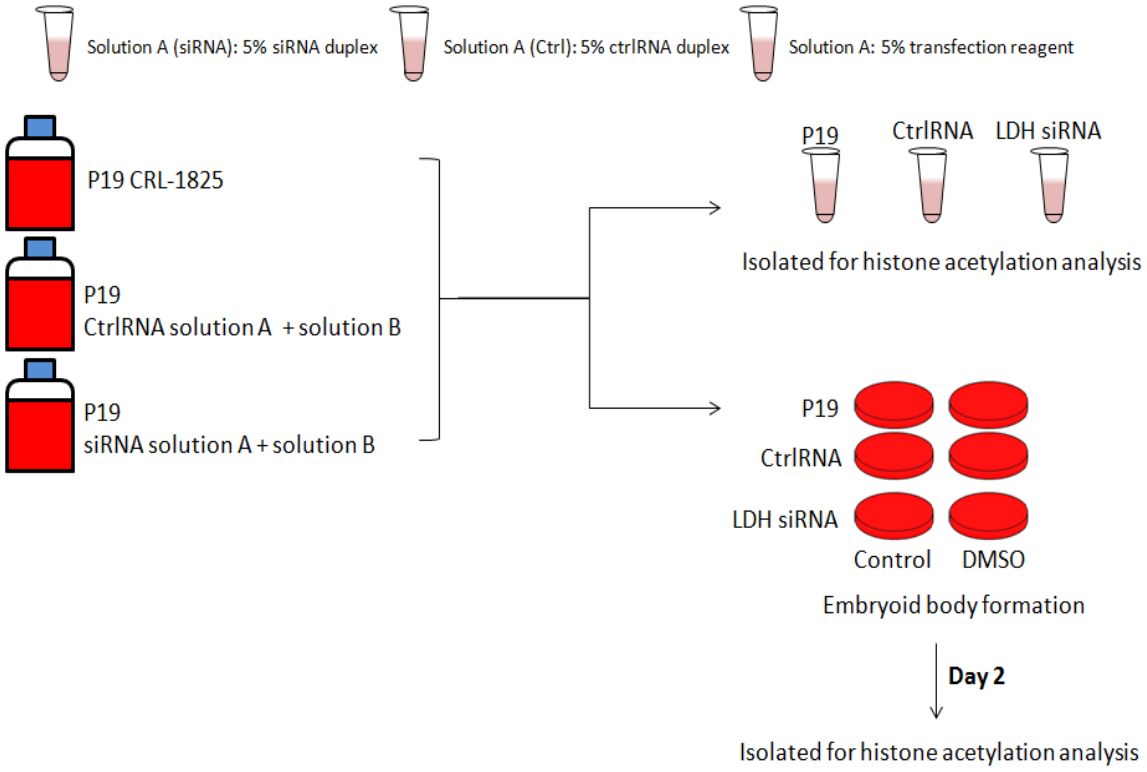

Figure 3. 8. siRNA inhibition experiment.

P19 cells were treated with control scrambled RNA and LDH siRNA as described by the manufacturer. After transfection, cells were incubated for another 24 hours. These cells were either isolated for histone acetylation analysis by HPLC as described previously or the cells were seeded for differentiation. Embryoid bodies were then isolated at day 2 and the level of histone acetylation was analysed. Note: embryoid bodies were only treated for 2 days in order to conserve the effect of LDH siRNA.

3.8 Statistical analysis

The student T-test was performed to determine the significance of results between control and differentiated cells. All experiments were performed at least in biological duplicates with 3 experimental replicates of each. The confidence interval of 95% was chosen ($p \leq 0.05$).

4. Results

4.1 Assessment of differentiation with OCT4 expression

DMSO is an established differentiating agent for P19 embryonal carcinoma cell lines [148]. DMSO (1%) was used during EB formation throughout the experiments (Figure 4.1). At day 4, cells were isolated and cell free extract (CFE) were subjected to western blot analysis for OCT4 expression. OCT4 is a master regulator of pluripotency and the expression level of OCT4 diminishes upon induction of differentiation [101]. The expression level of OCT4 was indeed shown to be decreased under 1% DMSO exposure (Figure 4.1).

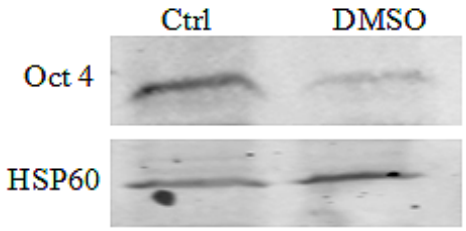

Figure 4. 1. Western blot analysis of OCT4 expression.

EBs of control and DMSO-treated cells were isolated at day 4 of differentiation. The OCT4 expression was examined in order to assess whether DMSO induced differentiation. HSP60 was used as a loading control. A representative electrogram is depicted.

4.2 Mitochondrial metabolism

4.2.1 Metabolic profile of CFE

To examine the change in metabolism, HPLC analysis was performed on CFE of undifferentiated (control) and differentiated (DMSO-treated) cells. Day 3 and day 7 was also chosen in order to demonstrate the change in metabolism as differentiation progressed. A number of metabolite standards were also subjected to analysis for peak

identity (Figure 4.2)

a)

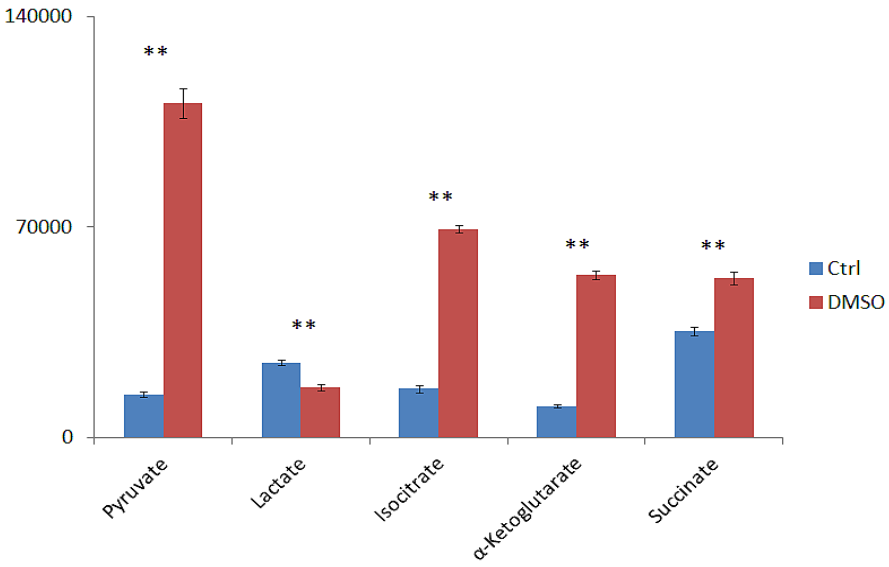

b)

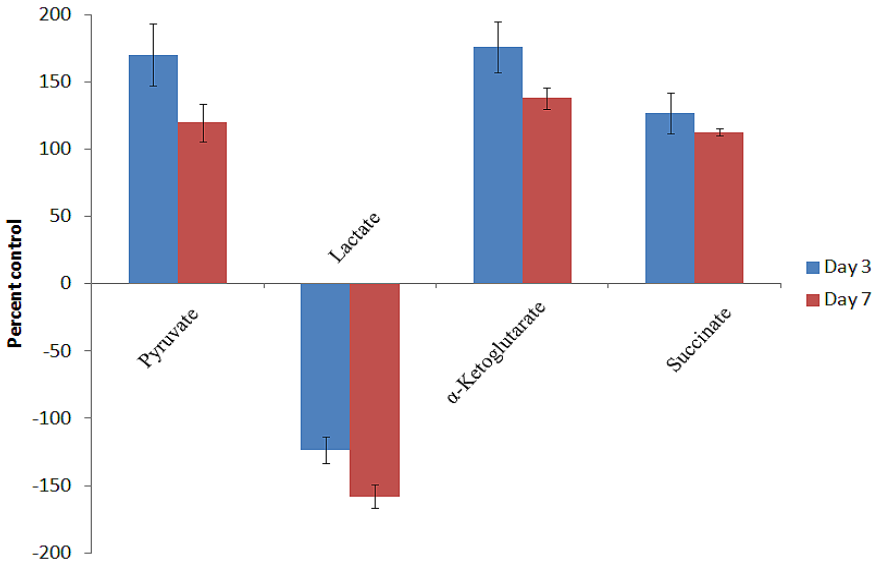

Figure 4. 2. Metabolite profile of differentiating stem cells.

a) HPLC analysis of day 4 CFE of the control and DMSO-treated cells. b) CFE metabolites in day 3 and day 7 of differentiation expressed as percentage of the control.

The negative value indicates decreased level of the metabolite. (Percentage of the control was taken as 0%) (n=3 ± SD; $p \leq 0.05$). ** Denotes a significant difference ($p \leq 0.01$).

Metabolites such as pyruvate, isocitrate, αKG and succinate were found to be significantly higher in differentiated cells, all analyzed to be significant. Lactate level, however, was found to be significantly reduced in differentiated cells compared to the control counterpart. Day 3 and day 7 metabolite profiles demonstrated similar results as the level of pyruvate, αKG and succinate was found to be increased over 100 fold. Again, the lactate presence was found to be reduced in day 3 and day 7 of DMSO-differentiated cells, thus suggesting the prominence of the TCA cycle in the differentiated cells.

To assess the level of energy metabolism, CFE of undifferentiated and differentiated cells were incubated in a) acetoacetate, a ketone body that can be metabolised into acetyl-CoA to produce energy via the TCA cycle, and b) succinate, an intermediate substrate of TCA cycle. The reaction was allowed to run for 1 hour. Consumption of these metabolites was then studied with HPLC. Additional experiments were performed with KCN in order to confirm that the consumption of acetoacetate and succinate was indeed a result of the TCA cycle and oxidative phosphorylation (Figure 4.3a,b). CFE of differentiated cells were found to consume significantly higher acetoacetate and succinate.

a)

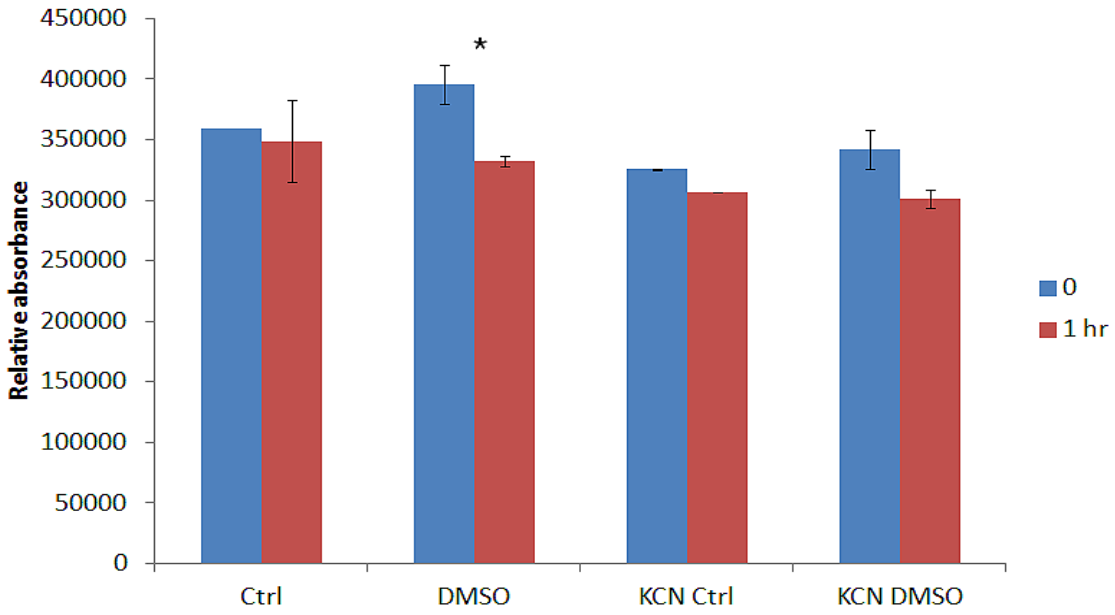

b)

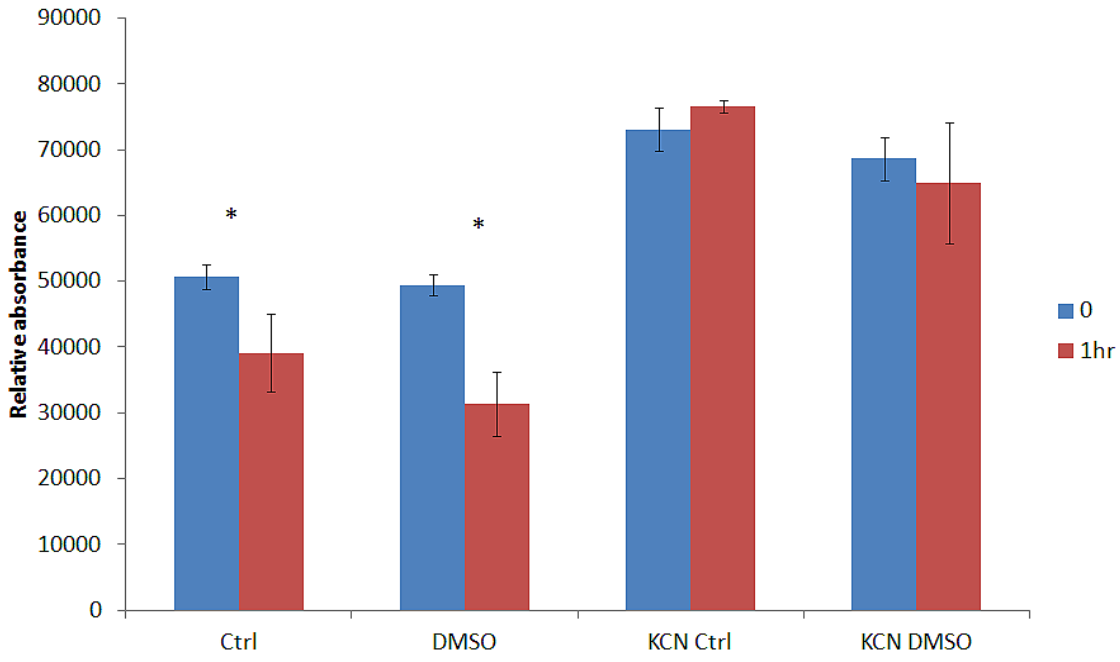

Figure 4. 3. Acetoacetate and succinate consumption of CFE.

a) DMSO-differentiated cells were shown to consume higher levels of acetoacetate. KCN treatment demonstrated that the consumption was indeed through metabolic enzymes. b) HPLC analysis of CFE succinate consumption. Undifferentiated (control) and

differentiated (DMSO) CFE both demonstrated consumption of succinate. However, DMSO-treated cells demonstrated trend of higher succinate consumption compared to the control. KCN treatment demonstrated that the succinate consumption was through metabolic activity. (n=3 ± SD; p≤0.05). * Denotes a significant difference (p ≤0.05)

As the metabolites in the oxidative phosphorylation were disparate between the undifferentiated and differentiated cells, it was important to assess the key enzymes involved in central energy metabolism.

4.2.2. Assessing enzymatic activities by BN-PAGE

To examine the enzymatic activity, cytosolic and mitochondrial proteins were isolated and prepared for BN-PAGE. The enzymes were probed using activity assay (recipes provided in Table 3.3) (Table 4.1).

Table 4. 1. In-gel activity of central metabolic network in cytoplasm and mitochondria.

Control and DMSO-differentiated cells were grown and isolated at day 3 and day 7. The samples were prepared for BN-PAGE and in-gel activity assay was performed to monitor the difference in the enzymatic activities (↑=high in-gel activity, ↓= low in-gel activity, - = no discernible bands)

Enzymes	Day 3 (differentiated)	Day 7 (differentiated)
HK	↓	↑
GPI	↓	↑
PK	↓	↑
Complex I	↓	↑
Complex II	↓	↑
Complex IV	↓	↑
Succinyl CoA transferase	↓	↑
Malate dehydrogenase	↑	↓
G6PDH	-	-
ICDH-NAD$^+$	-	-
KGDH	-	-
Malic enzyme	-	-
LDH (Cyt. & Mito.)	-	-
GAPDH	-	-

Alanine transaminase	-	-
Aspartate transaminase	-	-

Enzymes in glycolysis (HK,GPI and PK) and oxidative phosphorylation (Complex I, Complex II and Complex IV) were all found to have increased activity in day 7 compared to day 3 (Figure 4.4). Undifferentiated cells, however, consisted of very faint or no discernible bands. This may be due to the limits of BN-PAGE and not the presence of the enzyme. More sensitive techniques such as immunochemistry could reveal the expression. However, as the study mainly focuses on functional proteomics and metabolomics, no further experiments were performed to identify the expression of undetected enzymes. The enzyme activity was confirmed by excising the site of activity band and confirming with HPLC (Figure 4.5).

a)

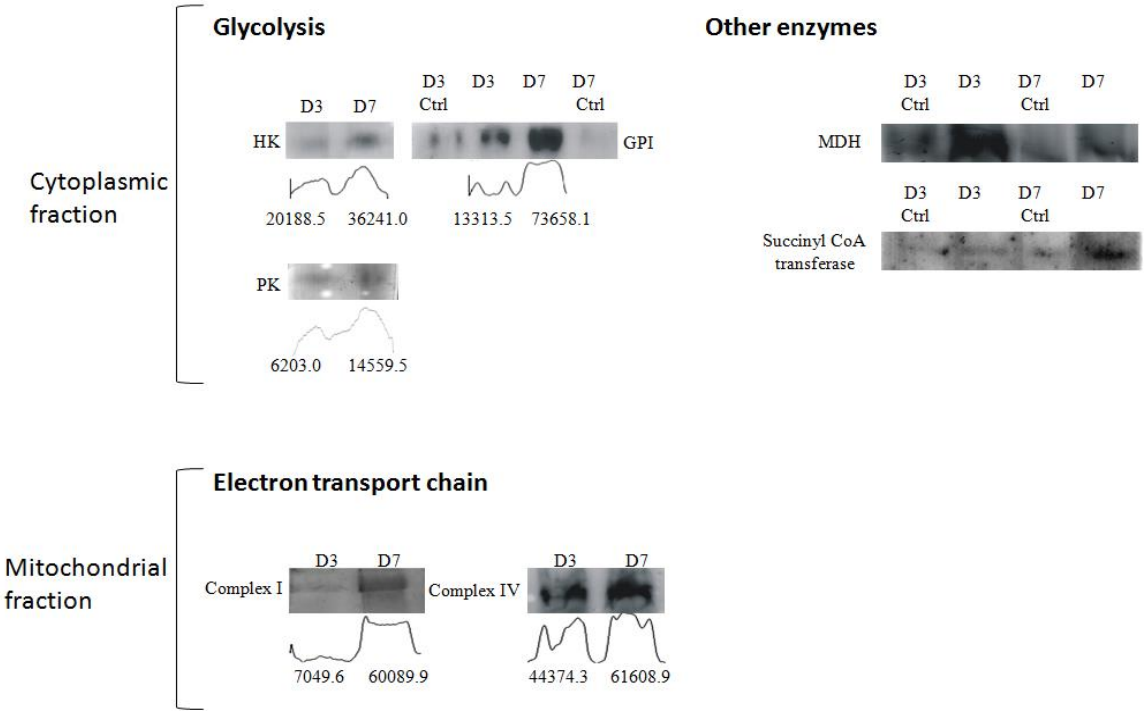

b)

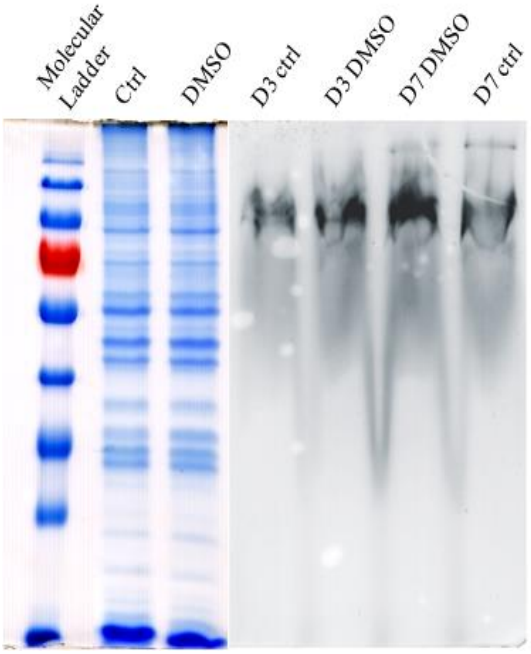

Figure 4. 4. BN-PAGE in-gel activity assay

a) Activity assays were performed for various metabolic enzymes. Image J software was used to quantify the band density. A representative electrogram is depicted. All the enzymes were assayed with control counter parts as shown in GPI and MDH in order to validate the differences are caused by differentiation. b) Equal loading was assured by staining total proteins with Coomassie R-250. Representative electrograms are depicted. Note: Complex IV enzymatic activity is depicted in the illustration.

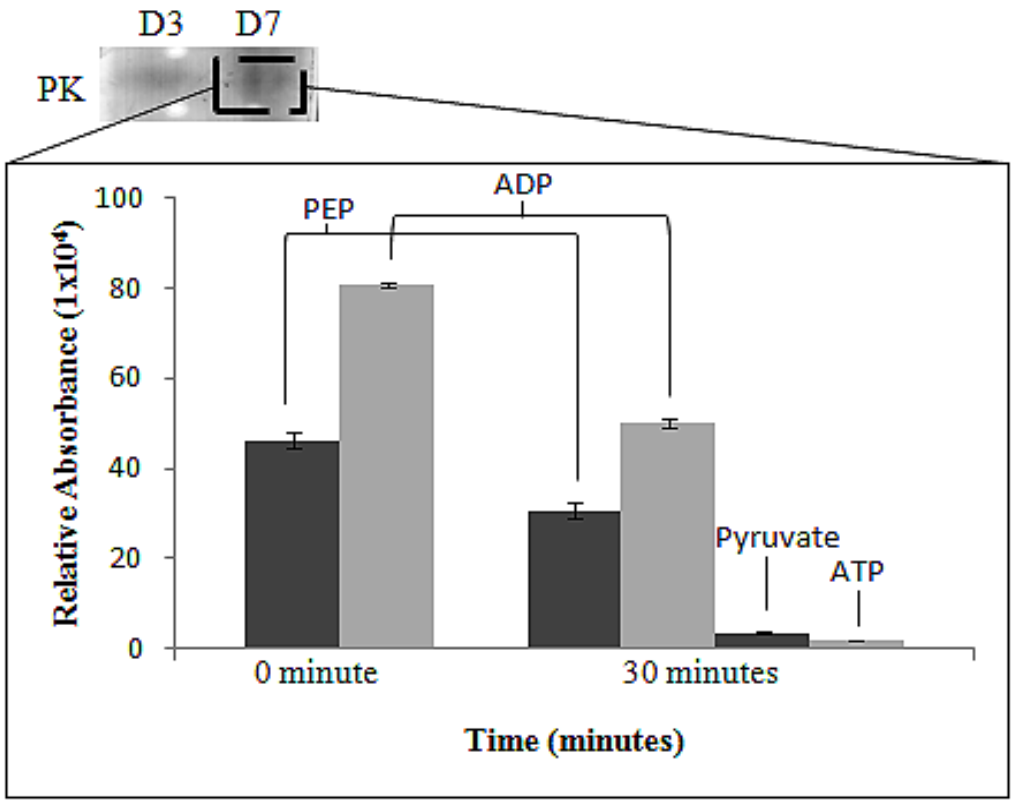

Figure 4. 5. A representative HPLC analysis performed on BN-PAGE activity assays.

The site of activity on the gel was excised and placed in reaction mixture containing appropriate substrates. The gel was incubated for 30 minutes. The consumption of substrates and formation of products were analyzed. For instance, PK activity band was excised and placed in reaction mixture containing PEP and ADP. The gel was incubated for 30 minutes and the sample was injected into HPLC. The level of PEP and ADP was found to decrease as the enzyme consumed these substrates. Pyruvate and ATP were found to increase after 30 minutes, confirming that the enzyme on BN-PAGE was indeed PK. ($n=3 \pm SD$; $p \leq 0.05$).

4.2.3 Mitochondrial ATP production

The enzymes involved in ETC and TCA cycle intermediate metabolites were observed to be increased in differentiated cells, suggesting an increased mitochondrial activity. Thus, it was important to assess and compare the ability of mitochondria to produce ATP in undifferentiated and differentiated cells. In order to examine the ability of mitochondria to generate ATP, the mitochondrial subcellular fraction of control and

DMSO-treated cells were isolated and incubated in 2 mM succinate or malate, TCA intermediates, and 0.5 mM ADP for 1 hour. HPLC analysis suggests that the presence of TCA cycle substrates and ADP, in the differentiated mitochondrial fraction produced higher levels of ATP (Figure 4.6).

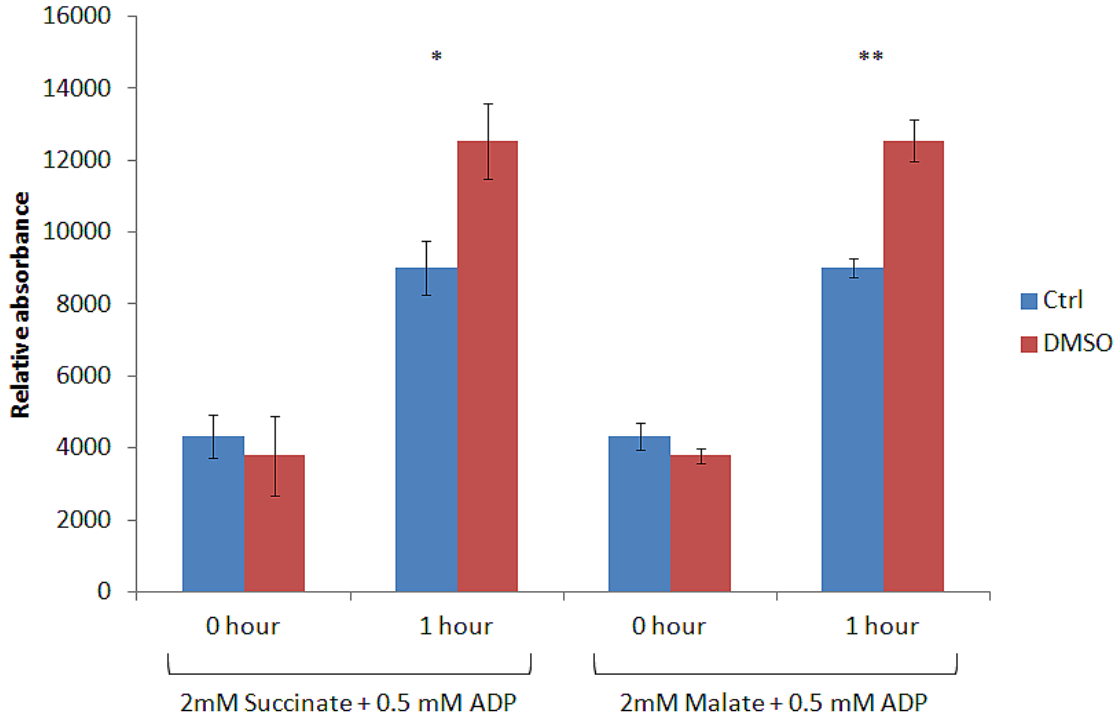

Figure 4. 6. ATP production in the mitochondria.

Mitochondrial fraction from control and DMSO-treated cells were incubated with 2 mM succinate or malate along with 0.5 mM ADP for one hour at 37 ˚C. Samples were boiled to stop the reactions and the amount of ATP was analyzed via HPLC analysis. (n=3 ± SD; $p \leq 0.05$) * Denotes a significant difference ($p \leq 0.05$). ** Denotes a very significant difference between the control and DMSO-subjected cells ($p \leq 0.001$).

As the activity of mitochondrial enzymes were elevated and mitochondrial fraction demonstrated higher ATP producing ability in differentiated cells, it was

imperative to investigate the changes in mitochondrial activity and biogenesis during differentiation of these stem cells.

4.2.4 Mitochondrial activity and biogenesis

Rhodamine dye is a well-known chemical agent that can be utilized to monitor membrane potential of mitochondria within the cell [172,173]. EBs were isolated and disaggregated at day 4. Cells were then seeded on coverslips and allowed to adhere overnight. Rhodamine dye was applied as described previously in the methods section. The results from microscopy showed that DMSO-exposed cells consisted of higher mitochondrial activity, even at an earlier stage of differentiation (Figure 4.7).

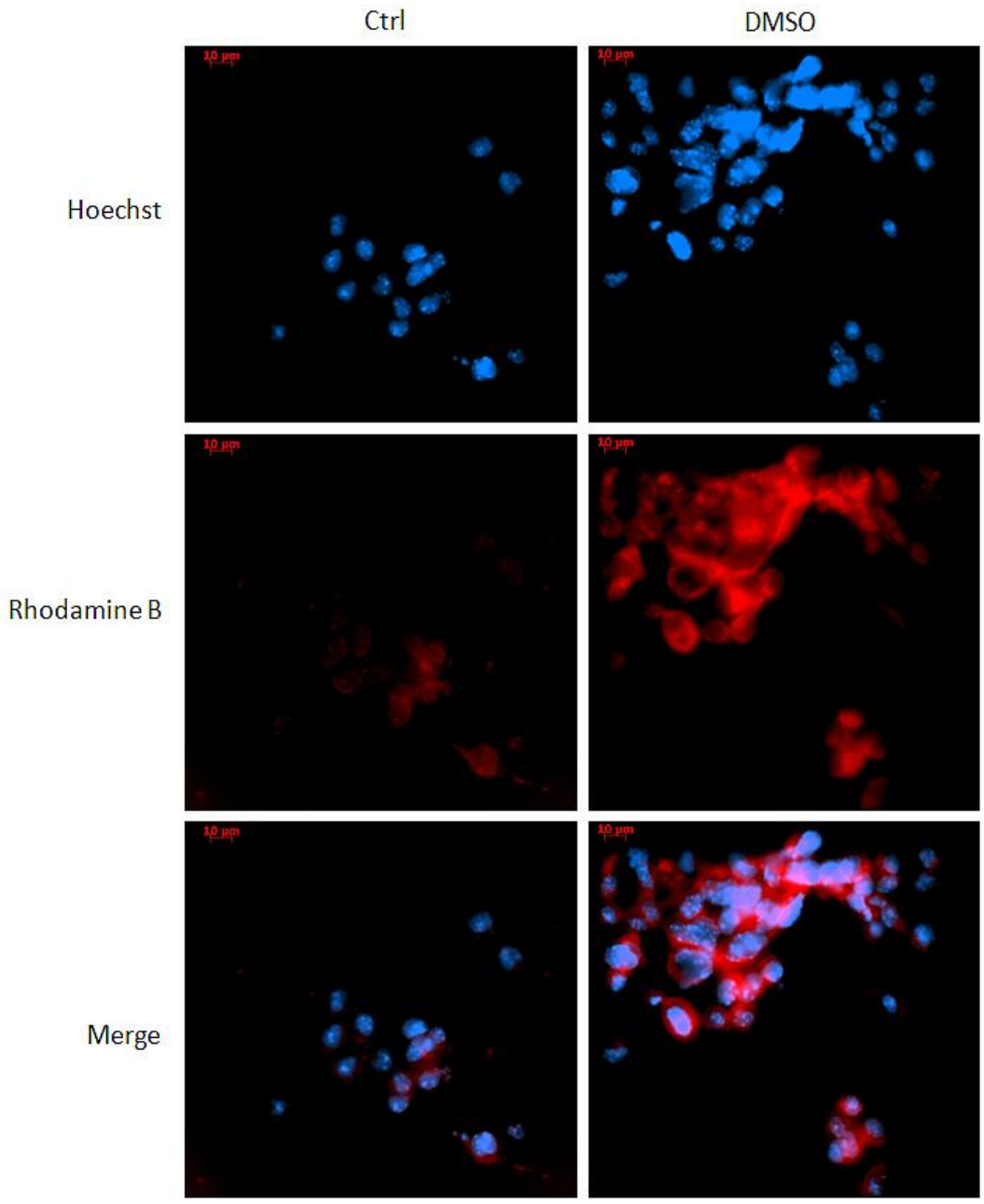

Figure 4. 7. Visualization of mitochondrial membrane potential via Rhodamine B dye.

Control and DMSO-treated EBs were disaggregated and seeded on coverslips. The cells were subjected to Hoechst, for nuclear identification, followed by rhodamine to visualize mitochondrial membrane potential. The cells were imaged on a deconvolution fluorescent microscope. (Scale bar = 10 μm). A representative micrograph is depicted in the figure.

To examine the difference in mitochondrial biogenesis between undifferentiated and differentiated cells, immunofluorescent microscopy was performed to visualize the level of VDAC, a mitochondrial marker, and PGC-1α, a master regulator of mitochondrial biogenesis. The results indicate elevated expression of VDAC and PGC-1α in DMSO-induced differentiated cells (Figure 4.8 and Figure 4.9).

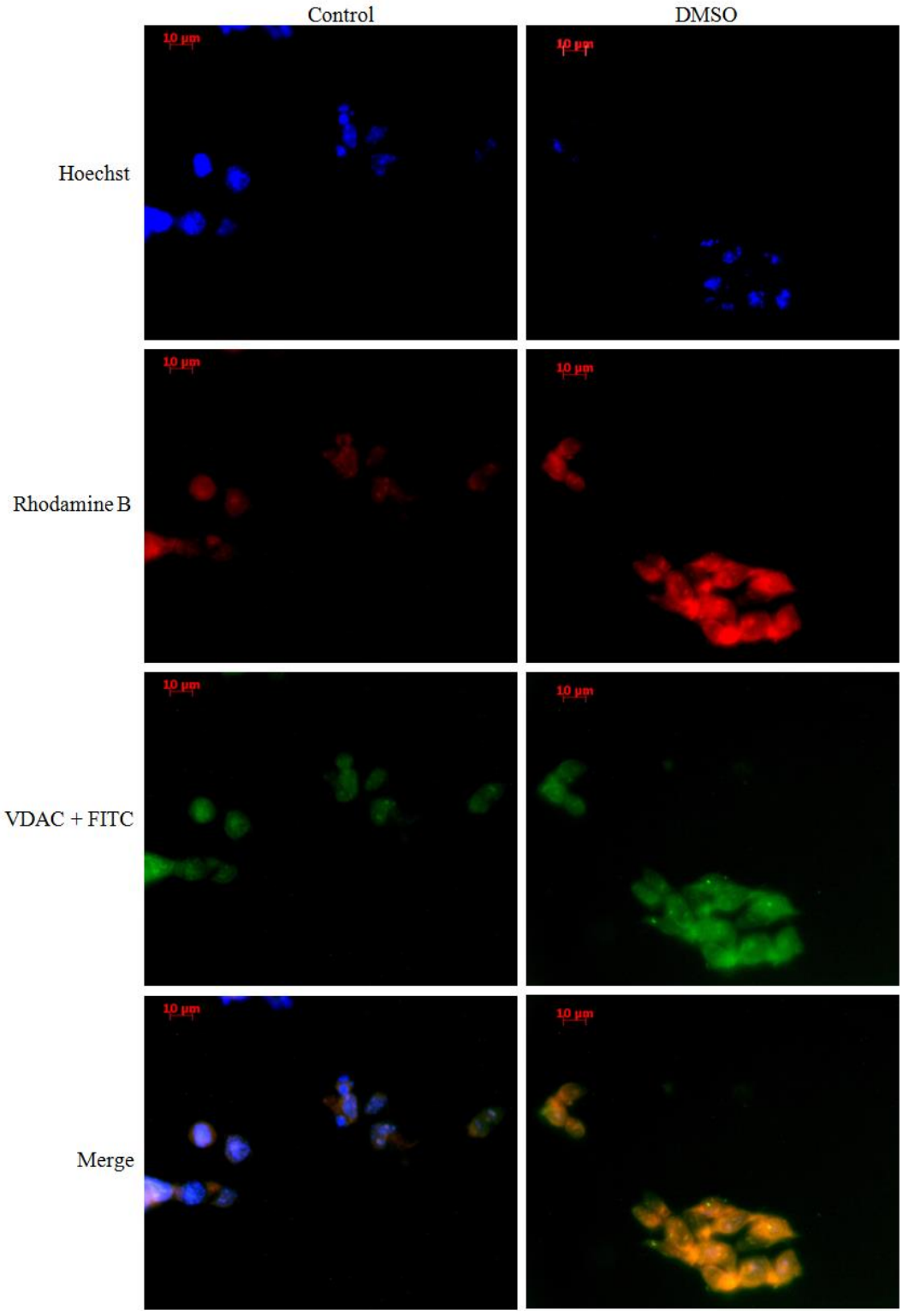

Figure 4. 8. VDAC expression in undifferentiated and differentiated cells.

In-cell western was performed using Hoescht as a counter stain to visualize the nucleus (blue), rhodamine B dye (red) and anti-VDAC primary antibody conjugated with FITC-

tagged secondary antibody (green). A deconvolution microscope was used to visualize the cells after treatment. (Scale bar = 20 μm). A representative micrograph is depicted in the figure.

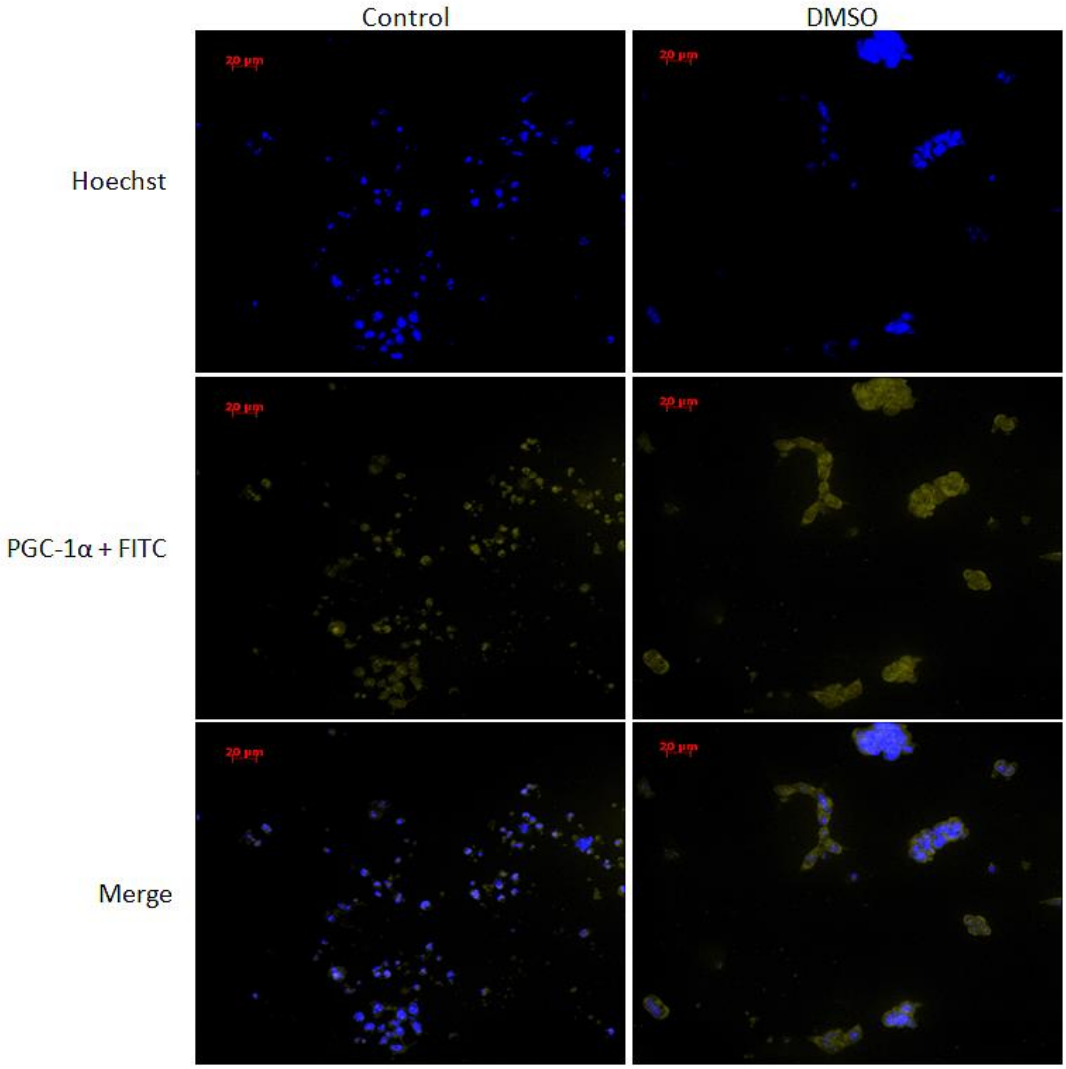

Figure 4. 9. PGC-1α expression in undifferentiated and differentiated cells.

In-cell western was performed using Hoescht as a counter stain to visualize the nucleus (blue) and anti-PGC-1α primary antibody conjugated with FITC-tagged secondary antibody (yellow). A deconvolution microscope was used to visualize the cells after treatment. (Scale bar = 20 μm). A representative micrograph is depicted in the figure.

Overall, these results suggest that mitochondrial activity and mitochondrial biogenesis undergo drastic changes during differentiation, even at an earlier stage of differentiation.

4.3 Nuclear metabolism

Previous work from our laboratory has uncovered an intricate connection between metabolism and epigenetics in HepG2 cells [80]. Nuclear lactate dehydrogenase was found to participate in the regulation of histone deacetylation by modulating NAD^+ concentration. These findings prompted us to investigate the potential role of nuclear metabolism in stem cell differentiation.

4.3.1 Nuclear purity

Prior to starting nuclear experiments, it was pivotal to assess nuclear purity in subcellular fractionations. Cells were separated into nuclear and cytosolic fractions through differential centrifugation as described in the methods section. Both fractions were probed for actin to examine potential cytosolic contamination in the nuclear fraction (Figure 4.9). Absence of actin expression in nuclear fraction confirmed the purity of nuclear fractions obtained during differential centrifugation.

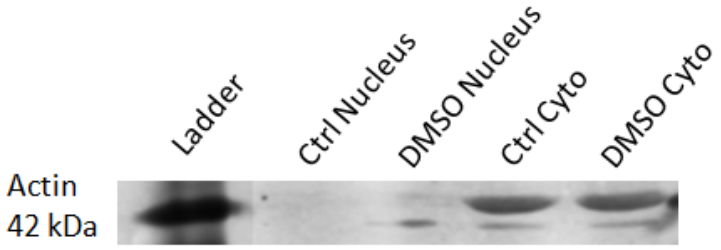

Figure 4. 10. Western blot analysis of nuclear purity.

Control and DMSO-treated cells were isolated and the cytosolic and nuclei were differentiated. Both fractions were tested for presence of actin to examine the purity of nuclear fraction.

4.3.2 Preliminary work

HPLC analysis was performed to examine the differences in the concentrations of key metabolites in the nucleus. Nuclear contents indicated that there were marked differences in metabolite levels in undifferentiated and differentiated cells. Differentiating cells consisted of generally higher metabolite level with the exception of acetate (Figure 4.10).

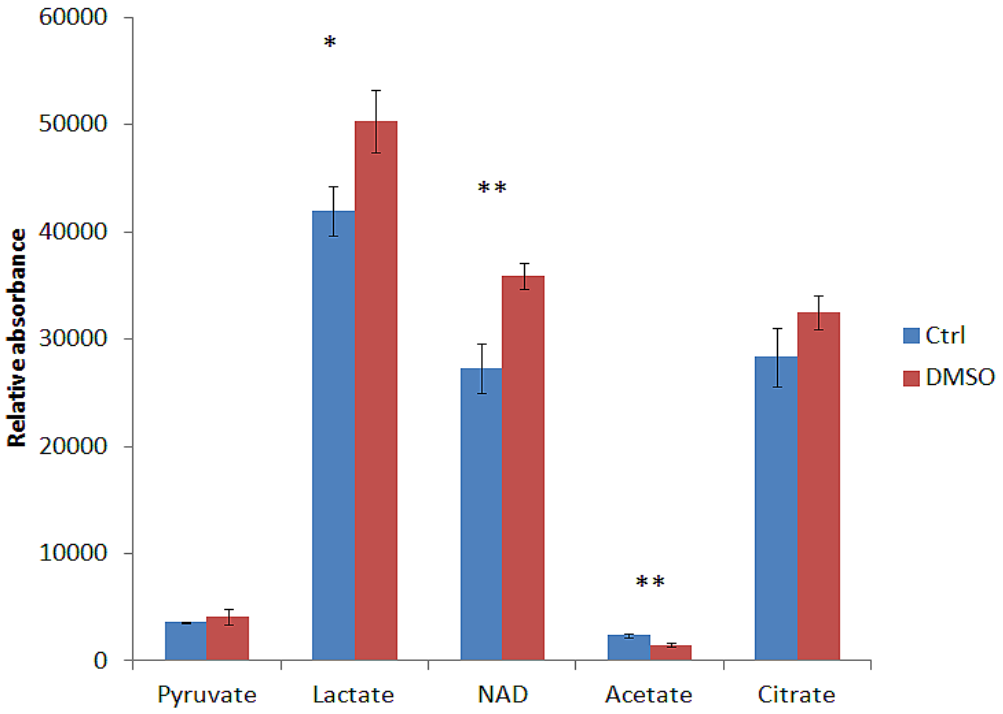

Figure 4. 11. Nuclear metabolic profile in control and DMSO-treated cells.

Nuclei were isolated from undifferentiated and differentiated cells and metabolic profile was obtained from HPLC analysis. (n=3 ± SD; $p \leq 0.05$). *Denotes a significant difference ($p \leq 0.05$). **Denotes a very significant difference ($p \leq 0.01$).

The presence of various metabolites and disparate metabolite levels indicates possible localization of metabolic enzymes in the nucleus. To determine this, nuclear subcellular fractions were isolated and subjected to BN-PAGE. Several metabolic enzymes were detected (Table 4.2). The enzymes LDH, ACL, PK and ICDH were prominent in the nucleus. The localization and function of nuclear ACL has been previous reported [73]. Although LDH has also been previously discovered in the nucleus, the role of this enzyme in the nucleus remained elusive to date.

Table 4. 2. In-gel activity of metabolic enzymes in the nucleus

The isolated nuclei from DMSO-differentiated cells (day 3 and day 7) were subjected to BN-PAGE. Enzymes from central metabolism were probed using activity assay (previous described) to examine the presence of these enzymes. (↑=high in-gel activity, ↓= low in-gel activity, - = no discernible bands).

Enzyme	Day 3	Day7
LDH	↑	↓
ACL	↓	↑
PK	↓	↑
ICDH	↑	↓
G6PDH	-	-
GPI	-	-
MDH	-	-
ME	-	-

No discernible band of indicative of the other enzymes such as G6PDH, GPI, MDH and ME, may be due to the limits of BN-PAGE and not the absence of the enzymes. More sensitive techniques could be used to further analyze the presence of these enzymes in the nucleus. As the role of nuclear LDH has been previously identified in a HepG2 cell line, particular attention was given to delineate possible roles of nuclear LDH in the differentiating stem cells.

4.3.3 Nuclear lactate dehydrogenase

To determine whether nuclear LDH plays a role in differentiation, nuclear fractions from undifferentiated and differentiated cells were subjected to in-gel activity assays. To confirm whether the bands were LDH, the activity bands were excised and placed in a reaction buffer containing 2 mM lactate and 0.5 mM NAD^+. The reaction mixture was incubated for 30 minutes and lactate consumption was monitored (Figure 4.12).

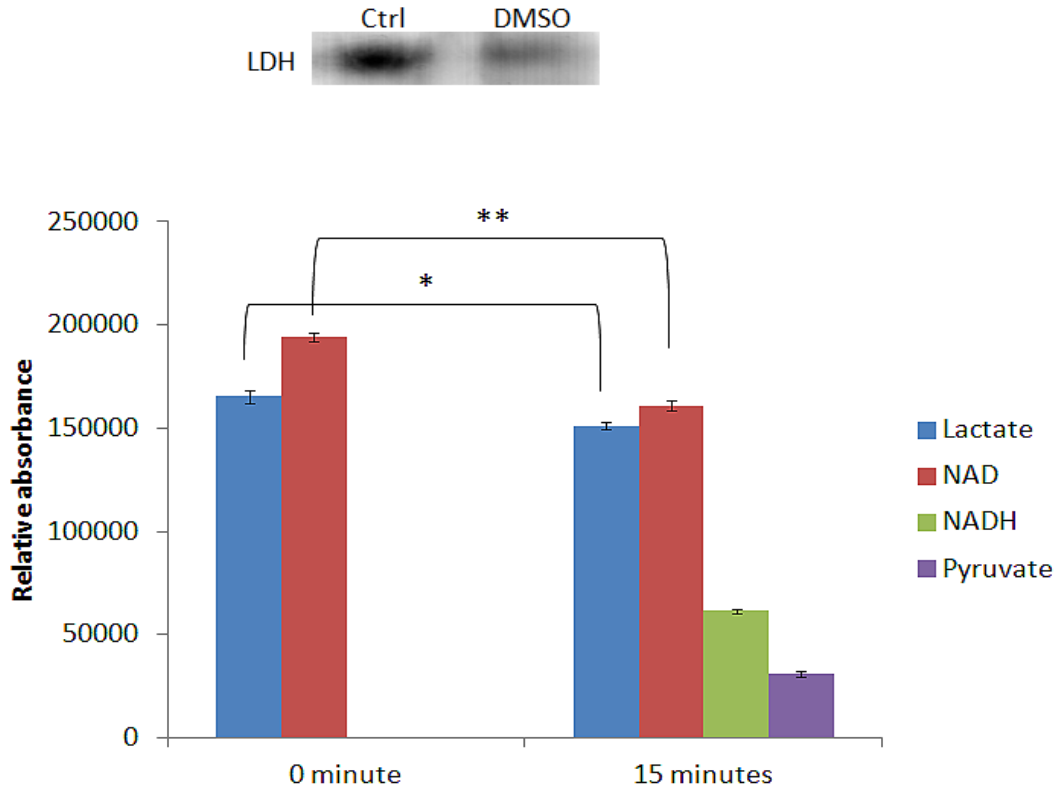

Figure 4. 12. LDH in-gel activity assay and HPLC confirmation.

Nuclear proteins (60 µg) was loaded into a blue native gel and subjected to electrophoresis. An activity assay was performed for LDH. Image J software was used to quantify the band density. The band from the control LDH was then excised and incubated in a solution of 2 mM lactate and 0.5 mM NAD^+ at 37˚C for 30 minutes. Lactate consumption was monitored by HPLC. Note: Control activity bands were used as no significant LDH activity was observed from DMSO-treated cells. A representative electrogram and chromatogram is depicted. (n=3 ± SD; $p \leq 0.05$). *Denote a significant difference ($p \leq 0.01$). ** Denotes a very significant difference ($p \leq 0.001$)

4.3.4 Expression of LDH in the nucleus

LDH expression was measured by immunofluorescent techniques. Western blot, immunofluorescent microscopy and 96-well plate in-cell western were used to examine the overall LDH expression and nuclear LDH expression. As LDH-5 is known to localize in the mitochondria, anti-LDH-5 was used in immunofluorescent microscopy. The results from immunofluorescent microscopy and 96-well plate in-cell western showed that the

expression of LDH was higher in undifferentiated cells (Figure 4.13a, c). An enlarged image of microscopy represents localization of LDH-5 in nucleus (Figure 4.12b). Western blot analysis of nuclear fraction with polyclonal anti-LDH demonstrated higher expression of LDH in nucleus (Figure 4.13d).

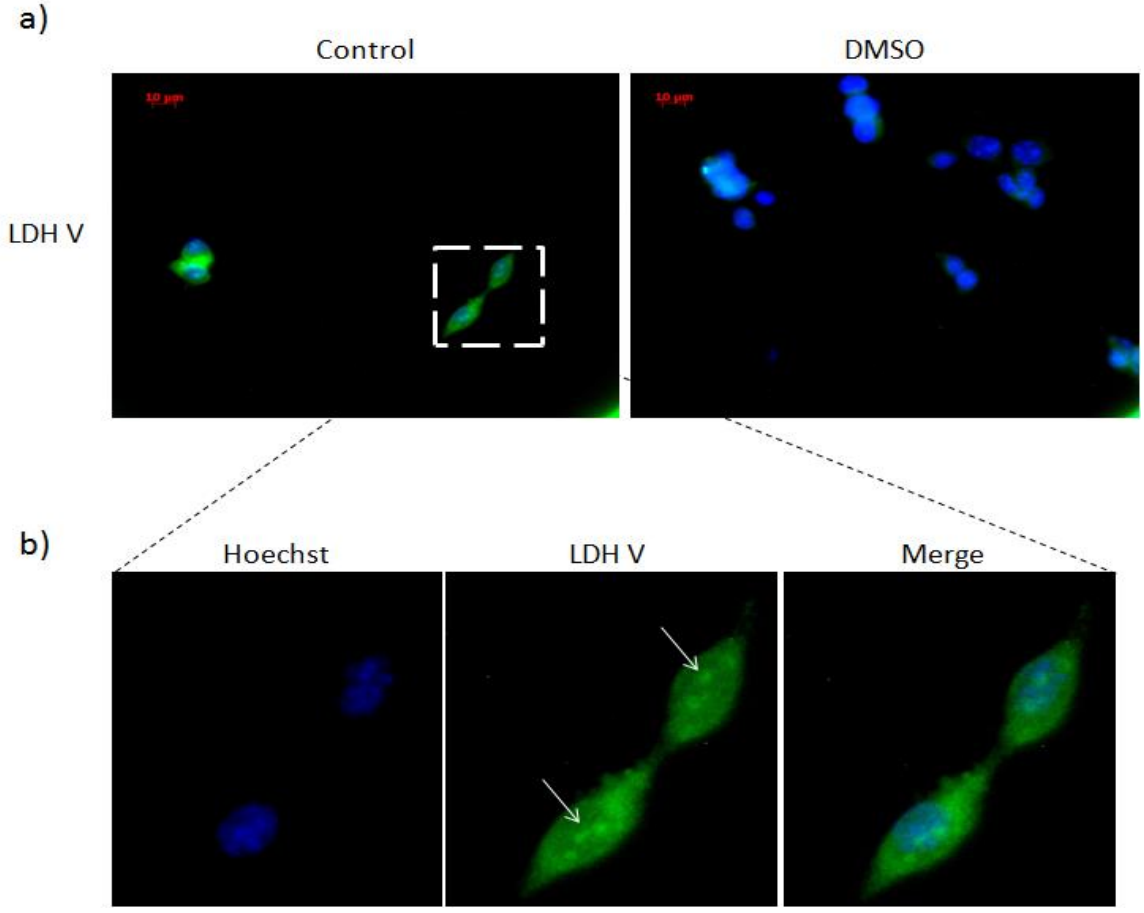

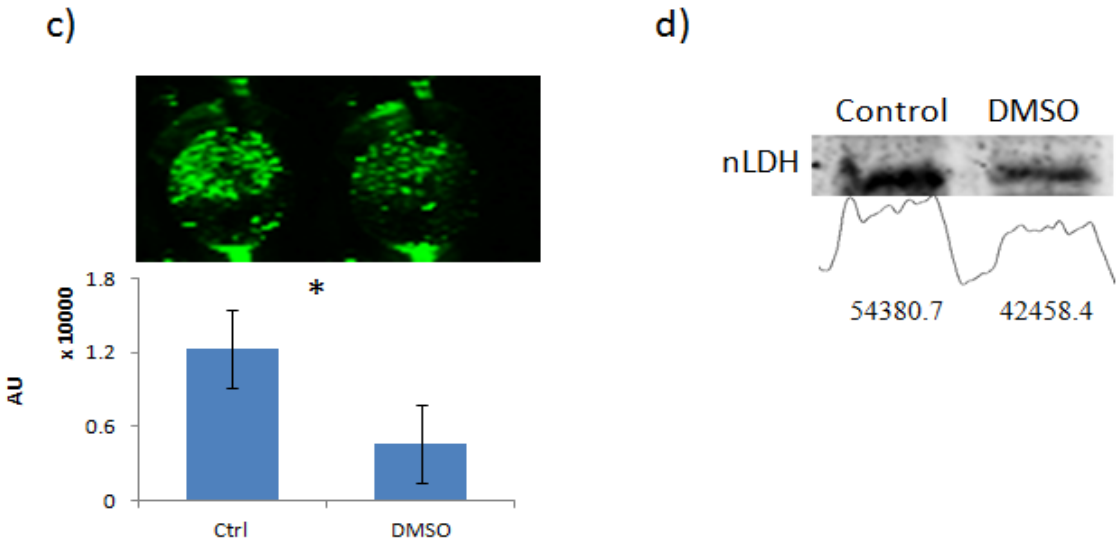

Figure 4. 13. Expression of LDH and proof of LDH nuclear localization.

a) EBs from control and DMSO-treated cells were disaggregated and seeded on coverslips. Immunofluorescent microscopy was performed with primary anti-LDH-5 and a secondary antibody conjugated to the FITC. Hoeschst was used to visualize the nucleus. The cells were visualized on deconvolution fluorescent microscope. (Scale bar = 10μm). b) Enlarged image of anti-LDH-5 immunofluorescent microscopy. White arrows indicate localization of LDH in nucleus. c) EBs were disaggregated and equal number of cells were seeded on 96-well plate. Immunostaining was performed with a primary anti-LDH and a secondary antibody conjugated to the FITC. (n=3 ± SD; $p \leq 0.05$). d) Nuclear fraction was isolated from undifferentiated and differentiated cells. Western blot was performed to examine the expression of LDH in the nucleus. Image J was used to quantify the band density. Representative results are depicted.

4.3.5 Nuclear lactate dehydrogenase, NAD^+ and sirtuins.

As nuclear LDH has been found to regulate the level of NAD^+ in HepG2 cells, the possibility that a similar role was being performed by the enzyme in the P19 embryonal carcinoma cells was assessed. First, the level of NAD^+ consumption in the nucleus was examined. Nuclear fractions of undifferentiated and differentiated cells were incubated with 2 mM NAD^+ at 37˚C for 1 hour and analyzed by HPLC. The results demonstrated that control nuclei consumed NAD^+ at an elevated rate (Figure 4.14).

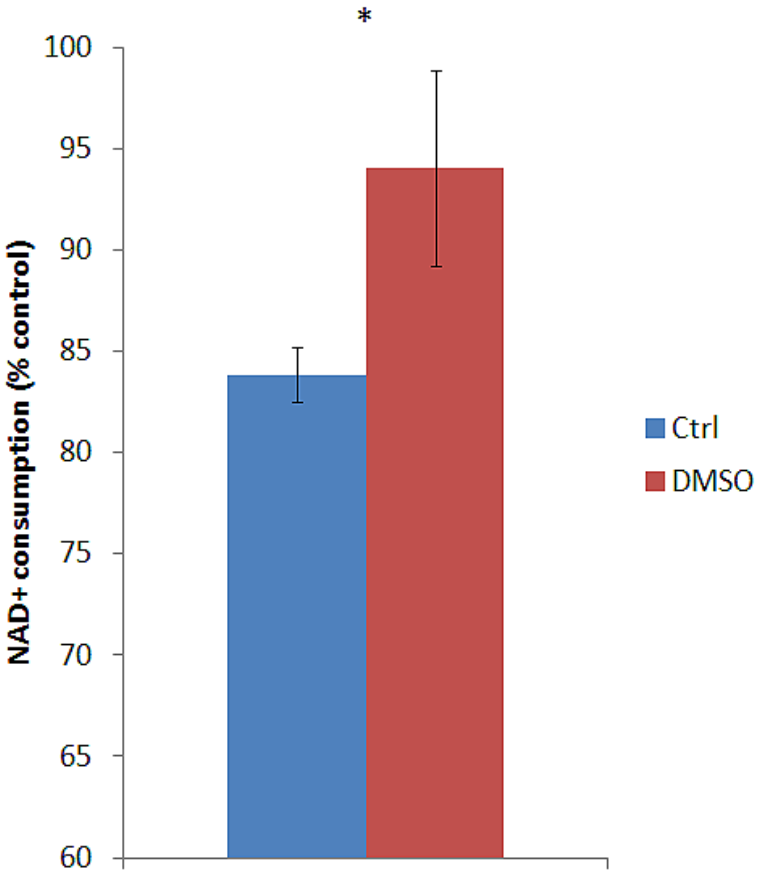

Figure 4. 14. NAD^+ utilization in the nucleus.

Whole nuclei isolated from undifferentiated and differentiated cells were incubated in a reaction mixture containing 2 mM NAD^+ for one hour at 37 ˚C. The level of NAD^+ consumption was measured and compared to time zero. n=3 ± SD; p≤ 0.05. * Denotes a significant difference ($p \leq 0.05$).

As NAD^+ participates in the regulation of sirtuin histone deacetylases, higher consumption of NAD^+ in control cells suggests increased histone deacetylation (lower acetylated histones). To examine the histone acetylation, histones were extracted and hydrolyzed from undifferentiated and differentiated cells. The results revealed that the level of histone acetylation was indeed significantly lower in the control cells (Figure 4.15).

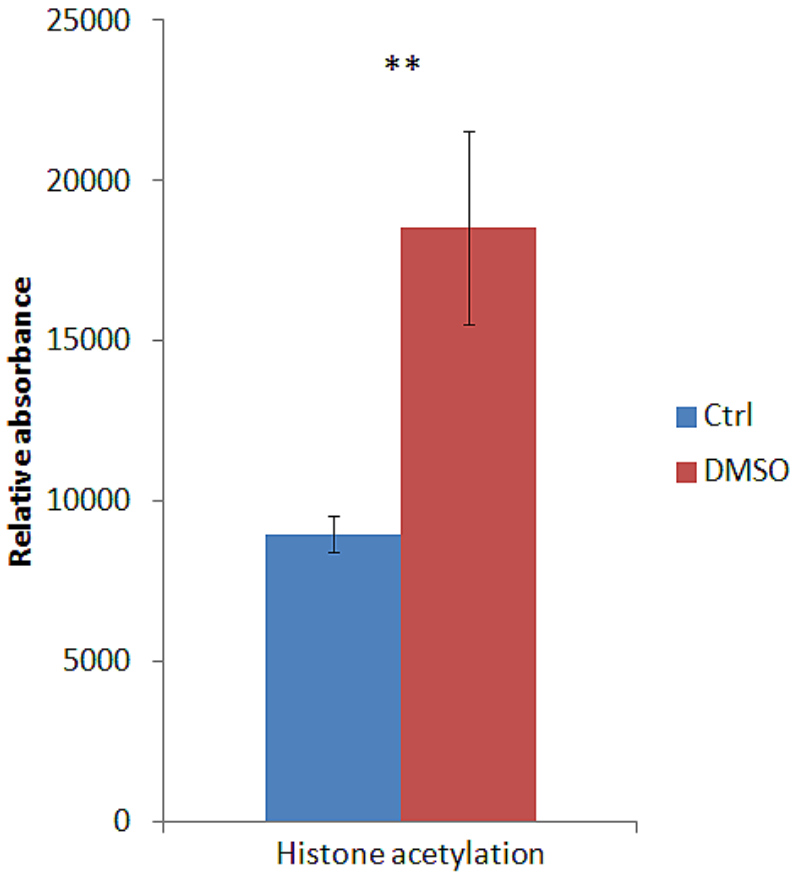

Figure 4. 15. Histone acetylation of nuclear extracts.

Nuclei from undifferentiated and differentiated cells were isolated. Histones were purified and hydrolyzed. The level of acetate from histones were then measured with HPLC at a flow rate of 0.2 mL/minute for 40 minutes. n=3 ± SD; $p \leq 0.05$. ** Denotes a very significant difference ($p \leq 0.001$).

To further support these results, the level of histone acetylation in the intact cell was examined with immunofluorescent microscopy and 96-well plate in-cell western blot. Indeed, the undifferentiated cells consisted of overall lower amounts of acetylated lysine residues as depicted in Figure 4.16a,b.

a)

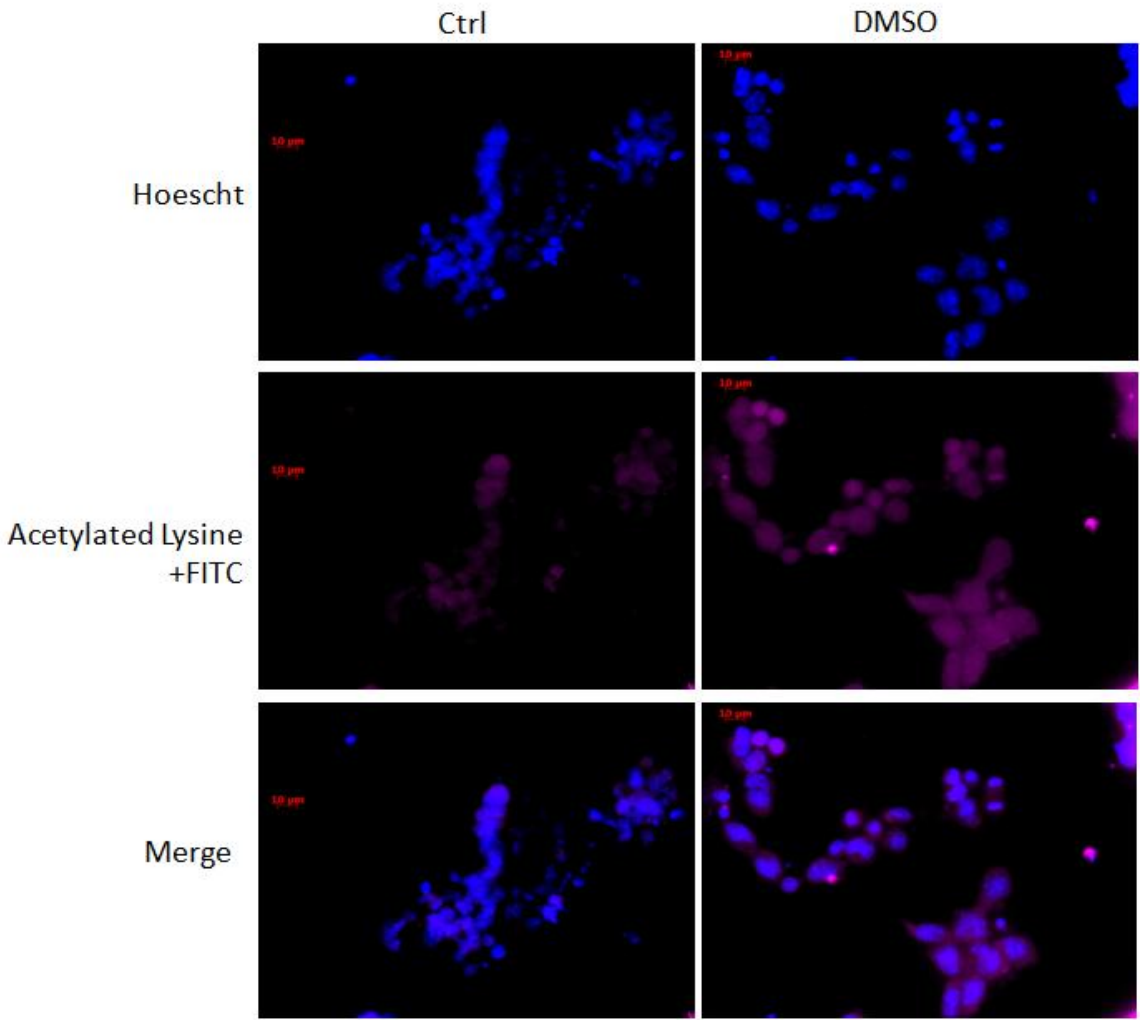

b)

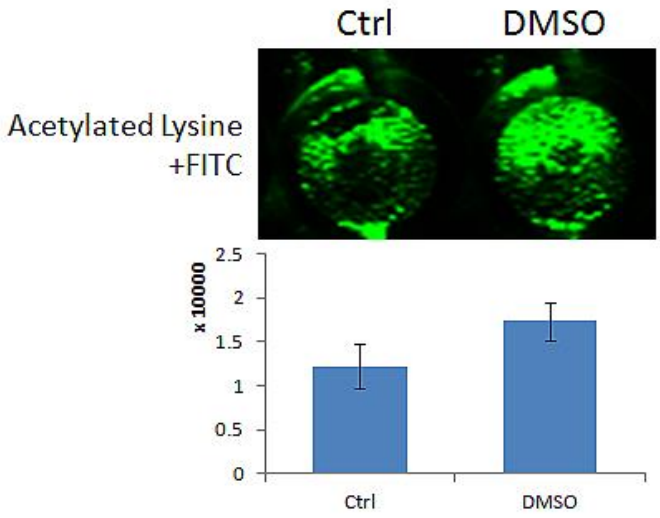

Figure 4. 16. Immunostaining of acetylated lysine residues in undifferentiated and differentiated cells.

a) Control and DMSO-treated EBs were disaggregated and grown on coverslips. Immunofluorescent microscopy was done using Hoescht to visualize the nucleus (blue) and an anti-acetylated lysine primary antibody. A FITC-tagged secondary antibody was used to visualize the images on a deconvolution microscope. (Scale bar = 10 μm). A representative micrograph is shown. b) EBs were disaggregated and equal number of cells were seeded on 96-well plate flask. Immunostaining was performed with a primary anti-acetylated lysine and a secondary antibody conjugated to the FITC. Image J was used to quantify the fluorescent density.

Sirtuins (SIRT1) are known to be responsible for histone deacetylation [49]. To examine whether the difference in histone acetylation was indeed a result of disparate nuclear LDH activity or just a result of an increase in sirtuin expression, SIRT1 expression was investigated. SIRT1 was chosen as this sirtuin is the predominantly localized in nucleus [174,175]. Utilizing anti-SIRT1 primary antibody and FITC-tagged secondary antibody, SIRT1 expression was visualized via immunofluorescent microscopy and 96-well plate in-cell western blot. The results showed that the expression of SIRT1 between undifferentiated and differentiated was relatively similar (Figure 4.17a,b).

a)

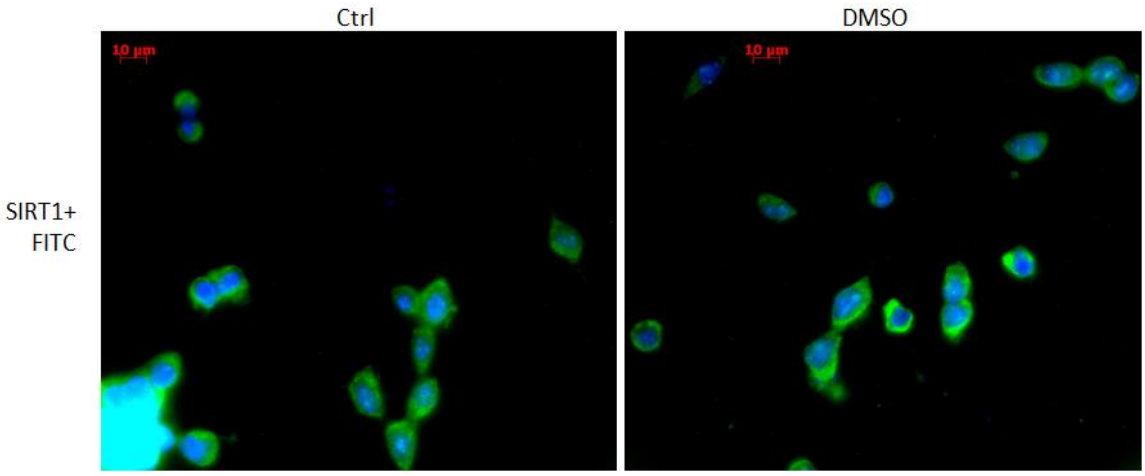

b)

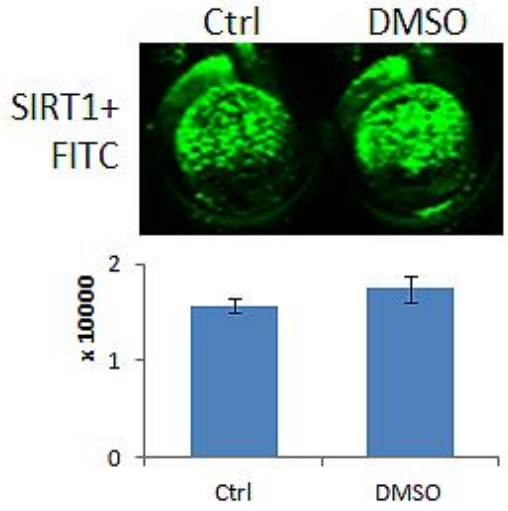

Figure 4. 17. SIRT1 expression in undifferentiated and differentiated cells.

a) EBs were disaggregated and seeded on coverslips. The cells were grown overnight and subjected to immunofluorescent microscopy. The nuclei were visualized by Hoescht and SIRT1 expression was examined by anti-SIRT1 primary antibody. A deconvolution microscope was used to visualize the cells after staining (scale bar = 20 µm). b) EBs were disaggregated and equal number of cells were seeded on 96-well plate flask. Immunostaining was performed with a primary anti-SIRT1 and a secondary antibody conjugated to the FITC. Image J was used to quantify the band density. Representative results are depicted.

These data suggest a link between LDH, NAD^+ and sirtuins. Nuclear LDH may contribute to the modulation of NAD^+ concentration in the nucleus, an event that can trigger the activity of sirtuin. Hence, an increase in deacetylation of histones would be observed during elevated nuclear LDH activity. Next, siRNA inhibition experiments were performed to solidify the evidences indicating the role of nuclear LDH in deacetylation of histones.

4.3.6 siRNA LDH inhibition

Double-stranded RNA (dsRNA) was used in attempt to inhibit LDH expression in P19 cells. LDHA specific small interfering RNA (siRNA) was chosen as LDH-5 is known to reside in the nucleus and it is comprised only of LDHA subunit. If indeed increased LDH activity in the nucleus promotes histone deacetylation, inhibition of LDH expression should result in elevated level of acetylation on histones (decreased histone deacetylation). The inhibition of LDHA via siRNA indeed revealed such a possibility (Figure 4.18). HPLC analyses indicated that histone acetylation increased by approximately 1.5-fold in the LDHA siRNA-treated cells compared to P19 non-treated and negative control siRNA subjected cells.

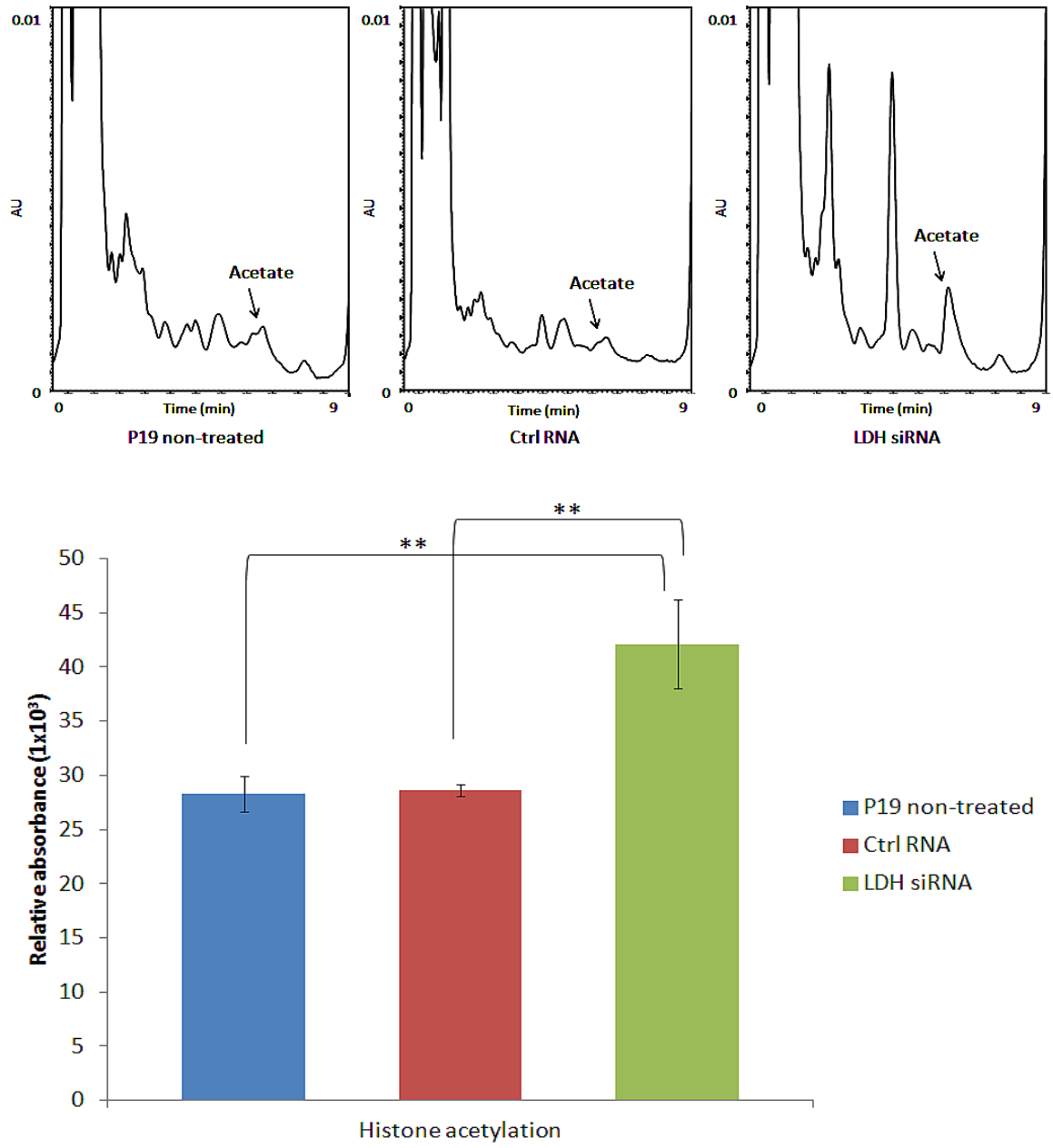

Figure 4. 18. HPLC analysis of histone acetylation under LDH siRNA inhibition.

P19 embryonal carcinoma cells were grown to 70% confluency and transfected with P19 non-treated, control siRNA and LDHA siRNA. Histones were isolated and the level of acetylation was analyzed by HPLC. (n=3 ± SD; $p \leq 0.05$) ** Denotes a very significant difference ($p \leq 0.001$).

The LDHA inhibited cells were also subjected to the differentiation protocol and histones were extracted. Differentiation was performed in liquid suspension promoting EB formation in the presence and absence of DMSO, respectively. The EBs were isolated at day 2 in order to conserve the effect of siRNA inhibition. Histones were extracted and hydrolyzed to monitor the level of acetylation. Acetylation of histones upon differentiation was again increased upon LDHA inhibition (Figure 4.19a). Differences in the level of histone acetylation among the samples were also examined. The results were expressed as percentage of control. It was shown that the LDHA siRNA inhibited cells exhibit reduced percent difference between DMSO-treated and control cells, indicating that the acetylation of histones were significantly increased in undifferentiated cells (Figure 4.19b).

a)

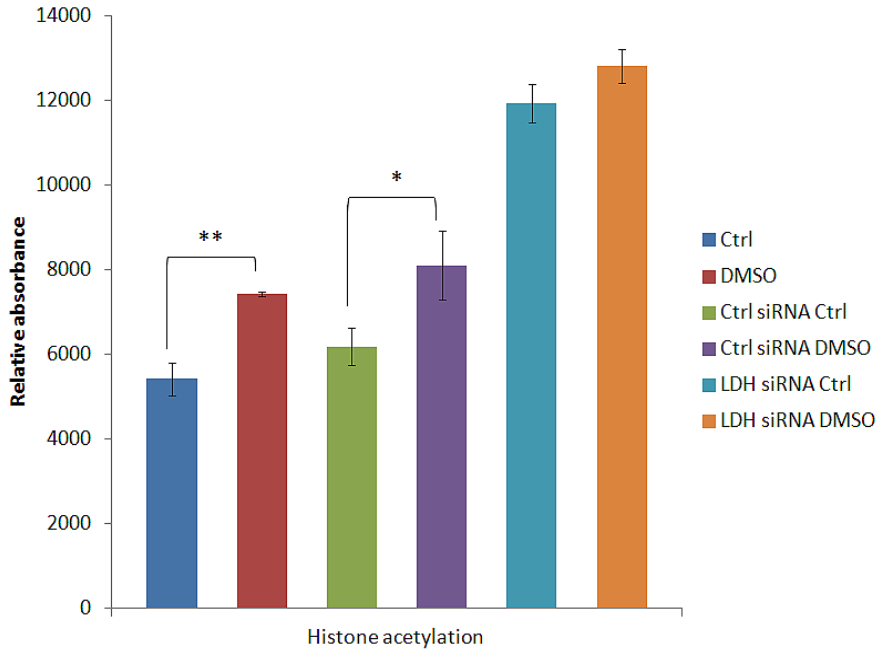

b)

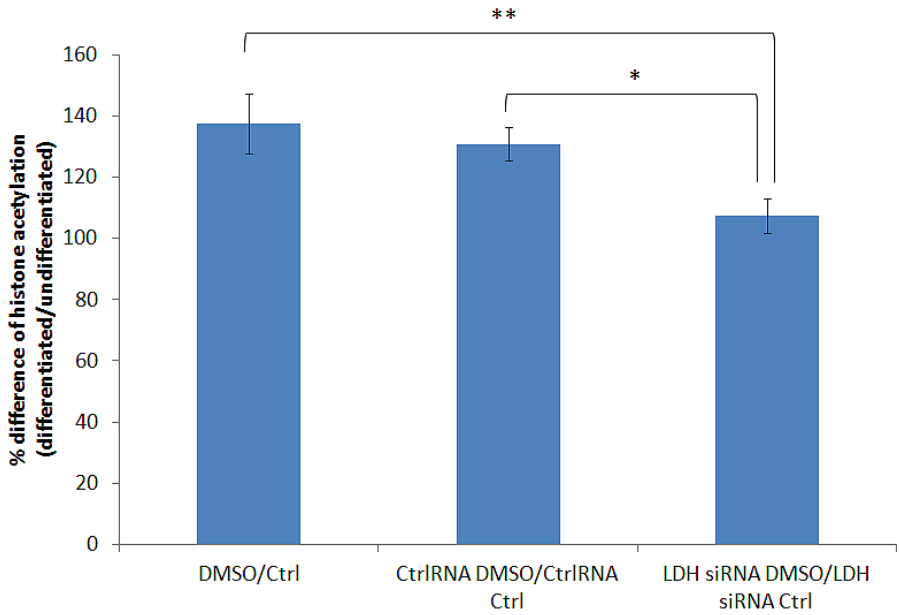

Figure 4. 19. HPLC analysis of histone acetylation under LDH siRNA inhibition during differentiation.

a) P19 embryonal carcinoma cells were grown to 70% confluency and transfected with control siRNA and LDHA siRNA. The cells were differentiated with 1% DMSO for 2 days prior to isolation (Control cells was grown without DMSO). Histones were isolated and the level of acetylation was analyzed by HPLC. b) Percent differentiation of histone

acetylation between differentiated and undifferentiated cells. (n=3 ± SD; p≤ 0.05) *Denotes a significant difference (p ≤ 0.05). **Denotes a very significant difference (p ≤ 0.001). Note: in the presence of LDHA siRNA, the difference of histone acetylation was decreased.

5. Discussion

5.1 Differentiation and metabolism in stem cells

The data suggest that DMSO treatment of the P19 embryonal carcinoma cells was effective as a morphogen, since the level of OCT4 expression, a marker of pluripotency, was sharply diminished. Hence, these DMSO-subjected cells were indeed differentiating (Figure 4.1). Since the discovery of stem cells and their potential for clinical applications, numerous studies are being undertaken in effort to fully delineate the molecular mechanism of pluripotency and differentiation. Global gene expression patterns and monitoring epigenetic regulation of ESCs have uncovered important genes involved in maintaining stemness and promoting differentiation [176,177]. Although these advancements have provided pivotal information about stem cells, the molecular frameworks governing these cells are yet to be fully understood.

Metabolism is an ideal candidate for investigation as it is considered the end products of various gene expressions and is often intimately connected to the regulation of gene expressions. For instance, activity of $NADP^+$-ICDH was shown to be up-regulated and produce the ketoacid αKG under ROS stress, which serves to neutralize ROS via non-enzymatic decarboxylation producing CO_2 and the organic acid, succinate. Accumulation of succinate can then stimulate hypoxia inducible factor-1α (HIF-1α) translocation by inhibiting prolyl hydroxylase 2 (PHD2). This nuclear translocation of HIF-1α then promotes hypoxic gene programs which encourage cell survival, glucose utilization, substrate level phosphorylation and glycolysis [178]. Metabolic enzymes are

also shown to participate in gene expression. GAPDH was found to serve as a co-activator to regulate the expression of histone H2B. The interaction, however, between GAPDH and DNA is suggested to be indirect [179]. However, studies identifying the connection between metabolism and stem cell differentiation are only beginning to emerge.

In the present work, DMSO-induced differentiation leads to the accumulation of elevated levels of TCA cycle intermediates and oxidative metabolism-related metabolites such as succinate, αKG, isocitrate and pyruvate (Figure 4.2a). Similar observations were evident at day 3 and day 7 stage of differentiation, thus suggesting drastic changes in metabolism (Figure 4.2b). Metabolic fluctuations in P19 cells and other types of stem cells have been indirectly shown [152,157,180]. These studies all demonstrate metabolic changes are necessary for the proper differentiation of stem cells. However, the primary focus on metabolic changes has been at the gene expression or protein expression levels. The activities of enzymes involved in this process has yet to be demonstrated, a shortcoming this work is attempting to rectify.

5.1.1 Mitochondrial metabolism

As mitochondria are responsible for energy metabolism and various other essential functions in cellular systems, it is becoming apparent that this organelle also plays an essential role in stemness and the differentiation of stem cells. Particular focus was directed towards the investigation of the changes in mitochondrial ATP metabolism during the differentiation of P19 embryonal carcinoma cells under DMSO treatment.

5.1.1.1 Up-regulation of oxidative metabolism in differentiated cells

To confirm if indeed disparate ATP-generating network were operative in undifferentiated and differentiated cells, the consumption of acetoacetate and succinate in these cells was monitored. Acetoacetate is a well-known energy source that is converted into acetyl-CoA, a metabolite that drives TCA cycle and eventually promotes production of ATP via oxidative phosphorylation. Succinate is a TCA cycle intermediate metabolite that can also partake in the oxidative phosphorylation. Thus, the cell with higher oxidative energy metabolism will consume these metabolites at an increased rate. This was indeed a case for DMSO-treated P19 cells as the acetoacetate and succinate were more readily consumed in the differentiated cells compared to undifferentiated cells (Figure 4.3). It was important to examine the metabolic enzymes involved in energy metabolism in these cells.

Various enzymes were subjected to BN-PAGE analysis for their enzymatic activities. Indeed cytosolic enzymes, such as HK, GPI and PK, demonstrated increased activities as the cells continue to mature post-differentiation. Mitochondrial enzymes such as Complex I, Complex II and Complex IV also exhibited enhanced activities (Table 4.1; Figure 4.4a). Interestingly, glycolytic enzymes in DMSO-treated cells demonstrated increased activity despite energy demands were being met by enhanced oxidative phosphorylation. However, the differentiated cells consisted of reduced amount of lactate while pyruvate level was increased (Figure 4.2a,b). Thus, the enzymatic activities and HPLC analyses suggest that the glycolytic pathway is providing pyruvate to fuel the TCA cycle and there are less substrate level phosphorylation occurring in the cell. These results indeed corroborate with other studies indicating reduced level of substrate level phosphorylation observed by limited lactate production in differentiated cells [157,181]

(Figure 5). However, this is the first demonstration of increased activities of glycolysis enzymes supplying pyruvate to enhance production of energy in the differentiated cells. The scheme in figure 5.1 depicts the metabolic pathway leading to enhanced oxidative ATP production in differentiating cells.

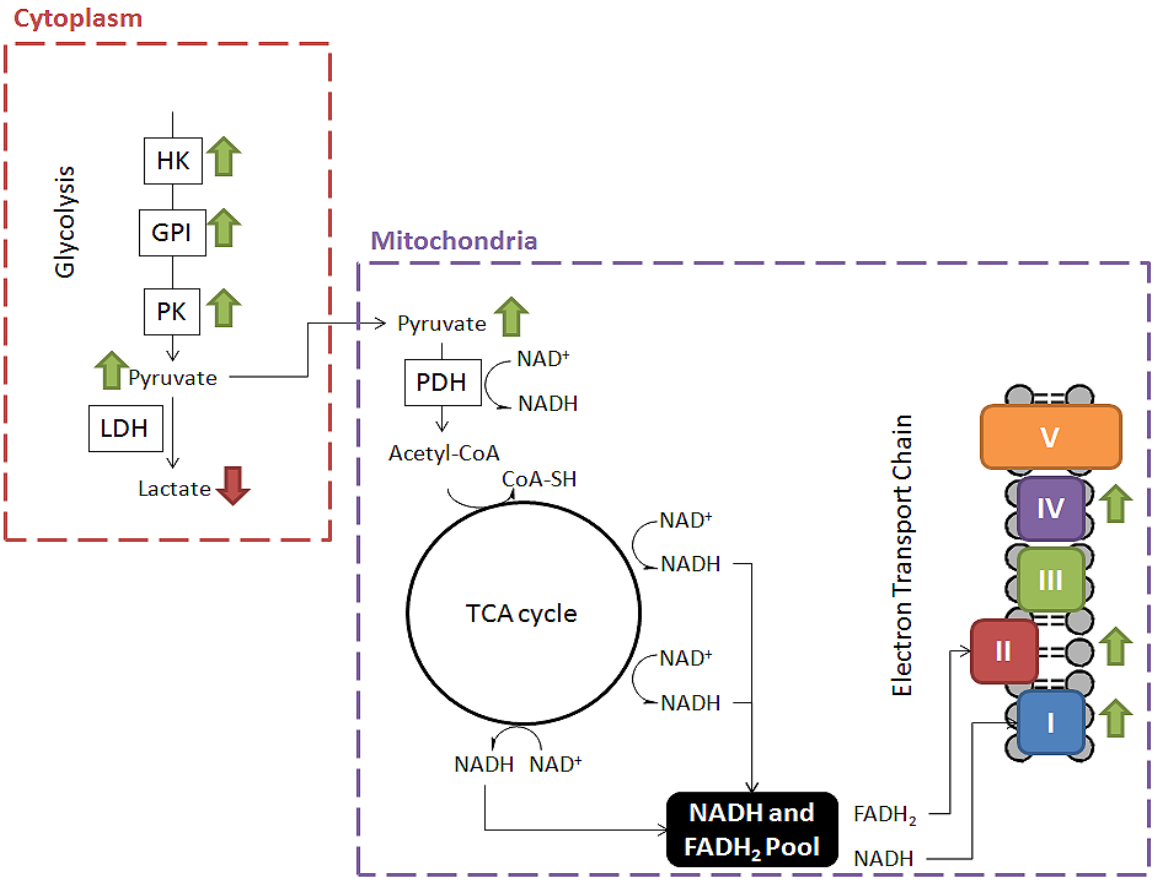

Figure 5. 1. Metabolic reconfiguration resulting in increased ATP production in DMSO-treated P19 cells.

The results of enzymatic activity assay suggest differentiation induces elevated central energy metabolism. Glycolysis is shown to be up-regulated to fuel pyruvate for TCA cycle. ETC enzyme activities were also up-regulated as a result of differentiation.

5.1.1.2 Differentiation promotes increased ATP production

The up-regulation of enzymes in the electron transport chain and the higher TCA cycle metabolites are a clear indication of elevated oxidative phosphorylation, which occurs in mitochondria. Therefore, our next step was to examine the ability of mitochondria to generate ATP. The results indeed showed that DMSO-treated cells produced significantly higher level of ATP when the mitochondrial fractions were exposed substrates like succinate and malate with ADP (Figure 4.5). As this experiment was performed only on mitochondrial fraction, it was evident that this organelle is undergoing dramatic changes during differentiation. Thus, we sought to confirm if indeed there was a shift towards increased mitochondrial biogenesis in the differentiating cells.

5.1.1.3 Mitochondrial activity and biogenesis is promoted during differentiation

HPLC analyses, enzymatic activities and ATP production all point to elevated mitochondrial activity in differentiated cells. To confirm this hypothesis, microscopy aided in the visualization of mitochondrial activity. Rhodamine dyes are recognized mitochondrial detectors as they help in the identification of membrane potential, a finger print of mitochondrial activity [172,182]. Enhanced mitochondrial activity will promote higher membrane potential across the mitochondrial membrane, in turn promoting greater ATP production via ETC. The results confirmed this postulation as rhodamine fluorescent was clearly higher in the differentiated cells (Figure 4.7).

Next, the level of mitochondrial biogenesis was examined. The increase in mitochondrial activity may be reflective of the presence of increased mitochondria in the cell. Although the change in mitochondrial biogenesis during differentiation has been shown in other cells lines, this phenomenon has yet to be proven in the P19 cells.

[157,183,184,185]. Thus, we investigated whether the alteration in metabolism of DMSO-differentiated P19 cells were also caused by up-regulated presence of mitochondria. First, VDAC expression was visualized by microscopy. VDACs, localized on the outer mitochondrial membrane often serve as mitochondrial marker as this protein is expressed specifically on mitochondria. Thus, DMSO-treated cells should consist of higher level of VDAC. The microscopy was performed with rhodamine B dye and VDAC to demonstrate overlap of mitochondrial activity and biogenesis. The result revealed that there were indeed increased amount of mitochondria present in the differentiated cells. Also the rhodamine B dye clearly overlaps the VDAC fluorescent, indicating rhodamine B dye was detecting mitochondrial membrane potential (Figure 4.8).

To provide further confirmation of increased mitochondrial biogenesis, PGC-1α expression was monitored. PGC-1α is a master regulator of mitochondrial biogenesis and the expression should be elevated in differentiated cells. The expression of PGC-1α has been shown in cells such as brown fat, mesoderm and neural differentiation [186,187,188]. To our knowledge, this the first study demonstrating the expression of PGC-1α in DMSO-treated P19 cells [189]. The in-cell western of PGC-1α confirmed our hypothesis of increased mitochondrial biogenesis as the expression of this transcription factor was higher in the differentiated cells (Figure 4.9) (Figure 5.2). Hence, DMSO promotes increased mitochondrial biogenesis, a feature that results in the loss of the stemness of P19 cells.

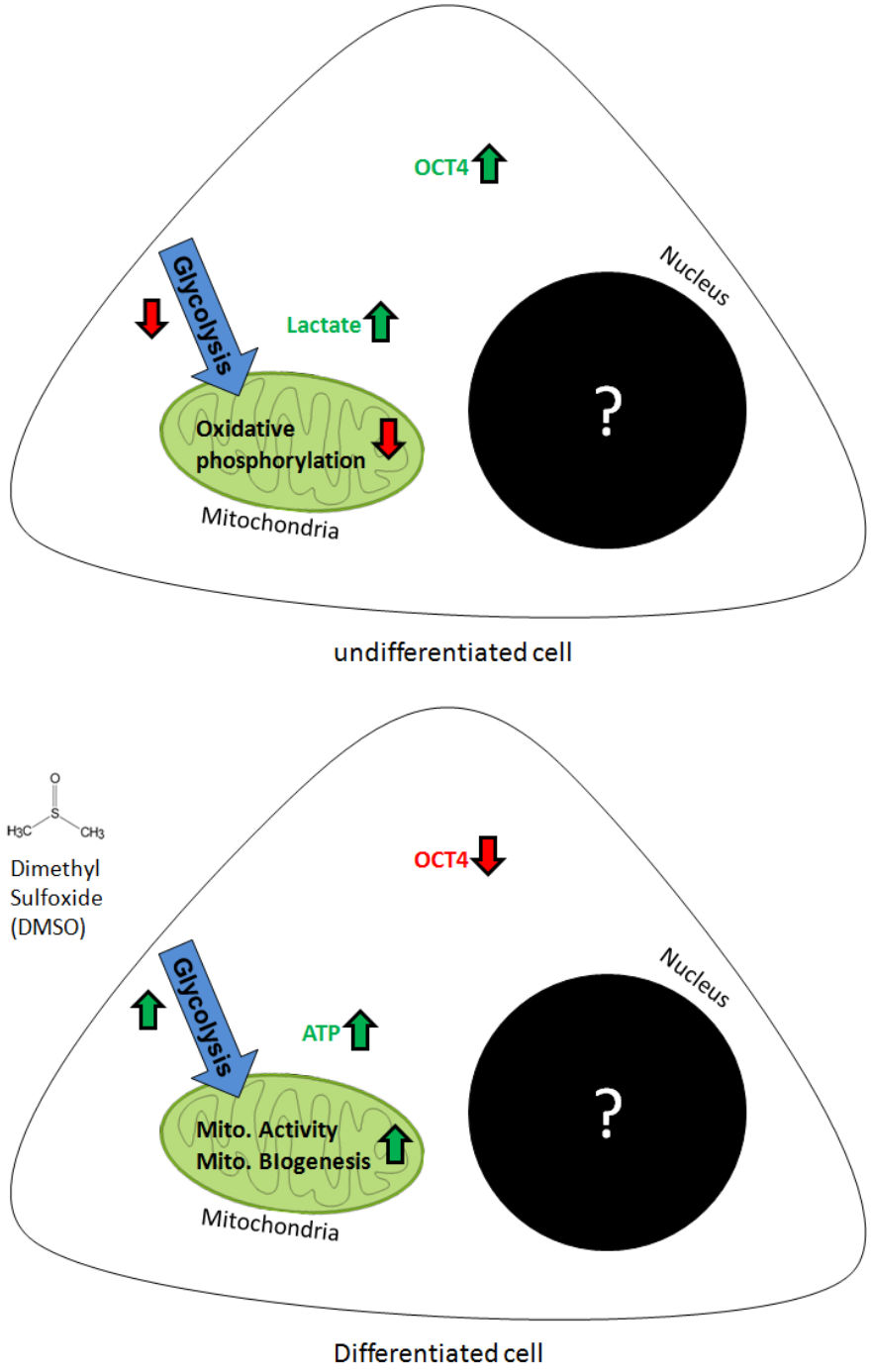

Figure 5. 2. Changing mitochondrial metabolism during stem cell differentiation

The result of mitochondrial study demonstrates drastic change in its energy metabolism. Several key glycolytic enzymes and ETC enzymes were up-regulated in differentiated cells. Monitoring the membrane potential and expression of VDAC and PGC-1α showed that mitochondrial activity and biogenesis were up-regulated in DMSO-treated cells.

5.1.2 Nuclear metabolism

Numerous studies have led to the discovery of a variety of biomolecules localized in the nucleus and their potential roles in epigenetic regulations [190]. However, the origin and interactions of these nuclear metabolites and the mechanism of action remain elusive to date. Recent work has demonstrated possible link between nuclear metabolic enzymes and histone modification. ACL has been shown to metabolize citrate in the nucleus into acetyl-CoA, a substrate required for HAT activity. HATs then acetylates histones, common epigenetic modifications found to up-regulate gene expressions of several glycolytic enzymes [73]. Also work done in our laboratory has unveiled the role of nuclear LDH in HepG2 cells. Nuclear LDH was found to regulate the level of NAD^+, thus modulating SIRT1 activity and promoting histone deacetylation [80]. Despite these efforts, the function of nuclear metabolism in epigenetics is still not fully understood. Especially, there is a dearth of studies dealing with the potential impact of nuclear metabolism in stem cell differentiation. Thus, in this project, the potential role of nuclear LDH in P19 embryonal carcinoma cells was also examined.

5.1.2.1 Nuclear lactate dehydrogenase is up-regulated in nucleus of undifferentiated stem cells.

Metabolomic analyses revealed significant change in the metabolic profile of the nucleus during differentiation (Figure 4.11). Electrophoretic studies led to the discovery of several metabolic enzymes residing in the nucleus of P19 cells (Table 4.2). As shown, ACL and LDH were present in the nucleus of the cell. The nuclear association of PK and ICDH were demonstrated. Since LDH has been reported to play a critical role in the epigenetic of HepG2 cells, the involvement of this enzyme in the nucleus of P19 cells

were further investigated. Interestingly, the activity of ACL and LDH appeared to be reversed where ACL is more active in day 7 and LDH activity was higher during day 3 of differentiation. This prompted us to consider whether the nuclear LDH has a potential role in pluripotency or differentiation of stem cells. The result indicated that nuclear LDH in undifferentiated cells maintain increased activity (Figure 4.12). The control band was excised and incubated in a reaction mixture containing lactate and NAD^+ to confirm that the enzyme is LDH (Figure 4.12). The LDH activity bands from DMSO-treated cells were barely discernible. This enzyme was confirmed by numerous techniques including HPLC, fluorescence microscopy, electrophoresis and siRNA inhibition. These clearly revealed the significance of LDH in the nucleus. Previous studies have identified LDH-5 in the nucleus [77,78,79,80]. LDH-5, consisting of only LDHA subunit, preferentially oxidizes NADH in the presence of pyruvate to form lactate and NAD^+. To confirm the presence of LDH-5 in the nucleus, anti-LDH-5 primary antibody was used to visualize the localization of LDH in the nucleus via immunofluorescent microscopy and western blot of nuclear fractions (Figure 4.13 a,b,d). Overall LDH expression in control and DMSO-treated cells were also monitored via 96-well plate in-cell western (Figure 4.13 c). The expression and localization studies indeed did confirm the presence of LDH in the nucleus.

5.1.2.2 Nuclear lactate dehydrogenase modulates level of nuclear NAD^+

Much like the nuclear ACL providing acetyl-CoA for HATs to promote histone acetylation [73], LDH appears to provide NAD^+ for sirtuins to promote histone deacetylation. It should be noted, however, nuclear NAD^+ can regulate a variety of other proteins in the nucleus also [191], thus, indicating a pivotal role of NAD^+ in the nucleus.

NAD^+ consumption experiment demonstrated that the nuclear extracts from the undifferentiated cells consumed significantly more NAD^+ than the nuclei from DMSO-treated cells, an observation indirectly confirming the higher level of LDH in the control cells (Figure 4.14). Since the major NAD^+ utilizing protein in the nucleus is sirtuin, attempts were made to identify the connection between the nuclear LDH and sirtuins. In particular, SIRT1 was studied as it is the best characterized, nuclear localized enzyme in this family and possesses HDAC activity [192].

The level of histone acetylation was examined as SIRT1 is known to deacetylate histones. HPLC analyses suggested that undifferentiated cells consisted of significantly less acetylated histones (Figure 4.15). In-cell western microscopy and 96-well plate in-cell western blot images confirmed these observations as the acetylated lysine residues in control cells were lower compared to the DMSO-treated cells. (Figure 4.17 a,b). However, further experiments were needed to ensure that nuclear LDH is indeed influencing the activity of sirtuin to modulate histone deacetylation. The level of SIRT1 expression was examined and similar SIRT1 expression level in undifferentiated and differentiated cells was detected. Hence, elevated histone deacetylation in control cells was not due to SIRT1 but rather to other factors like NAD^+ (Figure 4.17 a,b). Hence, histone acetylation was found to correlate with nuclear LDH expression and activity, independent of SIRT1 expression. As sirtuins are known to be regulated mainly by the NAD^+:NADH ratio [68], these results suggest that nuclear LDH modulates the NAD^+ concentration in the nucleus. This phenomenon appears to influence activity of sirtuins and histone deacetylation (Figure 5.3).

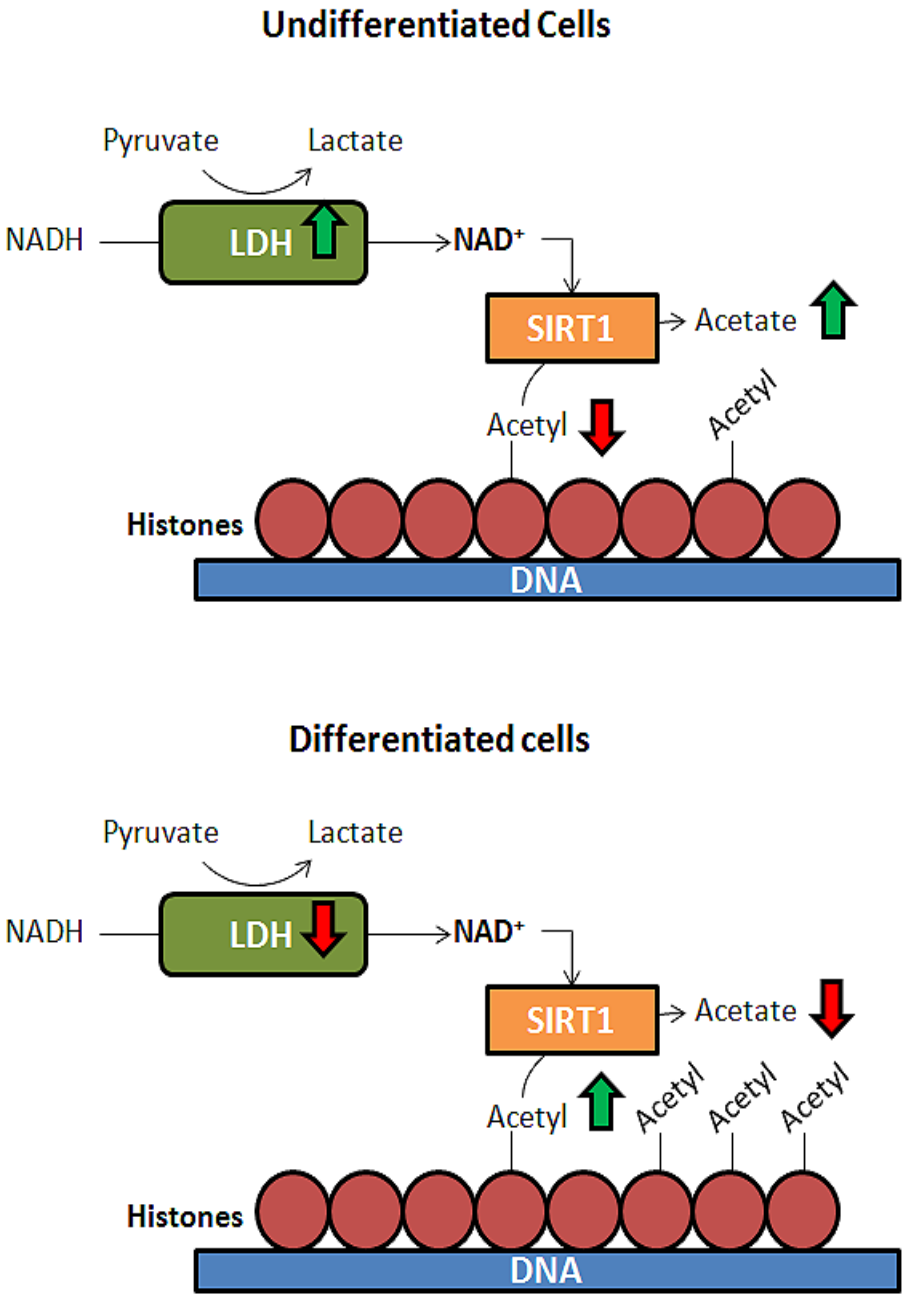

Figure 5. 3. LDH modulates nuclear NAD^+ concentration in order to influence histone deacetylation.

LDH expression and activity was found to be up-regulated in undifferentiated cells. Since SIRT1 expression remains similar in both control and DMSO-treated cells, LDH is suggested to provide NAD^+ to modulate activity of SIRT1. Higher activity of sirtuin in undifferentiated cells due to increased availability of NAD^+ induces histone deacetylation (lower acetyl content on histones).

5.1.2.3 Nuclear lactate dehydrogenase and histone deacetylation

To further solidify the connection between nuclear LDH, sirtuins and histone acetylation, LDH inhibition experiments were performed. To inhibit the activity of nuclear LDH, LDHA siRNA was utilized. SiRNAs are commonly used inhibitory molecules that can temporarily inhibit protein expression. LDHA subunit inhibiting siRNA was chosen in order to produce selective inhibition of nuclear LDH. If the nuclear LDH is indeed a regulator of NAD^+ concentration and histone deacetylation, inhibition of nuclear LDH should elevate the level of histone acetylation. Inhibition of LDH in P19 cells did indeed revealed such a scenario. Comparison of levels of histone acetylation in P19 non-treated, negative control siRNA and LDHA siRNA treated cell showed that LDHA inhibited cells exhibit significant higher histone acetylation (Figure 4.18) (Figure 5.4). The P19 cells (no treatment), control siRNA-treated and LDHA siRNA-treated cells were subjected to DMSO-induced differentiation (Figure 3.7). Since the effect of siRNA is temporary, cells were isolated at day 2 of differentiation to conserve the inhibition. Histones were again acetylated at increased level in LDH inhibited cultures (Figure 4.19a). The differences in histone acetylation of control (non DMSO-treated) and DMSO-treated cells were analyzed (Figure 4.19b). Upon LDHA siRNA inhibition, the control cells exhibited significantly higher level of acetylated histones compared to the control cells of P19 (no inhibition) and control siRNA-treated cells. Note the percentage difference in LDHA siRNA-treated cells was significantly reduced. Hence, the LDHA siRNA inhibition experiments suggest that LDH participates in modulating the level of histone deacetylation. In particular, higher LDH activity in undifferentiated cells indicates that the LDH could be involved in silencing gene expressions during self-renewal period of stem cells. Since SIRT1 has been linked to regulation of metabolic network in the cell,

it is possible that LDH participates in silencing certain metabolic pathways. Thus, further studies should be performed to identify the gene expressions influenced by the activity of nuclear LDH.

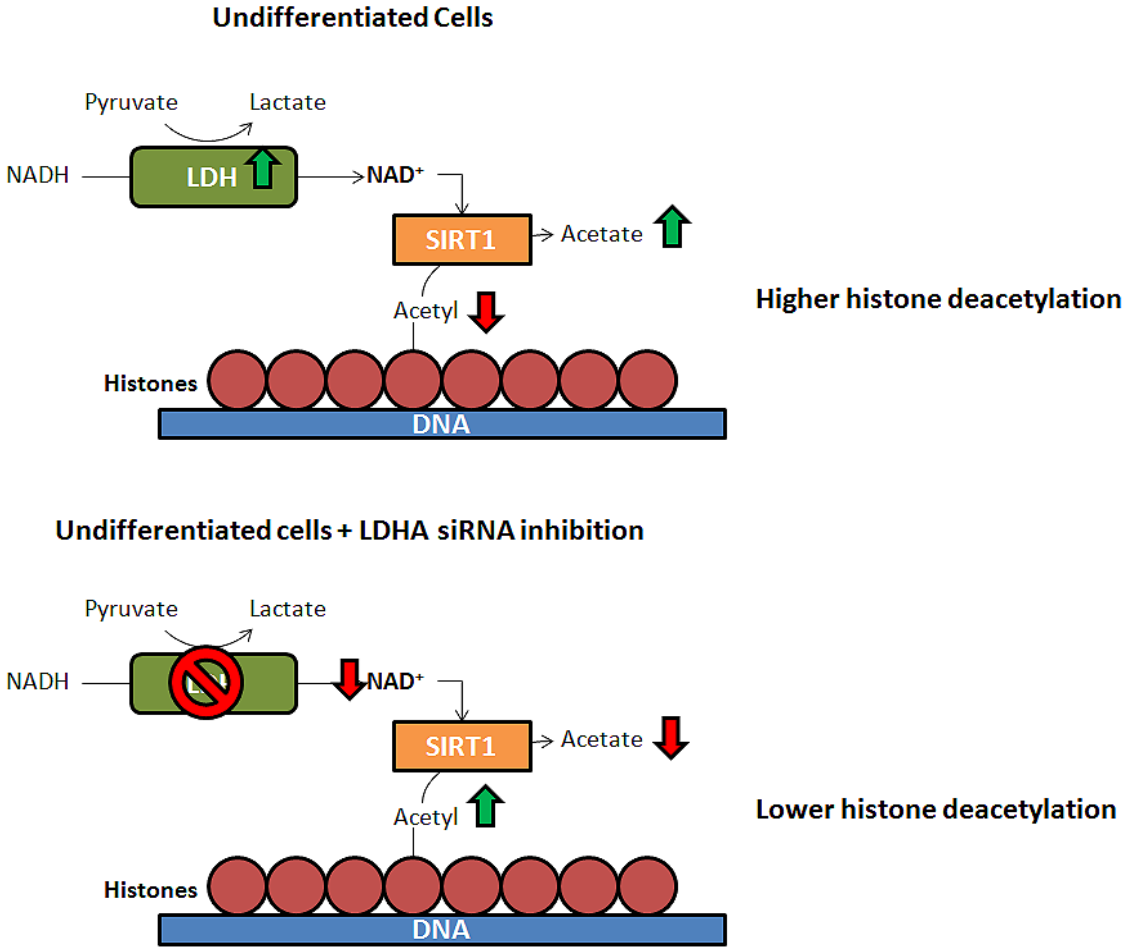

Figure 5. 4. Link between LDH, sirtuin and histone deacetylation.

If nuclear LDH was indeed a modulator of histone deacetylation, selective inhibition of LDH should promote lower histone deacetylase activity in the nucleus. Upon inhibition, the predicted metabolic shift indeed occurred. While uninhibited cells have lower level of acetylated histone residues, LDHA inhibited cells exhibit higher level of acetylated histone residues.

6. Conclusion

The importance of metabolism in stem cell biology is only beginning to emerge. Here we provide convincing evidence for changes in mitochondrial and nuclear metabolism in differentiating stem cells. Mitochondrial activity and biogenesis were found to be enhanced under DMSO-induced differentiation of P19 cells. Activities of several key glycolytic and ETC enzymes and elevated mitochondrial ATP production suggest increased mitochondrial activity in the DMSO-treated cells. Additionally, mitochondrial biogenesis is partly responsible for the increased energy metabolism in differentiated cells. This was indeed confirmed by the higher level of expression of VDAC and PGC-1α in the differentiated cells. These changes indicate drastic variation in mitochondrial characteristics in stem cells and suggest a key role for mitochondria in differentiation, findings that add to our understanding of the link between this organelle and stemness. The occurrence of LDH in P19 cells is a seminal observation that injects a new twist to stem cell differentiation (Figure 5.5).

Nuclear LDH was found to be over-expressed in pluripotent cells, but not in differentiated cells. The higher expression and activity of nuclear LDH were suggested to bridge a gap between the modulation of nuclear NAD^+ concentration, SIRT1 and the level of histone deacetylation. The nuclear LDH appears to control NAD^+ concentration in the nucleus via the oxidation of NADH into NAD^+ with the subsequent conversion of pyruvate into lactate. NAD^+ produced from this reaction is utilized by SIRT1 as a substrate to deacetylate histones. This metabolic regulation of histone deacetylation is indeed independent of SIRT1 expression, a discovery that bridges the gap between metabolism and epigenetics (Figure 5.5).

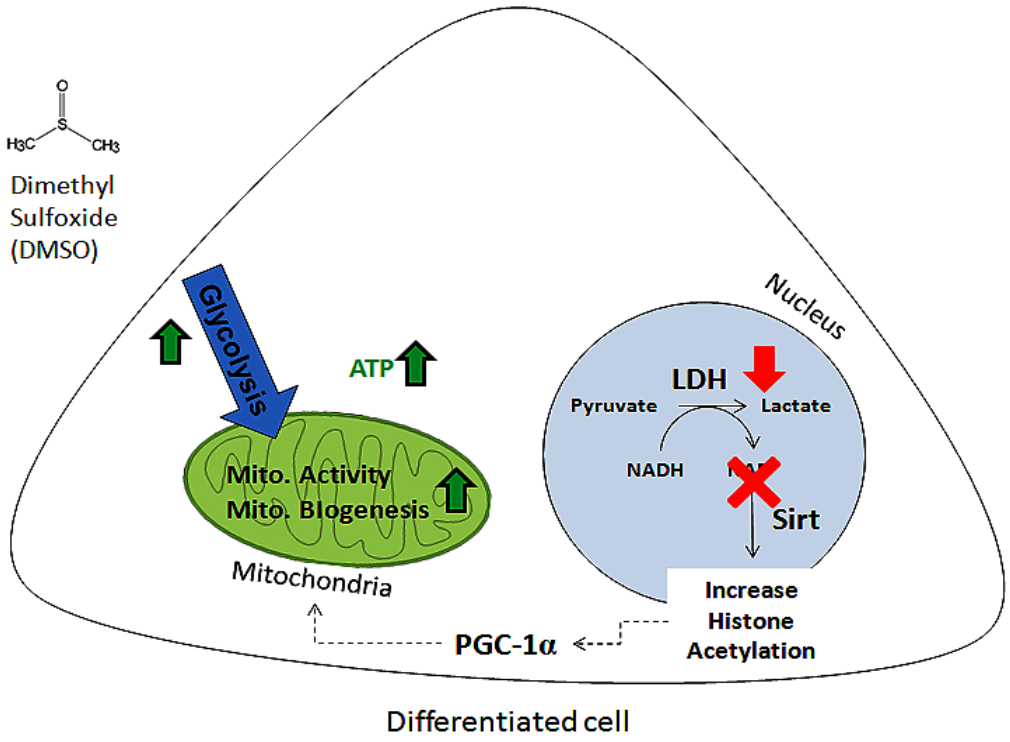

Figure 5. 5. Mitochondrial and nuclear metabolism undergoes drastic changes during differentiation.

The results of this study suggest that differentiation induces increase energy metabolism via up-regulation of mitochondrial activity and biogenesis, in turn producing higher level of ATP for the cell. The nucleus also experiences changes. Lactate dehydrogenase in nucleus produces NAD^+ in order to provide a key substrate for sirtuin-dependent epigenetic modification.

In conclusion, this study suggests an intimate connection between mitochondrial and nuclear metabolism and stem cells. Further studies should be performed to uncover detailed molecular mechanism of mitochondrial biogenesis during differentiation. The nuclear LDH should also be further investigated in order to unveil whether gene expression correlates with LDH activity and histone deacetylation. Delineating these molecular mechanisms of metabolic alterations can lead to a better understanding of pluripotent cells and provide an additional tool to direct stem cells to a desired fate during differentiation.

7. References

[1] J. Berg, J. Tymoczko, L. Stryer, Biochemistry 5th edition, W.H. Freeman, New Tork, 2002.

[2] A.R. Fernie, F. Carrari, L.J. Sweetlove, Respiratory metabolism: glycolysis, the TCA cycle and mitochondrial electron transport, Current Opinion in Plant Biology 7 (2004) 254-261.

[3] R.J. Mailloux, R. Bériault, J. Lemire, R. Singh, D.R. Chénier, R.D. Hamel, V.D. Appanna, The Tricarboxylic Acid Cycle, an Ancient Metabolic Network with a Novel Twist, PLoS ONE 2 (2007) e690.

[4] D.G. Hardie, AMP-activated protein kinase—an energy sensor that regulates all aspects of cell function, Genes & Development 25 (2011) 1895-1908.

[5] B. Desvergne, L. Michalik, W. Wahli, Transcriptional Regulation of Metabolism, Physiological Reviews 86 (2006) 465-514.

[6] P.J. Fernandez-Marcos, J. Auwerx, Regulation of PGC-1α, a nodal regulator of mitochondrial biogenesis, The American Journal of Clinical Nutrition 93 (2011) 884S-890S.

[7] P. Puigserver, Z. Wu, C.W. Park, R. Graves, M. Wright, B.M. Spiegelman, A Cold-Inducible Coactivator of Nuclear Receptors Linked to Adaptive Thermogenesis, Cell 92 (1998) 829-839.

[8] R.B. Vega, J.M. Huss, D.P. Kelly, The Coactivator PGC-1 Cooperates with Peroxisome Proliferator-Activated Receptor α in Transcriptional Control of Nuclear Genes Encoding Mitochondrial Fatty Acid Oxidation Enzymes, Molecular and Cellular Biology 20 (2000) 1868-1876.

[9] J.C. Yoon, P. Puigserver, G. Chen, J. Donovan, Z. Wu, J. Rhee, G. Adelmant, J. Stafford, C.R. Kahn, D.K. Granner, C.B. Newgard, B.M. Spiegelman, Control of hepatic gluconeogenesis through the transcriptional coactivator PGC-1, Nature 413 (2001) 131-138.

[10] P. Puigserver, B.M. Spiegelman, Peroxisome Proliferator-Activated Receptor-γ Coactivator 1α (PGC-1α): Transcriptional Coactivator and Metabolic Regulator, Endocrine Reviews 24 (2003) 78-90.

[11] P. Puigserver, J. Rhee, J. Donovan, C.J. Walkey, J.C. Yoon, F. Oriente, Y. Kitamura, J. Altomonte, H. Dong, D. Accili, B.M. Spiegelman, Insulin-regulated hepatic gluconeogenesis through FOXO1-PGC-1[alpha] interaction, Nature 423 (2003) 550-555.

[12] L. Gerosa, U. Sauer, Regulation and control of metabolic fluxes in microbes, Current Opinion in Biotechnology 22 (2011) 566-575.

[13] A.P. Oliveira, U. Sauer, The importance of post-translational modifications in regulating Saccharomyces cerevisiae metabolism, FEMS Yeast Research 12 (2012) 104-117.

[14] C.T. Walsh, S. Garneau-Tsodikova, G.J. Gatto, Protein Posttranslational Modifications: The Chemistry of Proteome Diversifications, Angewandte Chemie International Edition 44 (2005) 7342-7372.

[15] B. Bodenmiller, R. Aebersold, Chapter 13 - Quantitative Analysis of Protein Phosphorylation on a System-Wide Scale by Mass Spectrometry-Based Proteomics, in: W. Jonathan, G. Christine, R.F. Gerald (Eds.), Methods in Enzymology, Academic Press, 2010, pp. 317-334.
[16] B. Bodenmiller, D. Campbell, B. Gerrits, H. Lam, M. Jovanovic, P. Picotti, R. Schlapbach, R. Aebersold, PhosphoPep[mdash]a database of protein phosphorylation sites in model organisms, Nat Biotech 26 (2008) 1339-1340.
[17] B. Bodenmiller, S. Wanka, C. Kraft, J. Urban, D. Campbell, P.G. Pedrioli, B. Gerrits, P. Picotti, H. Lam, O. Vitek, M.-Y. Brusniak, B. Roschitzki, C. Zhang, K.M. Shokat, R. Schlapbach, A. Colman-Lerner, G.P. Nolan, A.I. Nesvizhskii, M. Peter, R. Loewith, C. von Mering, R. Aebersold, Phosphoproteomic Analysis Reveals Interconnected System-Wide Responses to Perturbations of Kinases and Phosphatases in Yeast, Sci. Signal. 3 (2010).
[18] S. Sharifpoor, A. Nguyen Ba, J.-Y. Young, D. van Dyk, H. Friesen, A. Douglas, C. Kurat, Y. Chong, K. Founk, A. Moses, B. Andrews, A quantitative literature-curated gold standard for kinase-substrate pairs, Genome Biology 12 (2011) R39.
[19] C.M. Taniguchi, B. Emanuelli, C.R. Kahn, Critical nodes in signalling pathways: insights into insulin action, Nat Rev Mol Cell Biol 7 (2006) 85-96.
[20] C.M. Jenkins, J. Yang, H.F. Sims, R.W. Gross, Reversible High Affinity Inhibition of Phosphofructokinase-1 by Acyl-CoA: A mechanism integrating glycolytic flux with lipid metabolism, Journal of Biological Chemistry 286 (2011) 11937-11950.
[21] N.-M. Grüning, M. Rinnerthaler, K. Bluemlein, M. Mülleder, Mirjam M.C. Wamelink, H. Lehrach, C. Jakobs, M. Breitenbach, M. Ralser, Pyruvate Kinase Triggers a Metabolic Feedback Loop that Controls Redox Metabolism in Respiring Cells, Cell Metabolism 14 (2011) 415-427.
[22] W. Martin, Evolutionary origins of metabolic compartmentalization in eukaryotes, Philosophical Transactions of the Royal Society B: Biological Sciences 365 (2010) 847-855.
[23] C.E. Lane, J.M. Archibald, The eukaryotic tree of life: endosymbiosis takes its TOL, Trends in ecology & evolution. 23 (2008) 268-275.
[24] T. Kleine, U.G. Maier, D. Leister, DNA Transfer from Organelles to the Nucleus: The Idiosyncratic Genetics of Endosymbiosis, Annual Review of Plant Biology 60 (2009) 115-138.
[25] A.G.M. Tielens, C. Rotte, J.J. van Hellemond, W. Martin, Mitochondria as we don't know them, Trends in biochemical sciences 27 (2002) 564-572.
[26] M. Van Der Giezen, Hydrogenosomes and Mitosomes: Conservation and Evolution of Functions1, Journal of Eukaryotic Microbiology 56 (2009) 221-231.
[27] E. Richly, D. Leister, An improved prediction of chloroplast proteins reveals diversities and commonalities in the chloroplast proteomes of Arabidopsis and rice, Gene 329 (2004) 11-16.
[28] C. Masters, Interactions between glycolytic enzymes and components of the cytomatrix, The Journal of Cell Biology (1984) 222-225.
[29] R.B. Robey, Hexokinase: a novel sugar kinase coupled to renal epithelial cell survival, Kidney Int 79 (2011) 1163-1165.
[30] J. Sibley, A. ALehninger, Determination of aldolase in animal tissues, The Journal of Biological Chemistry (1948) 859-873.

[31] E. Fermo, P. Bianchi, C. Vercellati, D.C. Rees, A.P. Marcello, W. Barcellini, A. Zanella, Triose phosphate isomerase deficiency associated with two novel mutations in TPI gene, European Journal of Haematology 85 (2010) 170-173.
[32] Y. Zhang, Z. Xie, G. Zhou, H. Zhang, J. Lu, W.J. Zhang, Fructose-1,6-Bisphosphatase Regulates Glucose-Stimulated Insulin Secretion of Mouse Pancreatic β-Cells, Endocrinology 151 (2010) 4688-4695.
[33] X. Tong, F. Zhao, C.B. Thompson, The molecular determinants of de novo nucleotide biosynthesis in cancer cells, Current Opinion in Genetics & Development 19 (2009) 32-37.
[34] T. Soderberg, Biosynthesis of ribose-5-phosphate and erythrose-4-phosphate in archaea: a phylogenetic analysis of archaeal genomes, Archaea 1 (2005) 347-352.
[35] C.S. Powell, R.M. Jackson, Mitochondrial complex I, aconitase, and succinate dehydrogenase during hypoxia-reoxygenation: modulation of enzyme activities by MnSOD, American Journal of Physiology - Lung Cellular and Molecular Physiology 285 (2003) L189-L198.
[36] M. Saraste, Oxidative Phosphorylation at the fin de siècle, Science 283 (1999) 1488-1493.
[37] S. Eaton, K. Bartlett, M. Pourfarzam, Mammalian mitochondrial beta-oxidation, Biochemical Journal (1996) 345-357.
[38] C. Wang, R.J. Youle, The role of mitochondria in apoptosis, Annual Review of Genetics 43 (2009) 95-118.
[39] M.R. Duchen, Mitochondria and calcium: from cell signalling to cell death, The Journal of Physiology 529 (2000) 57-68.
[40] B. Alberts, A. Johnson, L. J;, Molecular biology of the cell. 4th edition, Garland Science, New York, 2002.
[41] J.K. Reddy, T. Hashimoto, Peroxisomal β-oxidation and peroxisome proliferator-activated receptor α: An adaptive metabolic system, Annual Review of Nutrition 21 (2001) 193-230.
[42] S. Fu, Steven M. Watkins, Gökhan S. Hotamisligil, The Role of Endoplasmic Reticulum in Hepatic Lipid Homeostasis and Stress Signaling, Cell Metabolism 15 (2012) 623-634.
[43] R. Jaenisch, A. Bird, Epigenetic regulation of gene expression: how the genome integrates intrinsic and environmental signals, Nat Genet.
[44] M. Buratovich, Stem cell differentiation requires proper compaction of DNA, Beyond the Dish, Spring Arbor, Michigan, 2012.
[45] A.J. Bannister, T. Kouzarides, Regulation of chromatin by histone modifications, Cell Res 21 (2011) 381-395.
[46] P.A. Wade, Transcriptional control at regulatory checkpoints by histone deacetylases: molecular connections between cancer and chromatin, Human Molecular Genetics 10 (2001) 693-698.
[47] P. Bjerling, R.A. Silverstein, G. Thon, A. Caudy, S. Grewal, K. Ekwall, Functional Divergence between Histone Deacetylases in Fission Yeast by Distinct Cellular Localization and In Vivo Specificity, Molecular and Cellular Biology 22 (2002) 2170-2181.
[48] A.J.M. de Ruijter, A.H. van Gennip, H.N. Caron, S. Kemp, A.B.P. van Kuilenburg, Histone deacetylases (HDACs): characterization of the classical HDAC family, Biochem. J. 370 (2003) 737-749.

[49] T. Nakagawa, L. Guarente, Sirtuins at a glance, Journal of Cell Science 124 (2011) 833-838.
[50] C. Cantó, J. Auwerx, Targeting Sirtuin 1 to Improve Metabolism: All You Need Is NAD^+?, Pharmacological Reviews 64 (2012) 166-187.
[51] B.J. North, B.L. Marshall, M.T. Borra, J.M. Denu, E. Verdin, The Human Sir2 Ortholog, SIRT2, Is an NAD^+-Dependent Tubulin Deacetylase, Molecular cell 11 (2003) 437-444.
[52] S.C. Dryden, F.A. Nahhas, J.E. Nowak, A.-S. Goustin, M.A. Tainsky, Role for Human SIRT2 NAD-Dependent Deacetylase Activity in Control of Mitotic Exit in the Cell Cycle, Molecular and Cellular Biology 23 (2003) 3173-3185.
[53] P. Onyango, I. Celic, J.M. McCaffery, J.D. Boeke, A.P. Feinberg, SIRT3, a human SIR2 homologue, is an NAD^+- dependent deacetylase localized to mitochondria, Proceedings of the National Academy of Sciences 99 (2002) 13653-13658.
[54] W.C. Hallows, S. Lee, J.M. Denu, Sirtuins deacetylate and activate mammalian acetyl-CoA synthetases, Proceedings of the National Academy of Sciences 103 (2006) 10230-10235.
[55] B. Schwer, J. Bunkenborg, R.O. Verdin, J.S. Andersen, E. Verdin, Reversible lysine acetylation controls the activity of the mitochondrial enzyme acetyl-CoA synthetase 2, Proceedings of the National Academy of Sciences 103 (2006) 10224-10229.
[56] C. Schlicker, M. Gertz, P. Papatheodorou, B. Kachholz, C.F.W. Becker, C. Steegborn, Substrates and Regulation Mechanisms for the Human Mitochondrial Sirtuins Sirt3 and Sirt5, Journal of Molecular Biology 382 (2008) 790-801.
[57] H. Cimen, M.-J. Han, Y. Yang, Q. Tong, H. Koc, E.C. Koc, Regulation of Succinate Dehydrogenase Activity by SIRT3 in Mammalian Mitochondria, Biochemistry 49 (2009) 304-311.
[58] T. Shi, F. Wang, E. Stieren, Q. Tong, SIRT3, a Mitochondrial Sirtuin Deacetylase, Regulates Mitochondrial Function and Thermogenesis in Brown Adipocytes, Journal of Biological Chemistry 280 (2005) 13560-13567.
[59] N. Dali Youcef, M. Lagouge, S. Froelich, C. Koehl, K. Schoonjans, J. Auwerx, Sirtuins: The 'magnificent seven', function, metabolism and longevity, Annals of Medicine 39 (2007) 335-345.
[60] E. Michishita, J.Y. Park, J.M. Burneskis, J.C. Barrett, I. Horikawa, Evolutionarily Conserved and Nonconserved Cellular Localizations and Functions of Human SIRT Proteins, Molecular Biology of the Cell 16 (2005) 4623-4635.
[61] M.C. Haigis, R. Mostoslavsky, K.M. Haigis, K. Fahie, D.C. Christodoulou, Andrew J. Murphy, D.M. Valenzuela, G.D. Yancopoulos, M. Karow, G. Blander, C. Wolberger, T.A. Prolla, R. Weindruch, F.W. Alt, L. Guarente, SIRT4 Inhibits Glutamate Dehydrogenase and Opposes the Effects of Calorie Restriction in Pancreatic β Cells, Cell 126 (2006) 941-954.
[62] T. Nakagawa, D.J. Lomb, M.C. Haigis, L. Guarente, SIRT5 Deacetylates Carbamoyl Phosphate Synthetase 1 and Regulates the Urea Cycle, Cell 137 (2009) 560-570.
[63] I. Yefimenko, V. Fresquet, C. Marco-Marín, V. Rubio, J. Cervera, Understanding Carbamoyl Phosphate Synthetase Deficiency: Impact of Clinical Mutations on Enzyme Functionality, Journal of Molecular Biology 349 (2005) 127-141.
[64] R.I. Tennen, K.F. Chua, Chromatin regulation and genome maintenance by mammalian SIRT6, Trends in biochemical sciences 36 (2011) 39-46.

[65] T.L.A. Kawahara, E. Michishita, A.S. Adler, M. Damian, E. Berber, M. Lin, R.A. McCord, K.C.L. Ongaigui, L.D. Boxer, H.Y. Chang, K.F. Chua, SIRT6 Links Histone H3 Lysine 9 Deacetylation to NF-ºB-Dependent Gene Expression and Organismal Life Span, Cell 136 (2009) 62-74.
[66] M.F. Barber, E. Michishita-Kioi, Y. Xi, L. Tasselli, M. Kioi, Z. Moqtaderi, R.I. Tennen, S. Paredes, N.L. Young, K. Chen, K. Struhl, B.A. Garcia, O. Gozani, W. Li, K.F. Chua, SIRT7 links H3K18 deacetylation to maintenance of oncogenic transformation, Nature advance online publication (2012).
[67] A. Satoh, L. Stein, S. Imai, The Role of Mammalian Sirtuins in the Regulation of Metabolism, Aging, and Longevity, in: T.-P. Yao, E. Seto (Eds.), Histone Deacetylases: the Biology and Clinical Implication, Springer Berlin Heidelberg, 2011, pp. 125-162.
[68] J.L. Feldman, K.E. Dittenhafer-Reed, J.M. Denu, Sirtuin Catalysis and Regulation, Journal of Biological Chemistry (2012).
[69] G. Wang, E. Pichersky, Nicotinamidase participates in the salvage pathway of NAD^+ biosynthesis in Arabidopsis, The Plant Journal 49 (2007) 1020-1029.
[70] T. Zhang, J.G. Berrocal, K.M. Frizzell, M.J. Gamble, M.E. DuMond, R. Krishnakumar, T. Yang, A.A. Sauve, W.L. Kraus, Enzymes in the NAD^+ Salvage Pathway Regulate SIRT1 Activity at Target Gene Promoters, Journal of Biological Chemistry 284 (2009) 20408-20417.
[71] A.A. Sauve, C. Wolberger, V.L. Schramm, J.D. Boeke, The Biochemistry of Sirtuins, Annual Review of Biochemistry 75 (2006) 435-465.
[72] Y. Shi, Y. Shi, Metabolic enzymes and coenzymes in transcription – a direct link between metabolism and transcription?, Trends in Genetics 20 (2004) 445-452.
[73] K.E. Wellen, G. Hatzivassiliou, U.M. Sachdeva, T.V. Bui, J.R. Cross, C.B. Thompson, ATP-Citrate Lyase Links Cellular Metabolism to Histone Acetylation, Science 324 (2009) 1076-1080.
[74] M. Drent, N. Cobben, R. Henderson, E. Wouters, M. van Dieijen-Visser, Usefulness of lactate dehydrogenase and its isoenzymes as indicators of lung damage or inflammation, European Respiratory Journal 9 (1996) 1736-1742.
[75] A. Le, C.R. Cooper, A.M. Gouw, R. Dinavahi, A. Maitra, L.M. Deck, R.E. Royer, D.L. Vander Jagt, G.L. Semenza, C.V. Dang, Inhibition of lactate dehydrogenase A induces oxidative stress and inhibits tumor progression, Proceedings of the National Academy of Sciences 107 (2010) 2037-2042.
[76] J. Lemire, R.J. Mailloux, V.D. Appanna, Mitochondrial Lactate Dehydrogenase Is Involved in Oxidative-Energy Metabolism in Human Astrocytoma Cells (CCF-STTG1), PLoS ONE 3 (2008) e1550.
[77] X. Zhong, B. Howard, Phosphotyrosine-containing lactate dehydrogenase is restricted to the nuclei of PC12 pheochromocytoma cells., Molecular and Cellular Biology 10 (1990) 770-776.
[78] O. Popanda, G. Fox, H.W. Thielmann, Modulation of DNA polymerases α, δ and ε by lactate dehydrogenase and 3-phosphoglycerate kinase, Biochimica et Biophysica Acta (BBA) - Gene Structure and Expression 1397 (1998) 102-117.
[79] M. Koukourakis, A. Giatromanolaki, C. Simopoulos, A. Polychronidis, E. Sivridis, Lactate dehydrogenase 5 (LDH5) relates to up-regulated hypoxia inducible factor pathway and metastasis in colorectal cancer, Clinical & Experimental Metastasis 22 (2005) 25-30.

[80] Z. Castonguay, Nuclear Lactate Dehydrogenase, Bridging Central Metabolism to Epigenetic Modifications in Mammalian Cellular Systems, Chemistry and Biochemistry, Laurentian University, Sudbury, 2012.
[81] S.F. Gilbert, Developmental biology, 6th edition, Sinauer Associates, Sunderland (MA), 2000.
[82] D. Herzlinger, C. Koseki, T. Mikawa, Q. al-Awqati, Metanephric mesenchyme contains multipotent stem cells whose fate is restricted after induction, Development 114 (1992) 565-572.
[83] E. Gunsilius, G. Gastl, A.L. Petzer, Hematopoietic stem cells, Biomedicine & Pharmacotherapy 55 (2001) 186-194.
[84] E.C. Forsberg, D. Bhattacharya, I. Weissman, Hematopoietic stem cells, Stem Cell Reviews 2 (2006) 23-30.
[85] R.S.P. Beddington, E.J. Robertson, Axis Development and Early Asymmetry in Mammals, Cell 96 (1999) 195-209.
[86] C.C. Wong, K.E. Loewke, N.L. Bossert, B. Behr, C.J. De Jonge, T.M. Baer, R.A.R. Pera, Non-invasive imaging of human embryos before embryonic genome activation predicts development to the blastocyst stage, Nat Biotech 28 (2010) 1115-1121.
[87] E. Fuchs, T. Tumbar, G. Guasch, Socializing with the Neighbors: Stem Cells and Their Niche, Cell 116 (2004) 769-778.
[88] K. Takahashi, S. Yamanaka, Induction of pluripotent stem cells from mouse embryonic and adult fibroblast cultures by defined factors, Cell 126 (2006) 663-676.
[89] J. Yu, M.A. Vodyanik, K. Smuga-Otto, J. Antosiewicz-Bourget, J.L. Frane, S. Tian, J. Nie, G.A. Jonsdottir, V. Ruotti, R. Stewart, I.I. Slukvin, J.A. Thomson, Induced Pluripotent Stem Cell Lines Derived from Human Somatic Cells, Science 318 (2007) 1917-1920.
[90] M. Stojkovic, M. Lako, T. Strachan, A. Murdoch, Derivation, growth and applications of human embryonic stem cells, Reproduction 128 (2004) 259-267.
[91] P. Cartwright, C. McLean, A. Sheppard, D. Rivett, K. Jones, S. Dalton, LIF/STAT3 controls ES cell self-renewal and pluripotency by a Myc-dependent mechanism, Development 132 (2005) 885-896.
[92] S. Watanabe, H. Umehara, K. Murayama, M. Okabe, T. Kimura, T. Nakano, Activation of Akt signaling is sufficient to maintain pluripotency in mouse and primate embryonic stem cells, Oncogene 25 (2006) 2697-2707.
[93] K. Blair, J. Wray, A. Smith, The Liberation of Embryonic Stem Cells, PLoS Genet 7 (2011) e1002019.
[94] J. Li, G. Wang, C. Wang, Y. Zhao, H. Zhang, Z. Tan, Z. Song, M. Ding, H. Deng, MEK/ERK signaling contributes to the maintenance of human embryonic stem cell self-renewal, Differentiation 75 (2007) 299-307.
[95] N.V. Lifantseva, A.M. Koltsova, G.G. Poljanskaya, O.F. Gordeeva, Expression of TGFβ family factors and FGF2 in mouse and human embryonic stem cells maintained in different culture systems, Russian Journal of Developmental Biology 44 (2013) 7-18.
[96] S.A. Pryzyborski, V.B. Christie, M.W. Hayman, R. Stewart, Human Embryonal Carcinoma Stem Cells: Models of Embryonic Development in Humans, Stem Cells and Development 13 (2004) 400-408.

[97] M.W. McBurney, P19 embryonal carcinoma cells, International Journal of Developmental Biology 37 (1993) 135-140.
[98] Q. Zhou, H. Chipperfield, D.A. Melton, W.H. Wong, A gene regulatory network in mouse embryonic stem cells, Proceedings of the National Academy of Sciences 104 (2007) 16438-16443.
[99] L. Chen, G.Q. Daley, Molecular basis of pluripotency, Human Molecular Genetics 17 (2008) R23-R27.
[100] Z. Wang, E. Oron, B. Nelson, S. Razis, N. Ivanova, Distinct Lineage Specification Roles for NANOG, OCT4, and SOX2 in Human Embryonic Stem Cells, Cell Stem Cell 10 (2012) 440-454.
[101] Y.-H. Loh, Q. Wu, J.-L. Chew, V.B. Vega, W. Zhang, X. Chen, G. Bourque, J. George, B. Leong, J. Liu, K.-Y. Wong, K.W. Sung, C.W.H. Lee, X.-D. Zhao, K.-P. Chiu, L. Lipovich, V.A. Kuznetsov, P. Robson, L.W. Stanton, C.-L. Wei, Y. Ruan, B. Lim, H.-H. Ng, The Oct4 and Nanog transcription network regulates pluripotency in mouse embryonic stem cells, Nat Genet 38 (2006) 431-440.
[102] J. Kim, J. Chu, X. Shen, J. Wang, S.H. Orkin, An Extended Transcriptional Network for Pluripotency of Embryonic Stem Cells, Cell 132 (2008) 1049-1061.
[103] W. Herr, M.A. Cleary, The POU domain: versatility in transcriptional regulation by a flexible two-in one DNA-binding domain, Gene & Development 9 (1995) 1679-1693.
[104] A. Brehm, K. Ohbo, H. Scholer, The carboxy-terminal transactivation domain of Oct-4 acquires cell specificity through the POU domain, Molecular and Cellular Biology 17 (1997) 154-162.
[105] G. Zafarana, S.R. Avery, K. Avery, H.D. Moore, P.W. Andrews, Specific Knockdown of OCT4 in Human Embryonic Stem Cells by Inducible Short Hairpin RNA Interference, Stem Cells 27 (2009) 776-782.
[106] L. Li, L. Sun, F. Gao, J. Jiang, Y. Yang, C. Li, J. Gu, Z. Wei, A. Yang, R. Lu, Y. Ma, F. Tang, S. Won Kwon, Y. Zhao, J. Li, Y. Jin, Stk40 links the pluripotency factor Oct4 to the Erk/MAPK pathway and controls extraembryonic endoderm differentiation, Proceedings of the National Academy of Sciences 107 (2010) 1402-1407.
[107] H. Niwa, J.-i. Miyazaki, A.G. Smith, Quantitative expression of Oct-3/4 defines differentiation, dedifferentiation or self-renewal of ES cells, Nat Genet 24 (2000) 372-376.
[108] A. Rizzino, Sox2 and Oct-3/4: a versatile pair of master regulators that orchestrate the self-renewal and pluripotency of embryonic stem cells, Wiley Interdisciplinary Reviews: Systems Biology and Medicine 1 (2009) 228-236.
[109] Z.-X. Wang, C.H.-L. Teh, J.L.L. Kueh, T. Lufkin, P. Robson, L.W. Stanton, Oct4 and Sox2 Directly Regulate Expression of Another Pluripotency Transcription Factor, Zfp206, in Embryonic Stem Cells, Journal of Biological Chemistry 282 (2007) 12822-12830.
[110] A.A. Avilion, S.K. Nicolis, L.H. Pevny, L. Perez, N. Vivian, R. Lovell-Badge, Multipotent cell lineages in early mouse development depend on SOX2 function, Genes & Development 17 (2003) 126-140.
[111] K. Mitsui, Y. Tokuzawa, H. Itoh, K. Segawa, M. Murakami, K. Takahashi, M. Maruyama, M. Maeda, S. Yamanaka, The Homeoprotein Nanog Is Required for

Maintenance of Pluripotency in Mouse Epiblast and ES Cells, Cell 113 (2003) 631-642.
[112] A.M. Singh, T. Hamazaki, K.E. Hankowski, N. Terada, A Heterogeneous Expression Pattern for Nanog in Embryonic Stem Cells, STEM CELLS 25 (2007) 2534-2542.
[113] H. Niwa, K. Ogawa, D. Shimosato, K. Adachi, A parallel circuit of LIF signalling pathways maintains pluripotency of mouse ES cells, Nature 460 (2009) 118-122.
[114] H. Kurosawa, Methods for inducing embryoid body formation: in vitro differentiation system of embryonic stem cells, Journal of Bioscience and Bioengineering 103 (2007) 389-398.
[115] M. Wartenberg, J. Gunther, J. Hescheler, H. Sauer, The embryoid body as a novel in vitro assay system for antiangiogenic agents, Laboratory Investigation - Nature 78 (1998) 1301-1314.
[116] M. Banerjee, R. Bhonde, Application of hanging drop technique for stem cell differentiation and cytotoxicity studies, Cytotechnology 51 (2006) 1-5.
[117] H. Liu, S.F. Collins, L.J. Suggs, Three-dimensional culture for expansion and differentiation of mouse embryonic stem cells, Biomaterials 27 (2006) 6004-6014.
[118] T. Nakano, H. Kodama, T. Honjo, Generation of lymphohematopoietic cells from embryonic stem cells in culture, Science 265 (1994) 1098-1101.
[119] W. Ma, T. Tavakoli, E. Derby, Y. Serebryakova, M. Rao, M. Mattson, Cell-extracellular matrix interactions regulate neural differentiation of human embryonic stem cells, BMC Developmental Biology 8 (2008) 90.
[120] D. Evseenko, Y. Zhu, K. Schenke-Layland, J. Kuo, B. Latour, S. Ge, J. Scholes, G. Dravid, X. Li, W.R. MacLellan, G.M. Crooks, Mapping the first stages of mesoderm commitment during differentiation of human embryonic stem cells, Proceedings of the National Academy of Sciences 107 (2010) 13742-13747.
[121] C. Palena, D.E. Polev, K.Y. Tsang, R.I. Fernando, M. Litzinger, L.L. Krukovskaya, A.V. Baranova, A.P. Kozlov, J. Schlom, The Human T-Box Mesodermal Transcription Factor Brachyury Is a Candidate Target for T-Cell–Mediated Cancer Immunotherapy, Clinical Cancer Research 13 (2007) 2471-2478.
[122] E.S. Ng, L. Azzola, K. Sourris, L. Robb, E.G. Stanley, A.G. Elefanty, The primitive streak gene Mixl1 is required for efficient haematopoiesis and BMP4-induced ventral mesoderm patterning in differentiating, Development 132 (2005) 873-884.
[123] E. Piek, C.-H. Heldin, P. Ten Dijke, Specificity, diversity, and regulation in TGF-β superfamily signaling, The FASEB Journal 13 (1999) 2105-2124.
[124] S.I. Ashraf, X. Hu, J. Roote, Y.T. Ip, The mesoderm determinant Snail collaborates with related zinc-finger proteins to control Drosophila neurogenesis, EMBO J 18 (1999) 6426-6438.
[125] M. Takenaga, M. Fukumoto, Y. Hori, Regulated Nodal signaling promotes differentiation of the definitive endoderm and mesoderm from ES cells, Journal of Cell Science 120 (2007) 2078-2090.
[126] T.C. Doetschman, H. Eistetter, M. Katz, W. Schmidt, R. Kemler, The in vitro development of blastocyst-derived embryonic stem cell lines: formation of visceral yolk sac, blood islands and myocardium, Journal of Embryology and Experimental Morphology 87 (1985) 27-45.

[127] F. Shalaby, J. Rossant, T.P. Yamaguchi, M. Gertsenstein, X.-F. Wu, M.L. Breitman, A.C. Schuh, Failure of blood-island formation and vasculogenesis in Flk-1-deficient mice, Nature 376 (1995) 62-66.
[128] S.-I. Nishikawa, S. Nishikawa, H. Kawamoto, H. Yoshida, M. Kizumoto, H. Kataoka, Y. Katsura, In Vitro Generation of Lymphohematopoietic Cells from Endothelial Cells Purified from Murine Embryos, Immunity 8 (1998) 761-769.
[129] M. Hirashima, H. Kataoka, S. Nishikawa, N. Matsuyoshi, S.-I. Nishikawa, Maturation of Embryonic Stem Cells Into Endothelial Cells in an In Vitro Model of Vasculogenesis, Blood 93 (1999) 1253-1263.
[130] S.L. D'Souza, A.G. Elefanty, G. Keller, SCL/Tal-1 is essential for hematopoietic commitment of the hemangioblast but not for its development, Blood 105 (2005) 3862-3870.
[131] P. Faloon, E. Arentson, A. Kazarov, C.X. Deng, C. Porcher, S. Orkin, K. Choi, Basic fibroblast growth factor positively regulates hematopoietic development, Development 127 (2000) 1931-1941.
[132] K. Choi, M. Kennedy, A. Kazarov, J.C. Papadimitriou, G. Keller, A common precursor for hematopoietic and endothelial cells, Development 125 (1998) 725-732.
[133] C.A. Adelman, S. Chattopadhyay, J.J. Bieker, The BMP/BMPR/Smad pathway directs expression of the erythroid-specific EKLF and GATA1 transcription factors during embryoid body differentiation in serum-free media, Development 129 (2002) 539-549.
[134] K. Rajala, M. Pekkanen-Mattila, K. Alto-Setala, Cardiac differentiation of pluripotent stem cells, Stem cells International 2011 (2011) 12.
[135] A. Bondue, G. Lapouge, C. Paulissen, C. Semeraro, M. Iacovino, M. Kyba, C. Blanpain, Mesp1 Acts as a Master Regulator of Multipotent Cardiovascular Progenitor Specification, Cell Stem Cell 3 (2008) 69-84.
[136] A. Armiñán, C. Gandía, M. Bartual, J. M.García-Verdugo, E. Lledó, V. Mirabet, M. Llop, J. Barea, J. A.Montero, P. Sepúlveda, Cardiac Differentiation Is Driven by NKX2.5 and GATA4 Nuclear Translocation in Tissue-Specific Mesenchymal Stem Cells Stem Cells and Development 18 (2009) 907-918.
[137] H.S. Ip, D.B. Wilson, M. Heikinheimo, Z. Tang, C.N. Ting, M.C. Simon, J.M. Leiden, M.S. Parmacek, The GATA-4 transcription factor transactivates the cardiac muscle-specific troponin C promoter-enhancer in nonmuscle cells, Molecular and Cellular Biology 14 (1994) 7517-7526.
[138] T. Evans, Regulation of Cardiac Gene Expression by GATA-4/5/6, Trends in Cardiovascular Medicine 7 (1997) 75-83.
[139] T. Uchimura, Y. Komatsu, M. Tanaka, K.L. McCann, Y. Mishina, Bmp2 and Bmp4 genetically interact to support multiple aspects of mouse development including functional heart development, genesis 47 (2009) 374-384.
[140] J. Wang, S.B. Greene, M. Bonilla-Claudio, Y. Tao, J. Zhang, Y. Bai, Z. Huang, B.L. Black, F. Wang, J.F. Martin, Bmp Signaling Regulates Myocardial Differentiation from Cardiac Progenitors Through a MicroRNA-Mediated Mechanism, Developmental Cell 19 (2010) 903-912.
[141] K. Monzen, I. Shiojima, Y. Hiroi, S. Kudoh, T. Oka, E. Takimoto, D. Hayashi, T. Hosoda, A. Habara-Ohkubo, T. Nakaoka, T. Fujita, Y. Yazaki, I. Komuro, Bone Morphogenetic Proteins Induce Cardiomyocyte Differentiation through the

Mitogen-Activated Protein Kinase Kinase Kinase TAK1 and Cardiac Transcription Factors Csx/Nkx-2.5 and GATA-4, Molecular and Cellular Biology 19 (1999) 7096-7105.
[142] M.W. McBurney, B.J. Rogers, Isolation of male embryonal carcinoma cells and their chromosome replication patterns, Developmental Biology 89 (1982) 503-508.
[143] E.M.V. Jones-Villeneuve, M.W. McBurney, K.A. Rogers, Retinoic acid induces embryonal carcinoma cells to differentiate into neurons and glial cells, The Journal of Cell Biology 94 (1982) 253-262.
[144] L.J. Gudas, J.A. Wagner, Retinoids regulate stem cell differentiation, Journal of Cellular Physiology 226 (2011) 322-330.
[145] L. Cammas, R. Romand, V. Fraulob, C. Mura, P. Dollé, Expression of the murine retinol dehydrogenase 10 (Rdh10) gene correlates with many sites of retinoid signalling during embryogenesis and organ differentiation, Developmental Dynamics 236 (2007) 2899-2908.
[146] L.L. Sandell, B.W. Sanderson, G. Mioiseyev, T. Johnson, A. Mushegian, K. Young, J.-P. Rey, J.-x. Ma, K. Staehling-Hampton, P.A. Tainor, RDH10 is essential for synthesis of embryonic retinoic acid and is required for limb, craniofacial, and organ development, Genes & Development 21 (2007) 1113-1124.
[147] O.V. Belyaeva, M.P. Johnson, N.Y. Kedishvili, Kinetic Analysis of Human Enzyme RDH10 Defines the Characteristics of a Physiologically Relevant Retinol Dehydrogenase, Journal of Biological Chemistry 283 (2008) 20299-20308.
[148] M.A.G. van der Heyden, L.H.K. Defize, Twenty one years of P19 cells: what an embryonal carcinoma cell line taught us about cardiomyocyte differentiation, Cardiovascular Research 58 (2003) 292-302.
[149] J. Paquin, B.A. Danalache, M. Jankowski, S.M. McCann, J. Gutkowska, Oxytocin induces differentiation of P19 embryonic stem cells to cardiomyocytes, Proceedings of the National Academy of Sciences 99 (2002) 9550-9555.
[150] M.A. Rudnicki, G. Jackowski, L. Saggin, M.W. McBurney, Actin and myosin expression during development of cardiac muscle from cultured embryonal carcinoma cells, Developmental Biology 138 (1990) 348-358.
[151] P. Morley, J.F. Whitfield, The differentiation inducer, dimethyl sulfoxide, transiently increases the intracellular calcium ion concentration in various cell types, Journal of Cellular Physiology 156 (1993) 219-225.
[152] O. Yanes, J. Clark, D.M. Wong, G.J. Patti, A. Sánchez-Ruiz, H.P. Benton, S.A. Trauger, C. Desponts, S. Ding, G. Siuzdak, Metabolic oxidation regulates embryonic stem cell differentiation, Nat Chem Biol 6 (2010) 411-417.
[153] T. Lonergan, B. Bavister, C. Brenner, Mitochondria in stem cells, Mitochondrion 7 (2007) 289-296.
[154] J.C. St. John, J. Ramalho-Santos, H.L. Gray, P. Petrosko, V.Y. Rawe, C.S. Navara, The Expression of Mitochondrial DNA Transcription Factors during Early Cardiomyocyte In Vitro Differentiation from Human Embryonic Stem Cells, Cloning and Stem Cells 7 (2005) 141-153.
[155] A. Prigione, B. Fauler, R. Lurz, H. Lehrach, J. Adjaye, The Senescence-Related Mitochondrial/Oxidative Stress Pathway is Repressed in Human Induced Pluripotent Stem Cells, Stem Cells 28 (2010) 721-733.

[156] J.M. Facucho-Oliveira, J. Alderson, E.C. Spikings, S. Egginton, J.C. St. John, Mitochondrial DNA replication during differentiation of murine embryonic stem cells, Journal of Cell Science 120 (2007) 4025-4034.
[157] S. Chung, P.P. Dzeja, R.S. Faustino, C. Perez-Terzic, A. Behfar, A. Terzic, Mitochondrial oxidative metabolism is required for the cardiac differentiation of stem cells, Nat Clin Pract Cardiovasc Med (2006).
[158] A.-R. Ji, S.-Y. Ku, M.S. Cho, Y.Y. Kim, Y.J. Kim, S.K. Oh, S.H. Kim, S.Y. Moon, Y.M. Choi, Reactive oxygen species enhance differentiation of human embryonic stem cells into mesendodermal lineage, Exp Mol Med 42 (2010) 175-186.
[159] M. Schmelter, B. Ateghang, S. Helmig, M. Wartenberg, H. Sauer, Embryonic stem cells utilize reactive oxygen species as transducers of mechanical strain-induced cardiovascular differentiation, The FASEB Journal 20 (2006) 1182-1184.
[160] P. Vella, A. Scelfo, S. Jammula, F. Chiacchiera, K. Williams, A. Cuomo, A. Roberto, J. Christensen, T. Bonaldi, K. Helin, D. Pasini, Tet Proteins Connect the O-Linked N-acetylglucosamine Transferase Ogt to Chromatin in Embryonic Stem Cells, Molecular cell 49 (2013) 645-656.
[161] P.A. MacPherson, M.W. McBurney, P19 Embryonal Carcinoma Cells: A Source of Cultured Neurons Amenable to Genetic Manipulation, Methods 7 (1995) 238-252.
[162] M.A.G. van der Heyden, M.J.A. van Kempen, Y. Tsuji, M.B. Rook, H.J. Jongsma, T. Opthof, P19 embryonal carcinoma cells: a suitable model system for cardiac electrophysiological differentiation at the molecular and functional level, Cardiovascular Research 58 (2003) 410-422.
[163] J.M. Graham, Isolation of Mitochondria from Tissues and Cells by Differential Centrifugation, Current Protocols in Cell Biology, John Wiley & Sons, Inc., 2001.
[164] S. Han, C. Auger, Z. Castonguay, V. Appanna, S. Thomas, V. Appanna, The unravelling of metabolic dysfunctions linked to metal-associated diseases by blue native polyacrylamide gel electrophoresis, Analytical and Bioanalytical Chemistry 405 (2013) 1821-1831.
[165] M.M. Bradford, A rapid and sensitive method for the quantitation of microgram quantities of protein utilizing the principle of protein-dye binding., Analytical Biochemistry 7 (1976) 248-254.
[166] H. Schägger, G. von Jagow, Blue native electrophoresis for isolation of membrane protein complexes in enzymatically active form, Analytical Biochemistry 199 (1991) 223-231.
[167] R. Singh, D. Chénier, R. Bériault, R. Mailloux, R.D. Hamel, V.D. Appanna, Blue native polyacrylamide gel electrophoresis and the monitoring of malate- and oxaloacetate-producing enzymes, Journal of Biochemical and Biophysical Methods 64 (2005) 189-199.
[168] D. Shechter, H.L. Dormann, C.D. Allis, S.B. Hake, Extraction, purification and analysis of histones, Nat. Protocols 2 (2007) 1445-1457.
[169] D.M. Phillips, The presence of acetyl groups of histones, Biochemical Journal 87 (1963) 258-263.
[170] B.D. Zehr, T.J. Savin, R.E. Hall, A one-step, low background Coomassie staining procedure for polyacrylamide gels, Analytical Biochemistry 182 (1989) 157-159.
[171] H. Osterman, A. Schutz-Geschwender, White Paper: Near-Infrared Fluorescence Imaging: Seeing Beyond the Visible with IRDye® Infrared Dyes, Li-Cor Biosciences, Licoln Nebraska, 2007.

[172] P. Reungpatthanaphong, S. Dechsupa, J. Meesungnoen, C. Loetchutinat, S. Mankhetkorn, Rhodamine B as a mitochondrial probe for measurement and monitoring of mitochondrial membrane potential in drug-sensitive and -resistant cells, Journal of Biochemical and Biophysical Methods 57 (2003) 1-16.
[173] A. Baracca, G. Sgarbi, G. Solaini, G. Lenaz, Rhodamine 123 as a probe of mitochondrial membrane potential: evaluation of proton flux through F0 during ATP synthesis, Biochimica et Biophysica Acta (BBA) - Bioenergetics 1606 (2003) 137-146.
[174] M.C. Haigis, D.A. Sinclair, Mammalian Sirtuins: Biological Insights and Disease Relevance, Annual Review of Pathology: Mechanisms of Disease 5 (2010) 253-295.
[175] G. Donmez, L. Guarente, Aging and disease: connections to sirtuins, Aging Cell 9 (2010) 285-290.
[176] B.E. Bernstein, T.S. Mikkelsen, X. Xie, M. Kamal, D.J. Huebert, J. Cuff, B. Fry, A. Meissner, M. Wernig, K. Plath, R. Jaenisch, A. Wagschal, R. Feil, S.L. Schreiber, E.S. Lander, A Bivalent Chromatin Structure Marks Key Developmental Genes in Embryonic Stem Cells, Cell 125 (2006) 315-326.
[177] J. Graumann, N.C. Hubner, J.B. Kim, K. Ko, M. Moser, C. Kumar, J. Cox, H. Schöler, M. Mann, Stable Isotope Labeling by Amino Acids in Cell Culture (SILAC) and Proteome Quantitation of Mouse Embryonic Stem Cells to a Depth of 5,111 Proteins, Molecular & Cellular Proteomics 7 (2008) 672-683.
[178] R.J. Mailloux, S. Puiseux-Dao, V.D. Appanna, α-Ketoglutarate abrogates the nuclear localization of HIF-1α in aluminum-exposed hepatocytes, Biochimie 91 (2009) 408-415.
[179] L. Zheng, R.G. Roeder, Y. Luo, S Phase Activation of the Histone H2B Promoter by OCA-S, a Coactivator Complex that Contains GAPDH as a Key Component, Cell 114 (2003) 255-266.
[180] S. Varum, A.S. Rodrigues, M.B. Moura, O. Momcilovic, C.A.I.V. Easley, J. Ramalho-Santos, B. Van Houten, G. Schatten, Energy Metabolism in Human Pluripotent Stem Cells and Their Differentiated Counterparts, PLoS ONE 6 (2011) e20914.
[181] S. Chung, D.K. Arrell, R.S. Faustino, A. Terzic, P.P. Dzeja, Glycolytic network restructuring integral to the energetics of embryonic stem cell cardiac differentiation, Journal of Molecular and Cellular Cardiology 48 (2010) 725-734.
[182] B. Chazotte, Labeling Mitochondria with Rhodamine 123, Cold Spring Harbor Protocols 2011 (2011) pdb.prot5640.
[183] C. Mantel, S. Messina-Graham, H.E. Broxmeyer, Upregulation of nascent mitochondrial biogenesis in mouse hematopoietic stem cells parallels upregulation of CD34 and loss of pluripotency: A potential strategy for reducing oxidative risk in stem cells, Cell Cycle 9 (2010) 2008-2017.
[184] L. Wilson-Fritch, A. Burkart, G. Bell, K. Mendelson, J. Leszyk, S. Nicoloro, M. Czech, S. Corvera, Mitochondrial Biogenesis and Remodeling during Adipogenesis and in Response to the Insulin Sensitizer Rosiglitazone, Molecular and Cellular Biology 23 (2003) 1085-1094.
[185] S. Mandal, A.G. Lindgren, A.S. Srivastava, A.T. Clark, U. Banerjee, Mitochondrial Function Controls Proliferation and Early Differentiation Potential of Embryonic Stem Cells, Stem Cells 29 (2011) 486-495.

[186] M. Uldry, W. Yang, J. St-Pierre, J. Lin, P. Seale, B.M. Spiegelman, Complementary action of the PGC-1 coactivators in mitochondrial biogenesis and brown fat differentiation, Cell Metabolism 3 (2006) 333-341.
[187] S. Kang, L. Bajnok, K.A. Longo, R.K. Petersen, J.B. Hansen, K. Kristiansen, O.A. MacDougald, Effects of Wnt Signaling on Brown Adipocyte Differentiation and Metabolism Mediated by PGC-1α, Molecular and Cellular Biology 25 (2005) 1272-1282.
[188] A.B.J. Prowse, F. Chong, D.A. Elliott, A.G. Elefanty, E.G. Stanley, P.P. Gray, T.P. Munro, G.W. Osborne, Analysis of Mitochondrial Function and Localisation during Human Embryonic Stem Cell Differentiation In Vitro, PLoS ONE 7 (2012) e52214.
[189] J. Watkins, S. Basu, D.F. Bogenhagen, A Quantitative Proteomic Analysis of Mitochondrial Participation in P19 Cell Neuronal Differentiation, Journal of Proteome Research 7 (2007) 328-338.
[190] S. Katada, A. Imhof, P. Sassone-Corsi, Connecting Threads: Epigenetics and Metabolism, Cell 148 (2012) 24-28.
[191] Q. Zhang, D. Piston, R. Goodman, Regulation of Corepressor Function by Nuclear NADH, Science 295 (2002) 1895-1197.
[192] W. Stünkel, R.M. Campbell, Sirtuin 1 (SIRT1): The Misunderstood HDAC, Journal of Biomolecular Screening 16 (2011) 1153-1169.